An introduction to Radio Loud AGN

Paola Grandi & Eleonora Torresi

INAF-IASF Bologna

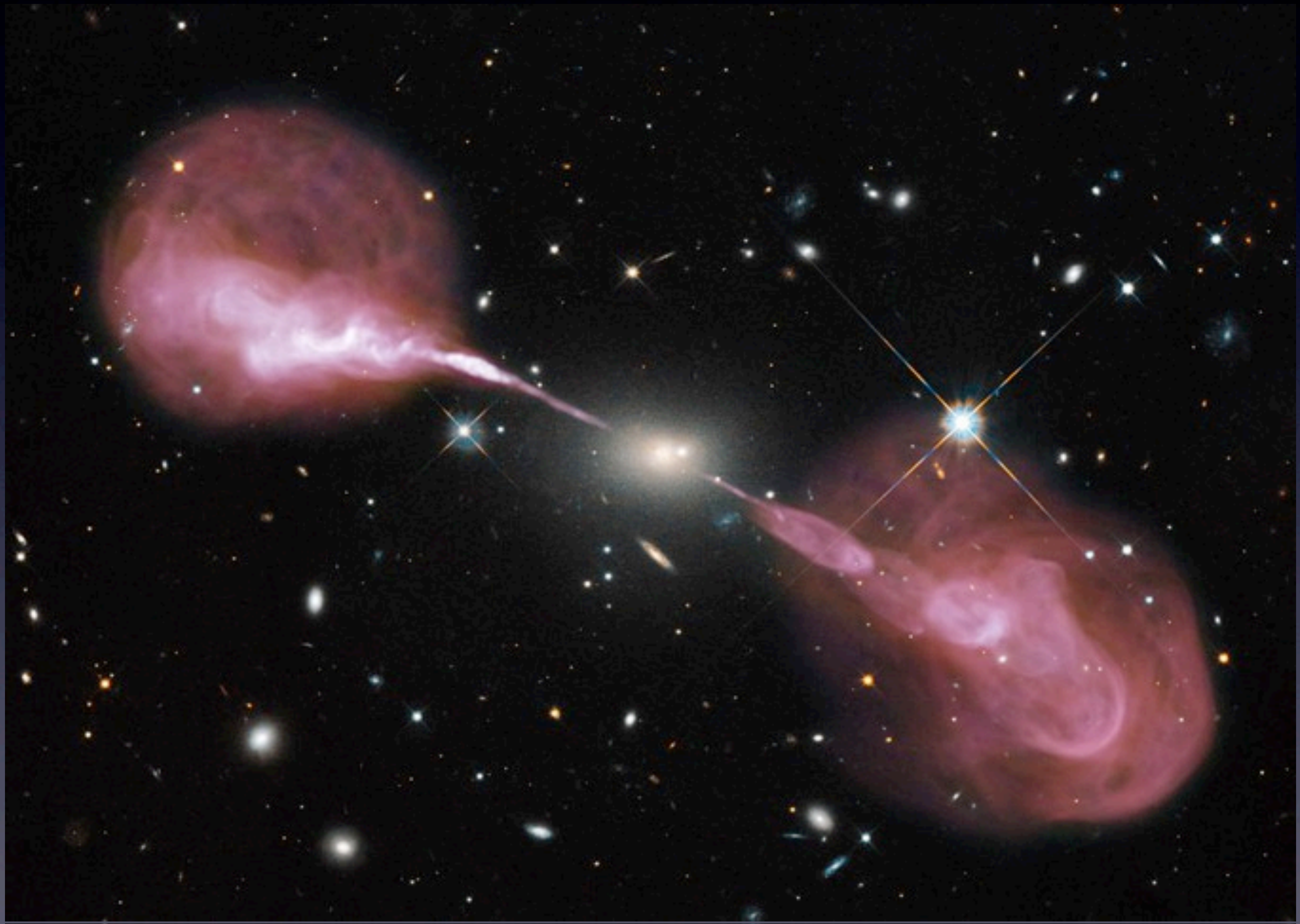

Laboratorio X

7.10.2014

Outline

- AGN IN GENERAL
  1) AGN classification
  2) Different SED in AGN
  3) The FRI/FRII dichotomy
  4) The X-ray spectra of radio galaxies

- RADIATIVE PROCESSES
  1) Thermal emission (accretion)
     - Accretion flow
     - Thermal Comptonization
     - Reprocessed features

  2) Non-thermal emission (jets and lobes)
     - Synchrotron process
     - Inverse Compton process

Almost every galaxy hosts a black hole

but...

Almost every galaxy hosts a black hole

but...

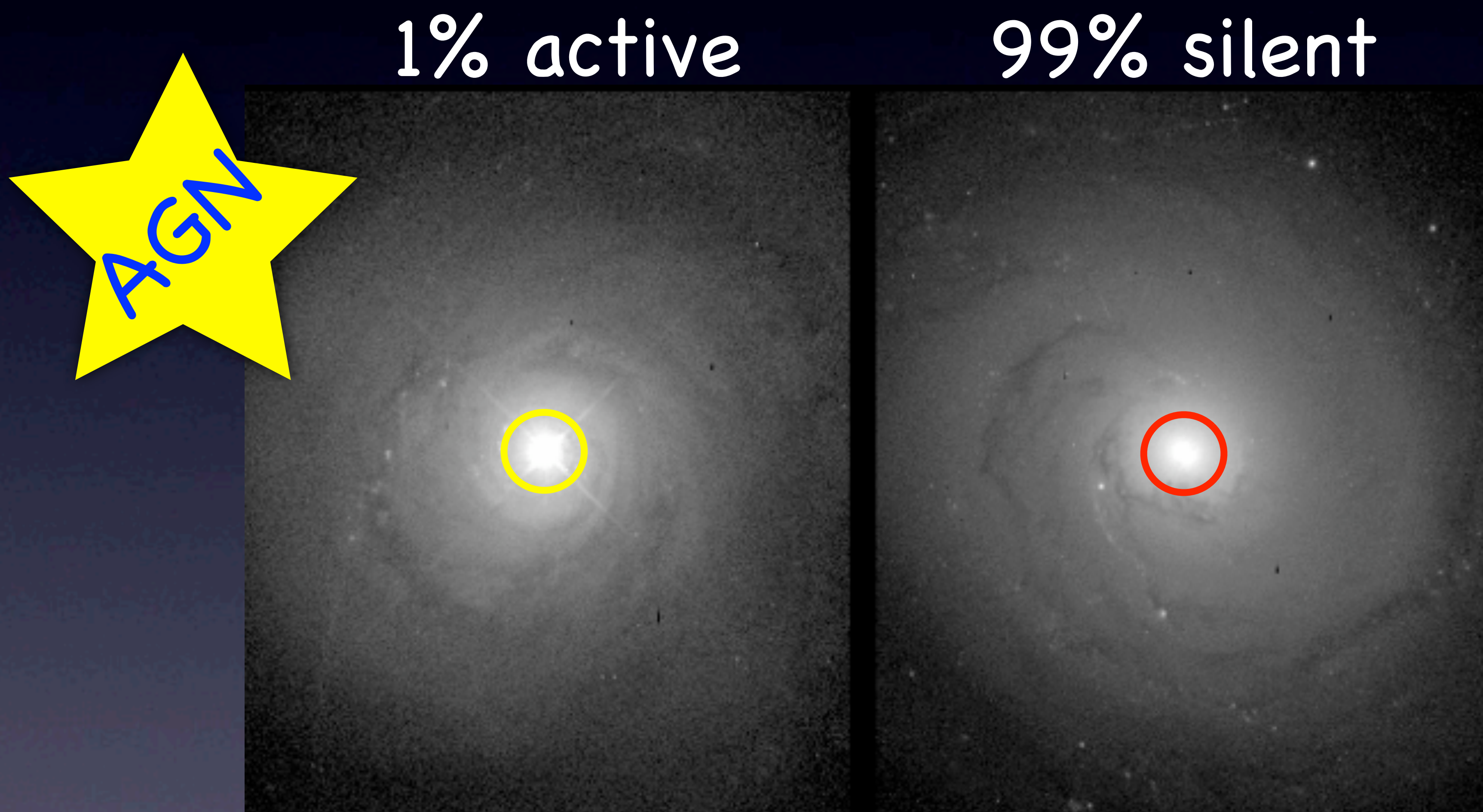

Almost every galaxy hosts a black hole

but...

1% active

99% silent

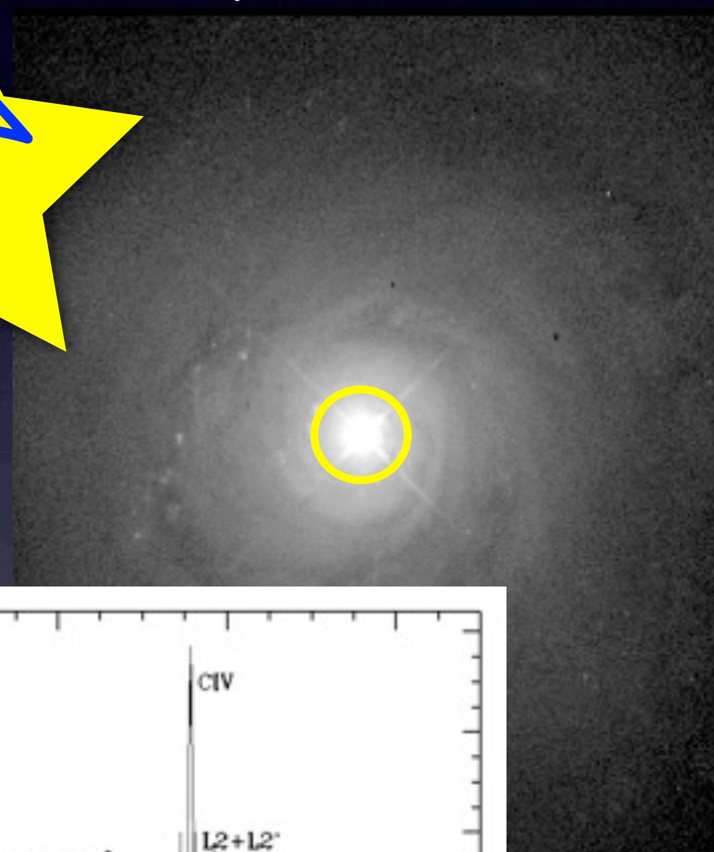

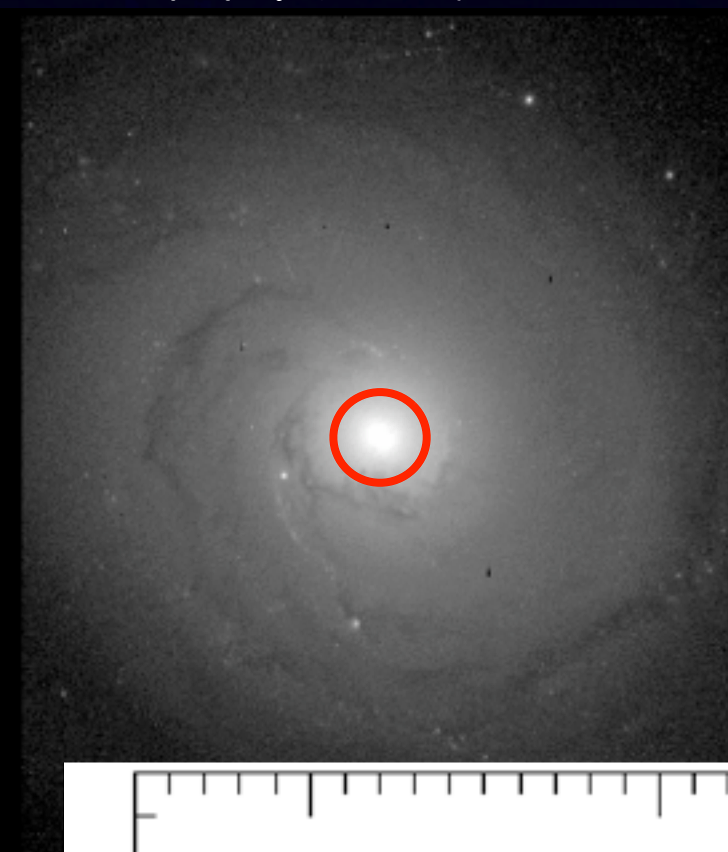

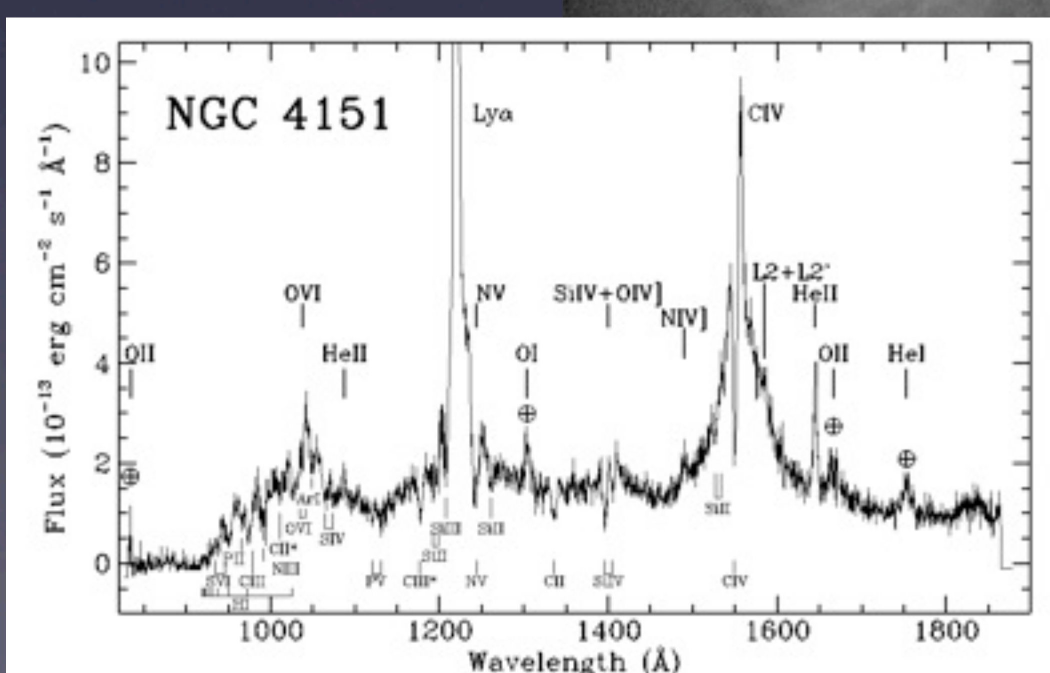

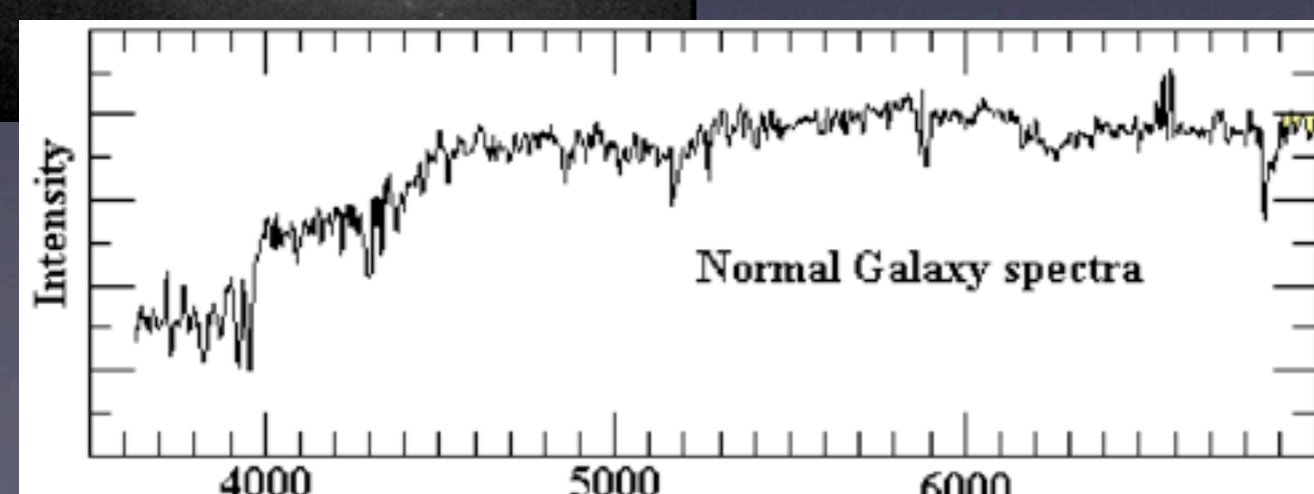

The engine occupies a tiny region in the center of the galaxy

30 kpc

2–3 pc

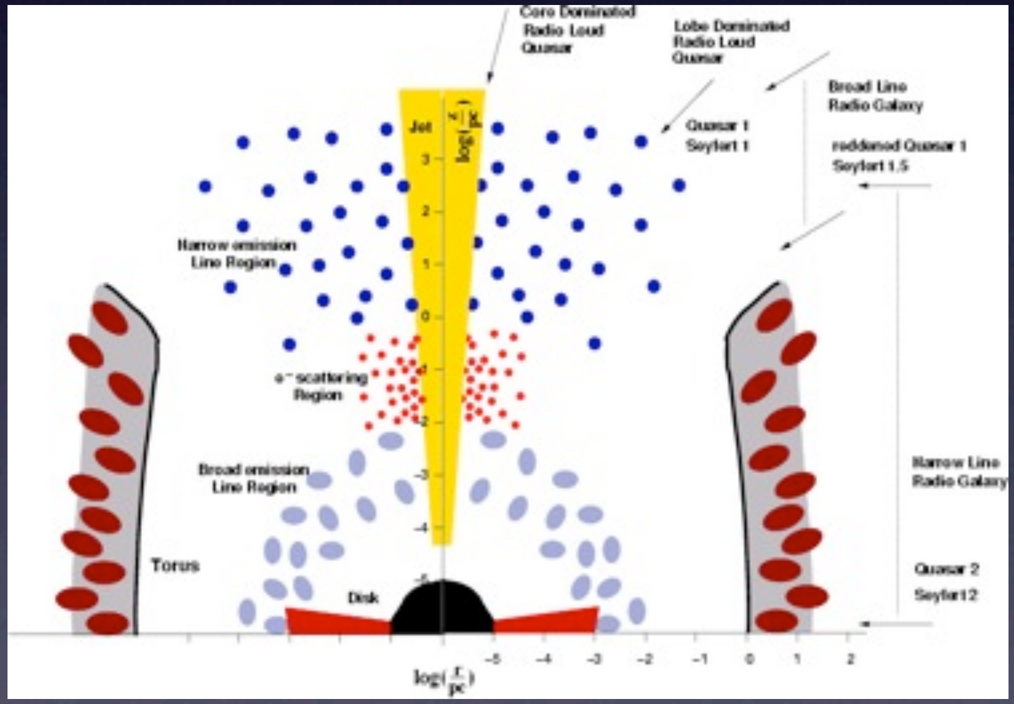

The extraordinary amount of energy is produced through accretion of gas close to a SMBH

About 15-20% of AGNs is Radio-Loud (RL) (Urry & Padovani 95)

An AGN is RL when

$$R = \frac{F_{5GHz}}{F_B} \geq 10$$

Kellermann et al. 1989

$$\log R_X = \frac{\nu L_\nu (5\mathrm{GHz})}{L_X} <= -4.5$$

Terashima & Wilson 2003

R= radio loudness parameter

RL AGNs lie in ellipticals

RQ AGNs lie in spirals and ellipticals

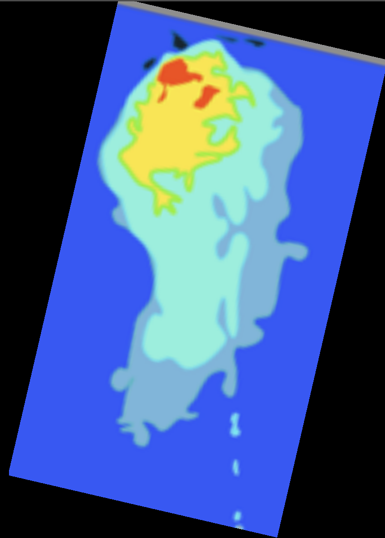

Radio Lobe

Some numbers for a typical AGN

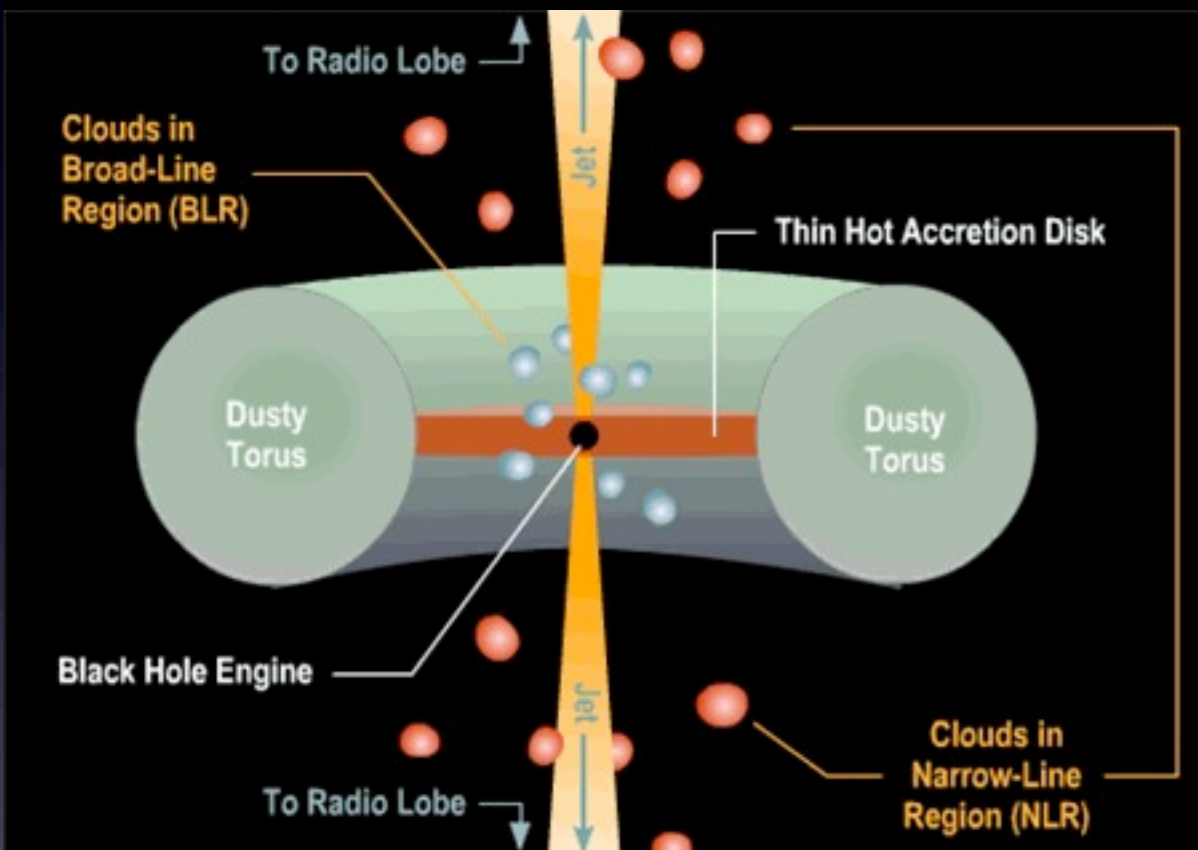

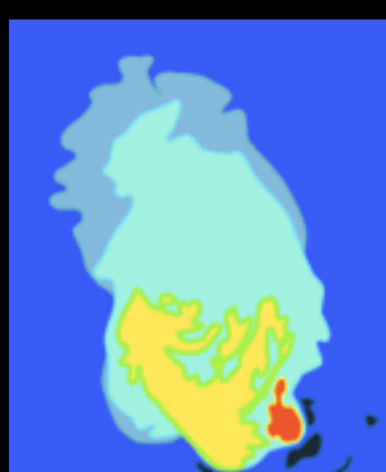

BH Mass $\sim 10^8 M_\odot$

Luminosity $\sim 10^{44}\ erg\ s^{-1}$

BH radius $\sim 3 \times 10^{13}\ cm$

BLR radius $\sim 2 - 20 \times 10^{16}\ cm$

NLR radius $\sim 10^{18} - 10^{20}\ cm$

In RL AGNs

Jet can be observed at $\sim 10^{17}\ cm$

Jets end at Kpc distances forming radio lobes

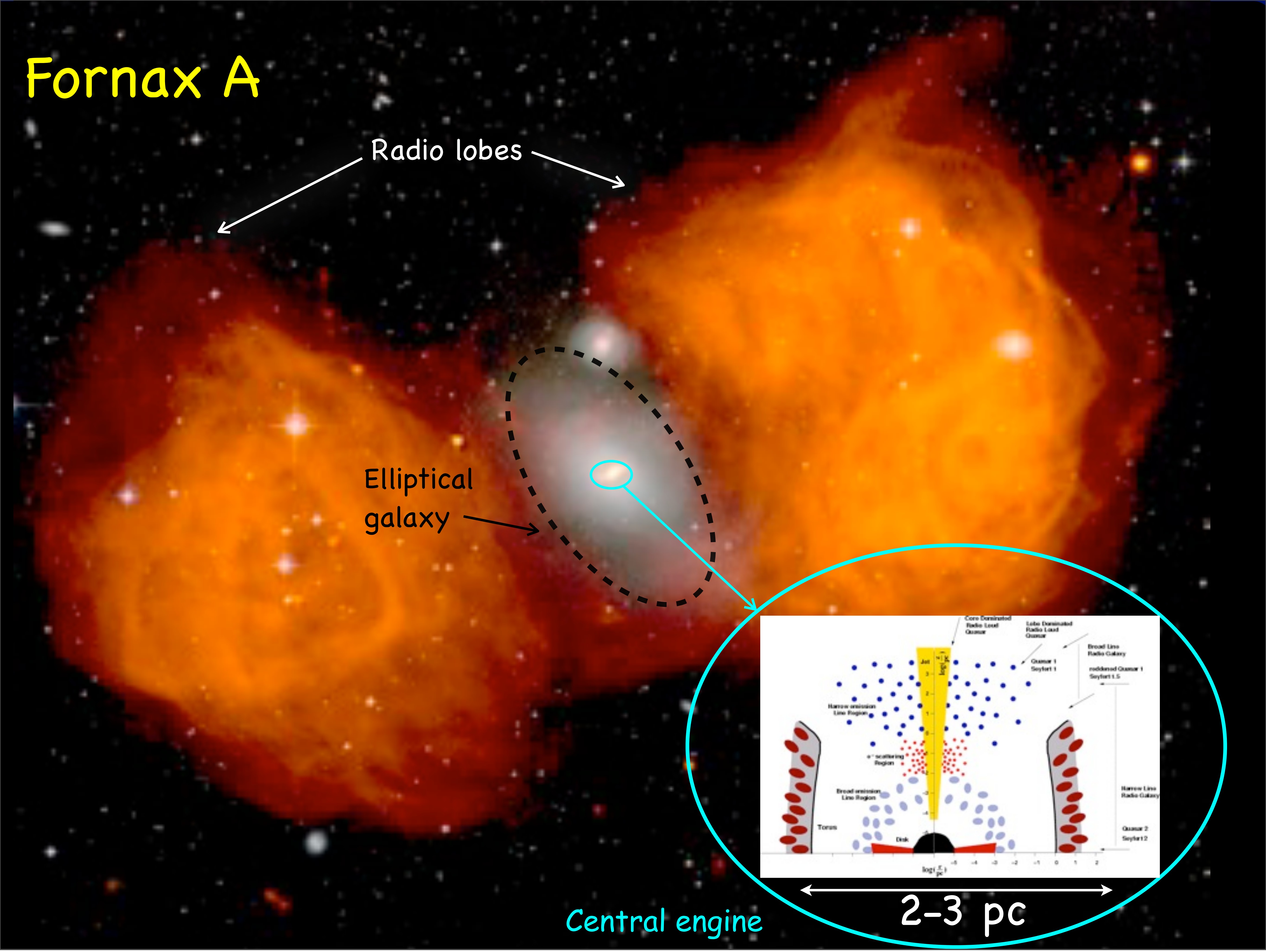
Fornax A
Radio lobes
Elliptical galaxy
Core Dominated Radio Loud Quasar
Lobe Dominated Radio Loud Quasar
Broad Line Radio Galaxy
Quasar 1 Seyfert 1
reddened Quasar 1 Seyfert 1.5
Jet
Narrow emission Line Region
e⁻ scattering Region
Broad emission Line Region
Narrow Line Radio Galaxy
Torus
Disk
Quasar 2 Seyfert 2
2–3 pc
Central engine

Black hole-galaxy feedback

Supermassive black holes have a profound effect on the formation and evolution of galaxies (Silk & Rees 1998, Fabian 1999, and many others) by regulating the amount of gas available for the star formation

-> strong link between BH formation and properties of the stellar bulge (correlations between host galaxy properties and masses of SMBHs)

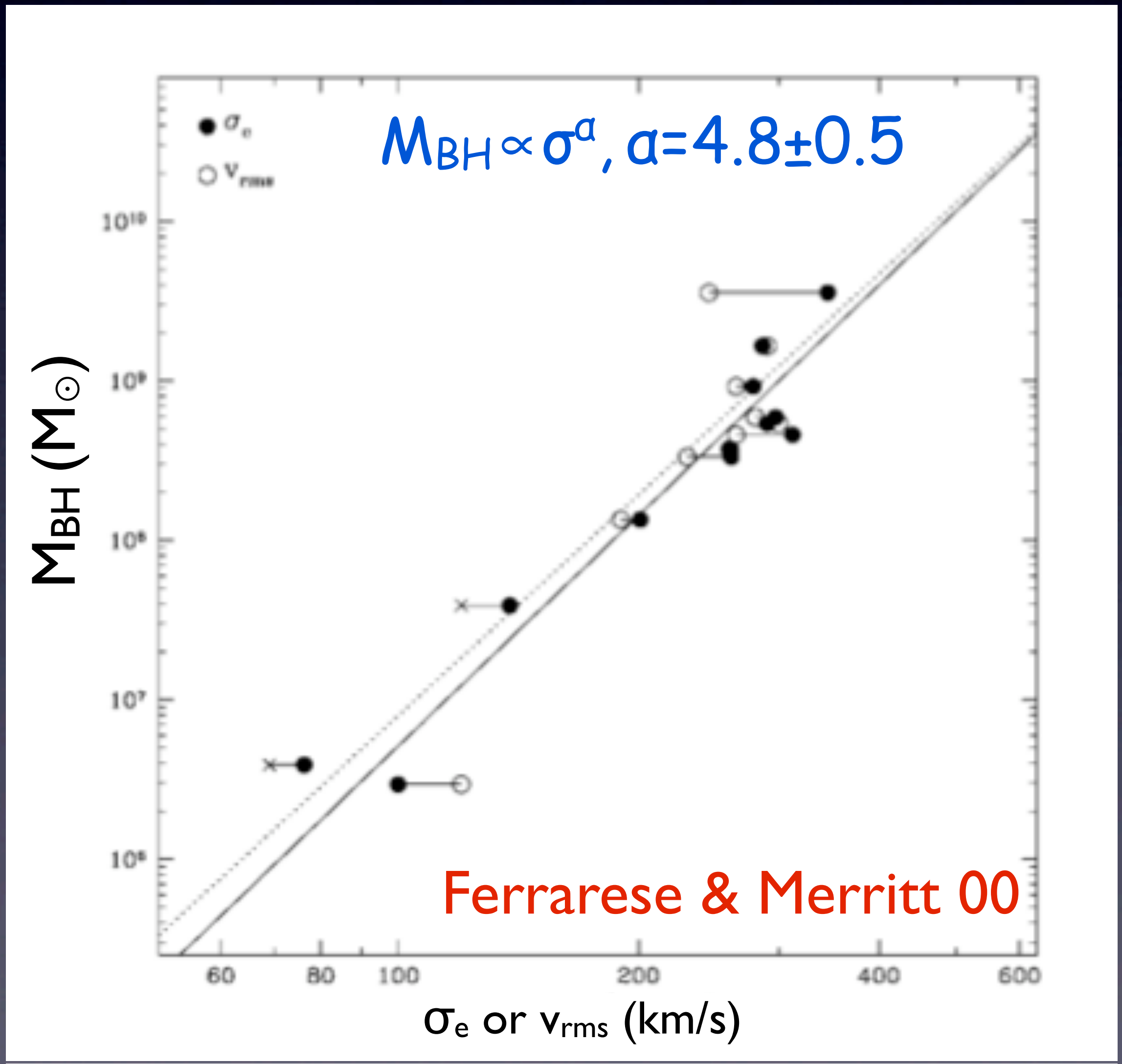

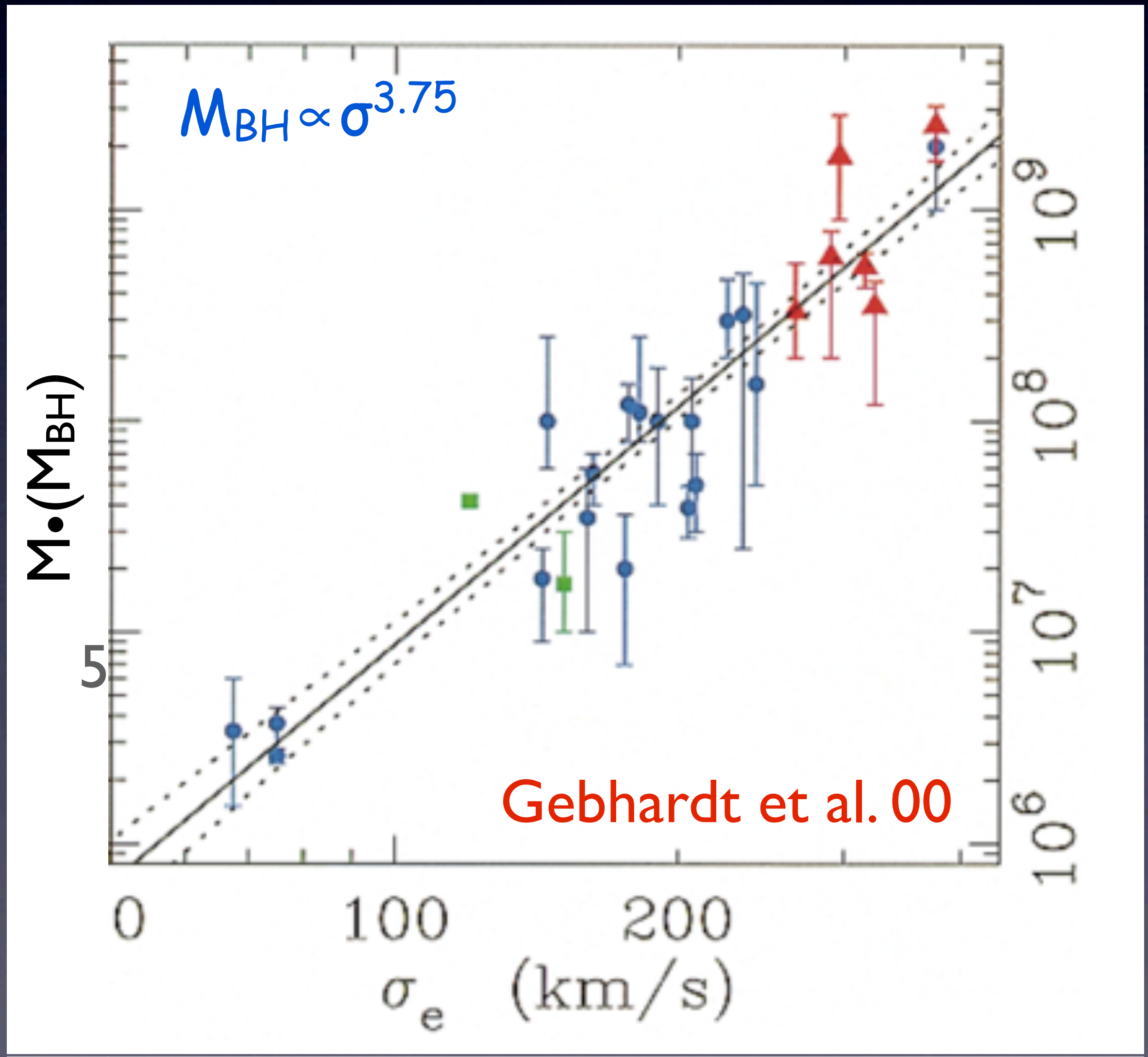

There are two types of feedback

RADIATIVE FEEDBACK radiative heating (primarily X-rays) nearby the SMBH (Ciotti & Ostriker 2007) that reduces cooling flows at the 10^2-10^3 pc scale.

MECHANICAL FEEDBACK feedback due to mechanical and thermal deposition of energy from jets and winds emitted by the accretion disk around the central BH (Ciotti, Ostriker & Proga 2009). The inner parts (10^1-10^2 pc) of elliptical galaxies are heated and the inflow to the central BH is reduced.

BOTH TYPES OF FEEDBACK (acting on different radial scales) ARE REQUIRED
(Ciotti, Ostriker & Proga 2009; 2010)
radiative feedback is required to balance and consume the cooling flow gas ;
mechanical feedback is required to limit the growth of the SMBH.

1. AGN classification

AGN classification

Optical classification

Type I	bright continuum and BROAD emission lines from hot high velocity gas (FWHM~10^{3-4} km s^{-1})
Type II	weak continuum and only NARROW emission lines (FWHM~10^{2} km s^{-1})

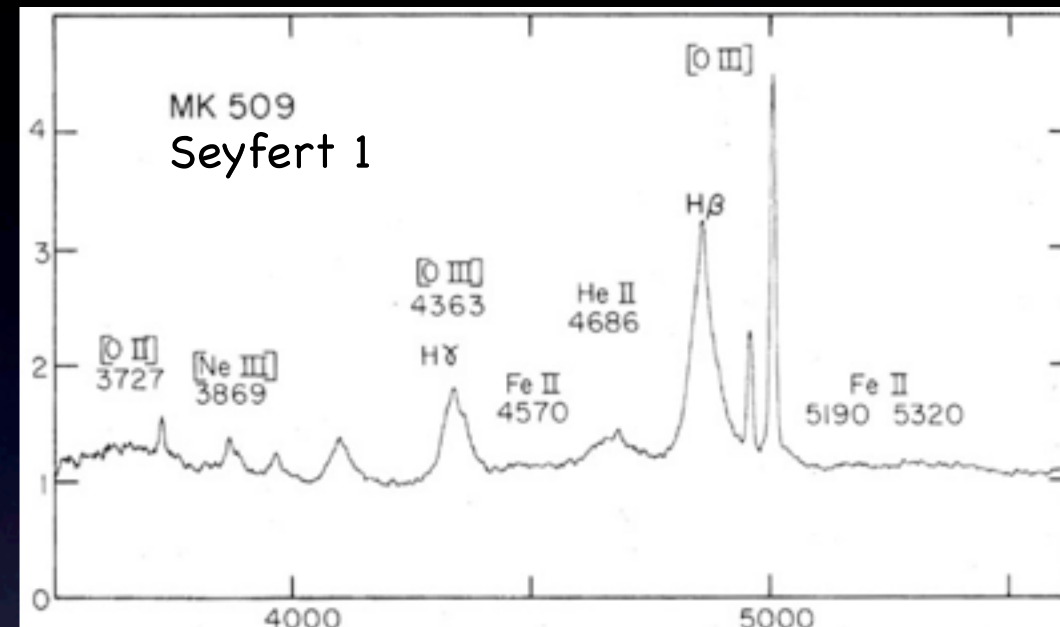

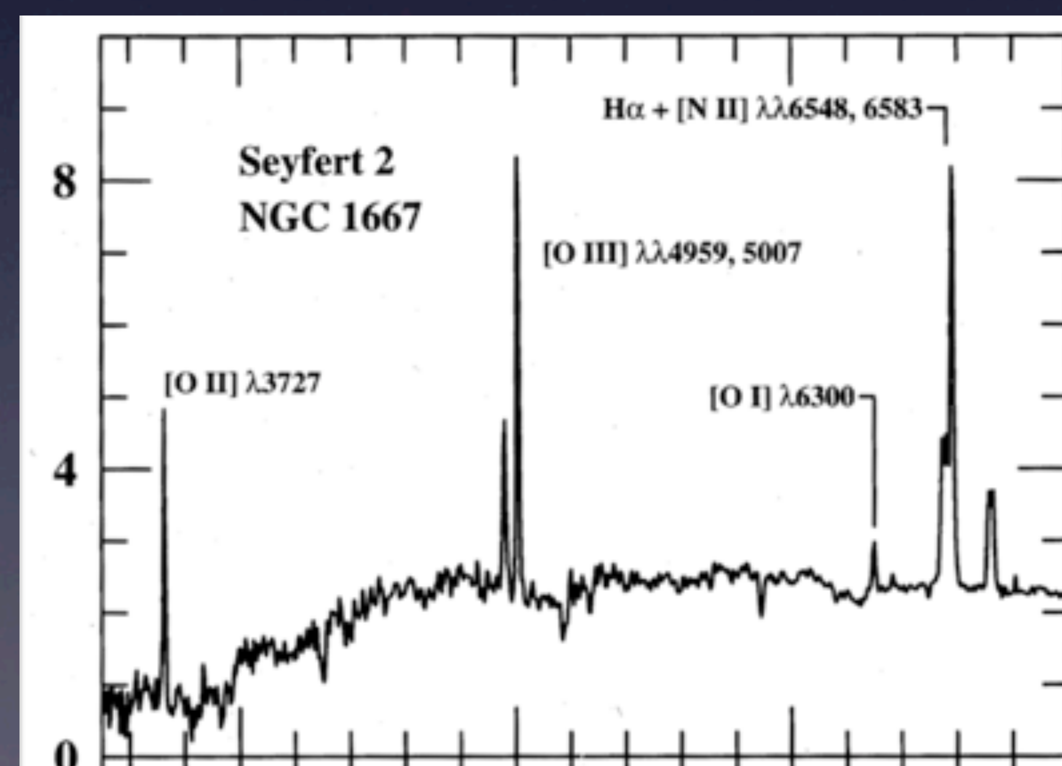

RL AGN classification

Optical classification — Radio classification

Type I/BLRGs Broad Line Radio Galaxies	bright continuum and BROAD emission lines from hot high velocity gas (FWHM~10^{3-4} km s^{-1})	FRII
Type II/NLRGs HEG Narrow Line Radio Galaxies/ High Excitation Galaxies	weak continuum and only NARROW emission lines (FWHM~10^2 km s^{-1})	FRII
Type II/NLRGs LEG Narrow Line Radio Galaxies/ Low Excitation Galaxies	narrow emission lines: $EW_{[OIII]}$>10 Å and/or O[II]/O[III]>1	FRII FRI
Type 0	Almost featureless in the optical band and extremely variable	BL Lac

FRI - $P_{178MHz} < 10^{25}$ W Hz^{-1} sr^{-1}

FRII - $P_{178MHz} > 10^{25}$ W Hz^{-1} sr^{-1}

(Fanaroff & Riley 1974)

RL AGN classificati

Optical classification

Rad

Type I/BLRGs Broad Line Radio Galaxies	**bright continuum and BROAD emission lines from hot high velocity gas (FWHM~10^{3-4} km s^{-1})**
Type II/NLRGs HEG Narrow Line Radio Galaxies/ High Excitation Galaxies	**weak continuum and only NARROW emission lines (FWHM~10^{2} km s^{-1})**
Type II/NLRGs LEG Narrow Line Radio Galaxies/ Low Excitation Galaxies	**narrow emission lines: $EW_{[OIII]}$>10 Å and/or O[II]/O[III]>1**
Type 0	**Almost featureless in the optical band and extremely variable**

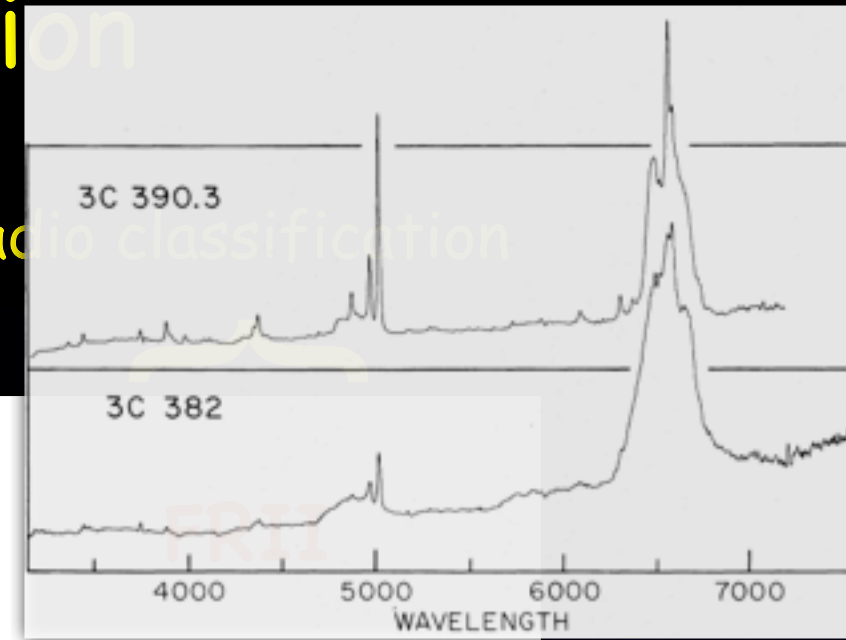

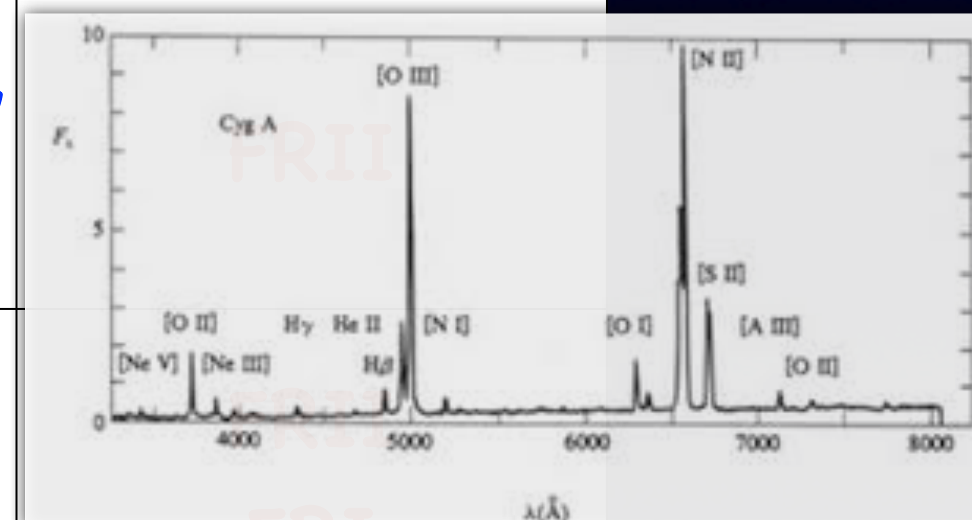

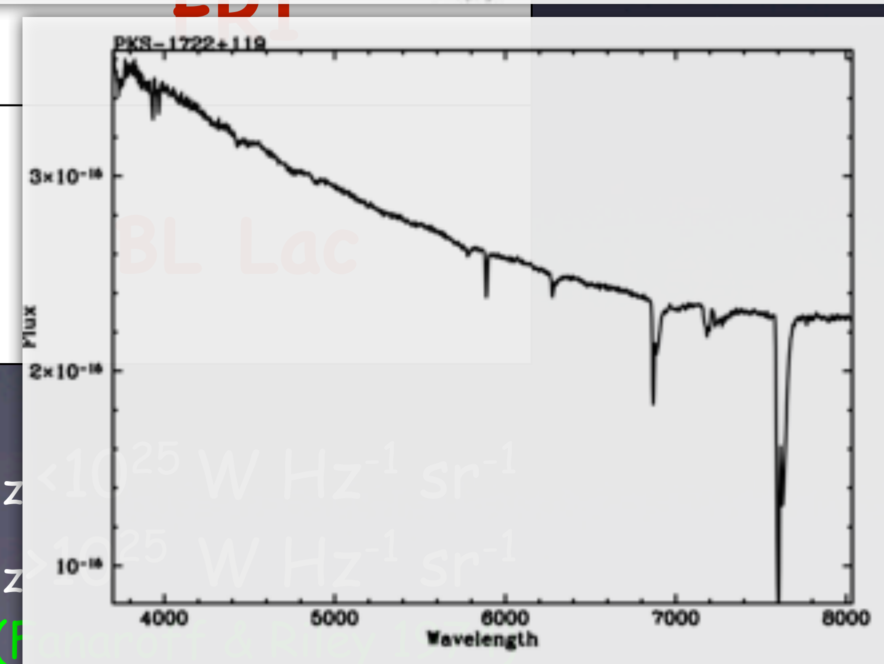

FRI - P_{178MHz}

FRII - P_{178MHz}

Observed radio morphologies:
The Fanaroff-Riley classification

FRI/jet dominated

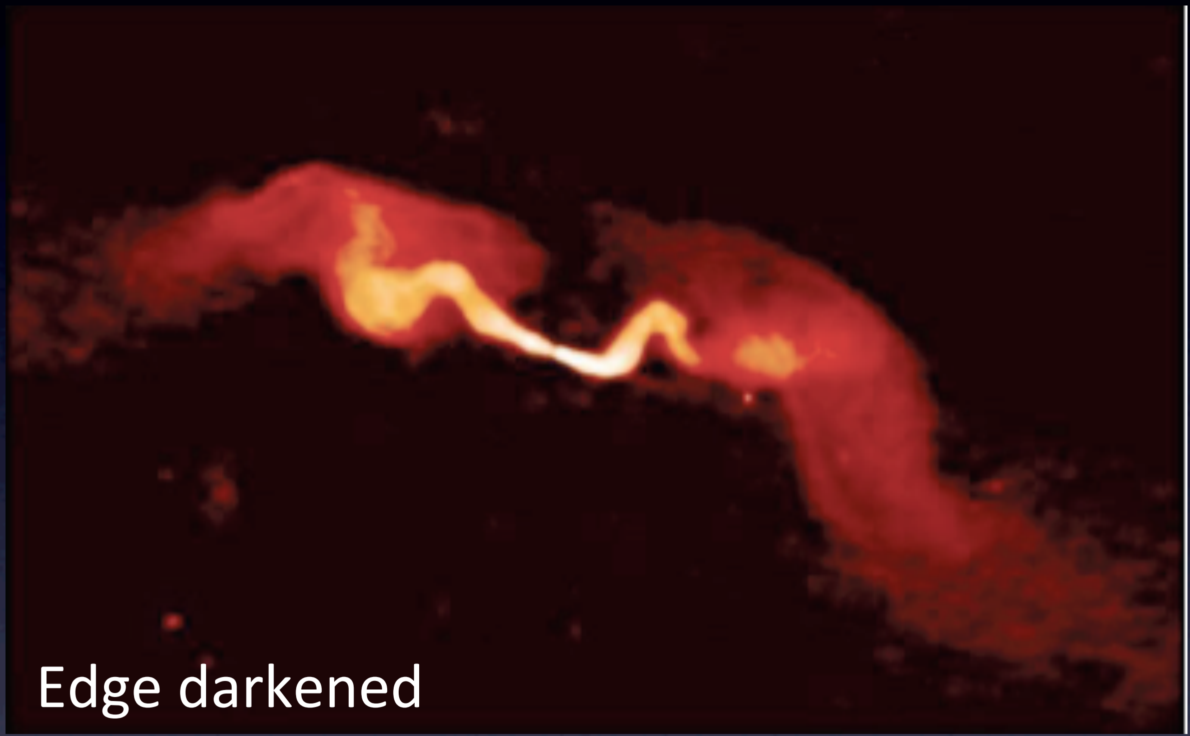

In FRI the jets are thought to decelerate and become sub-relativistic on scales of hundred of pc to kpc.

The nuclei of FRI are not generally absorbed and probably powered by inefficient accretion flows.

FRII/lobe dominated

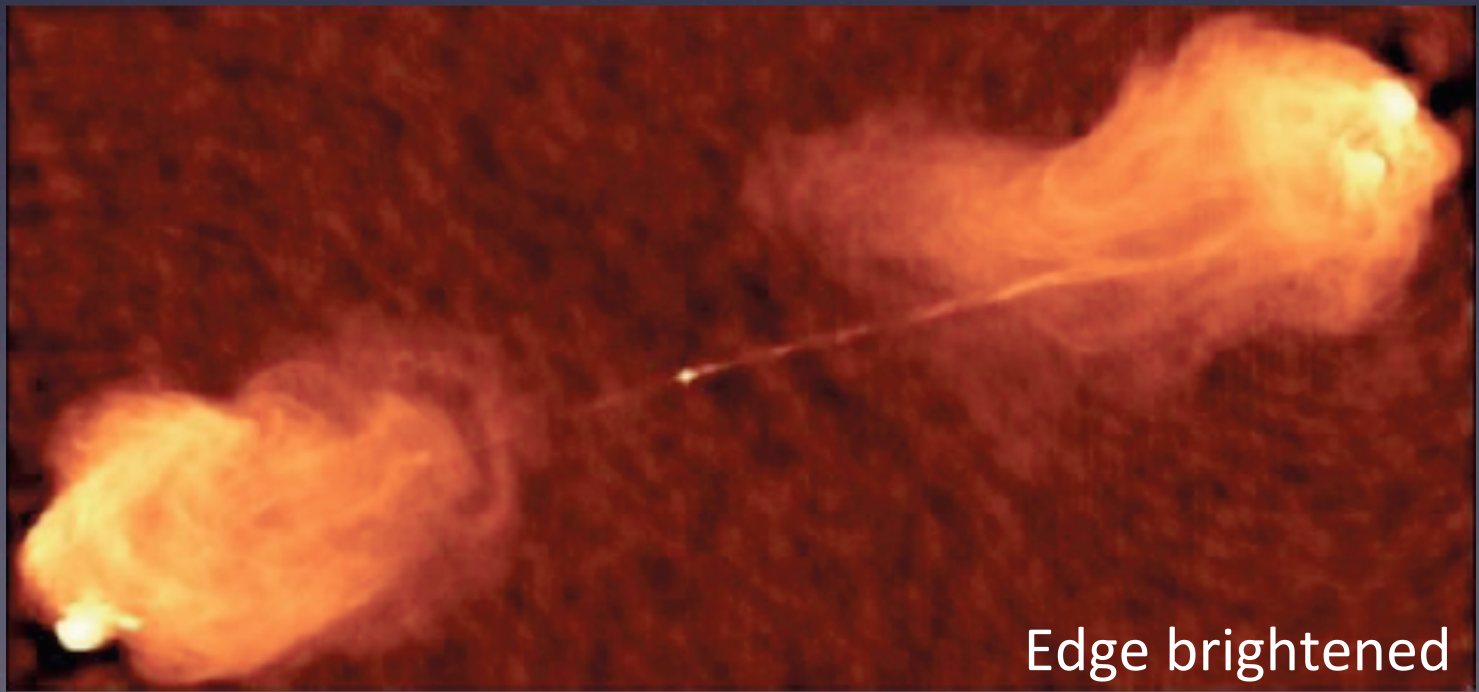

The jets in FRII are at least moderately relativistic and supersonic from the core to the hot spots.

Most FRII are thought to have an efficient engine and a dusty torus.

FRIs are considered the PARENT POPULATION of BL LACs

(Urry & Padovani 1995)

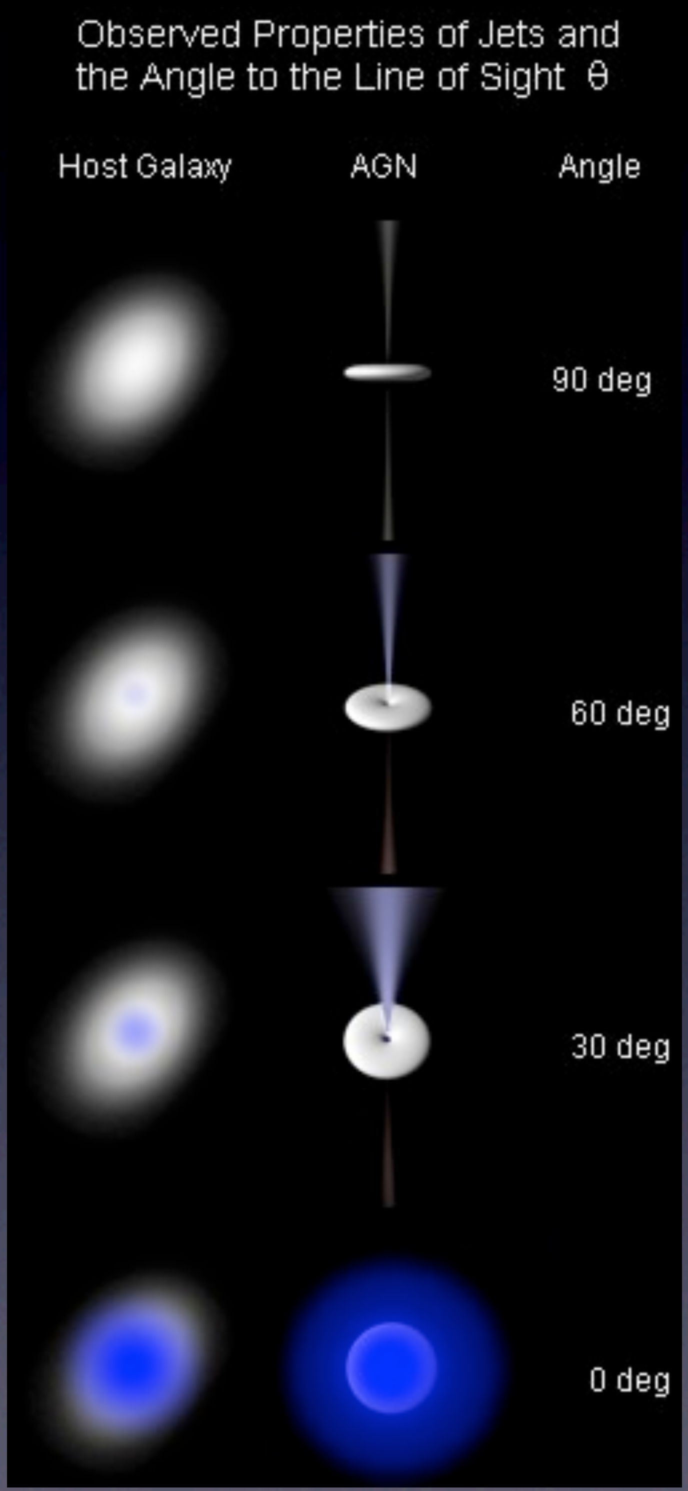

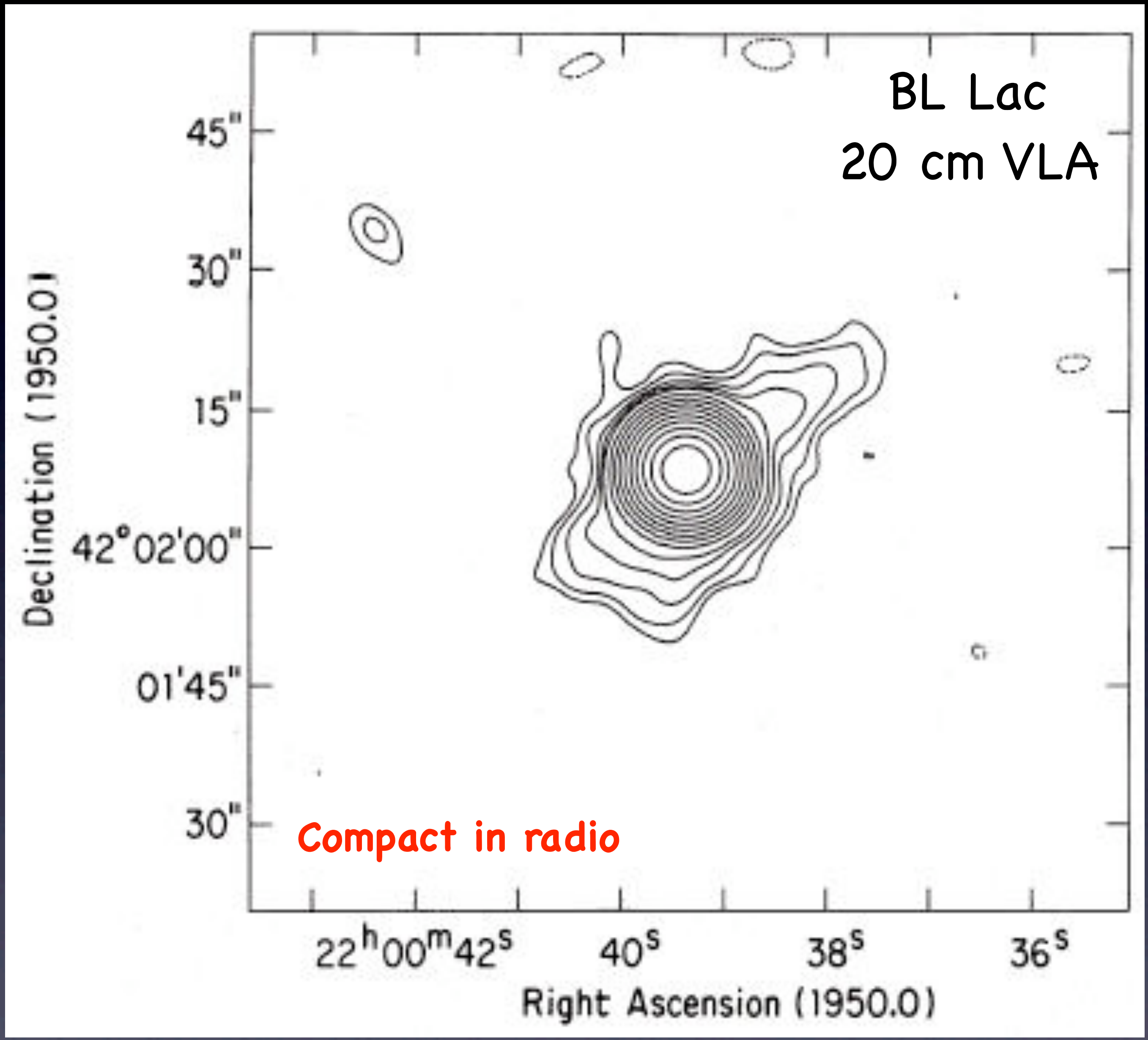

(Antonucci 1986)

FRIIs are considered the PARENT POPULATION of Flat Spectrum Radio Quasars (Urry & Padovani 1995)

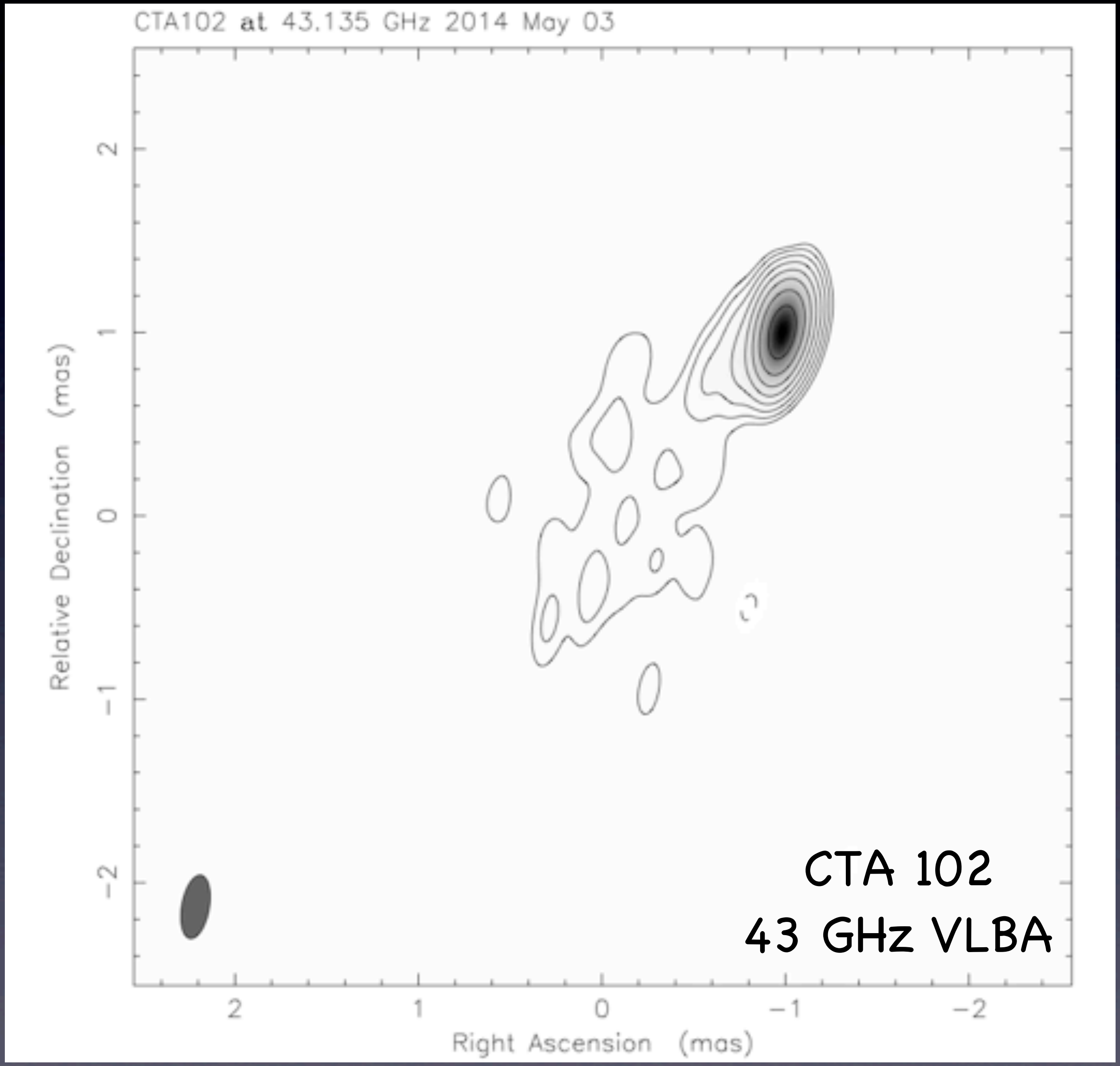

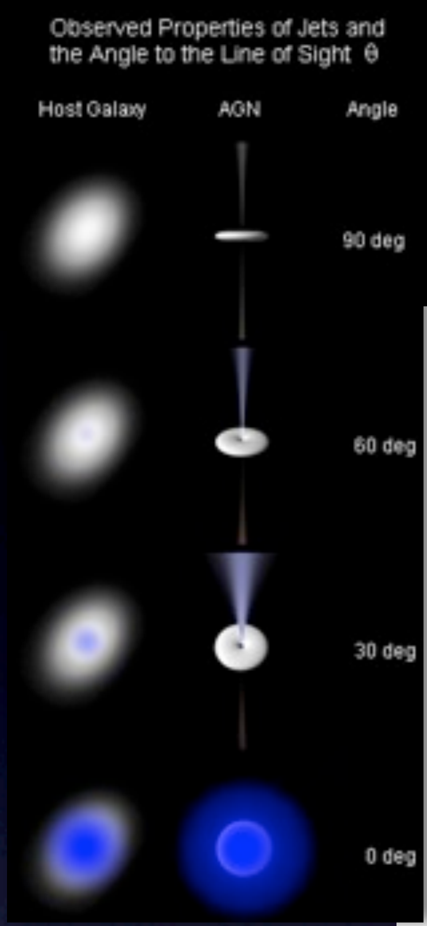
Observed Properties of Jets and
the Angle to the Line of Sight θ
Host Galaxy
AGN
Angle
90 deg
60 deg
30 deg
0 deg

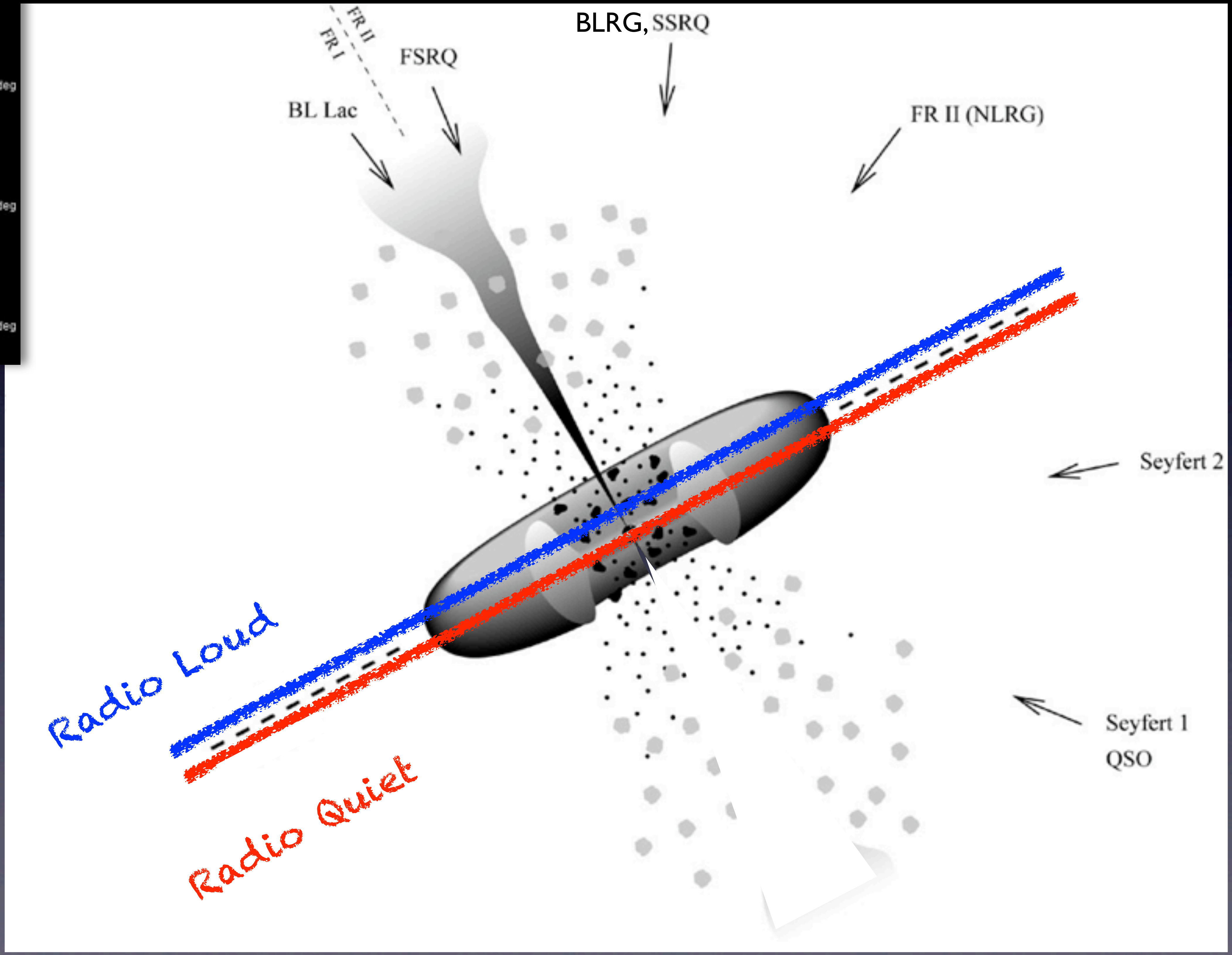
FR II
FR I
BLRG, SSRQ
FSRQ
BL Lac
FR II (NLRG)
Seyfert 2
Seyfert 1
QSO
Radio Loud
Radio Quiet

2. Spectral Energy Distribution of AGN

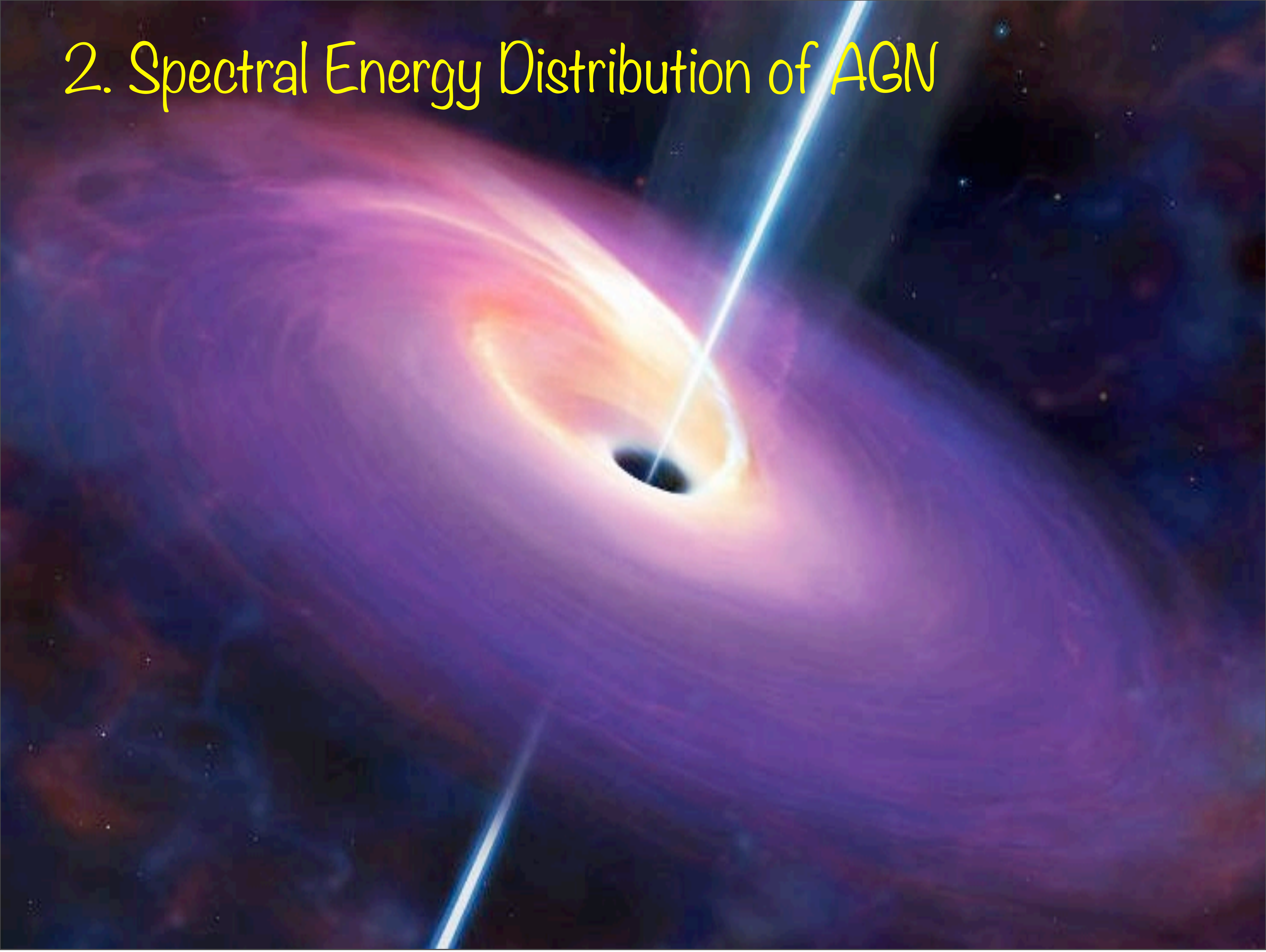

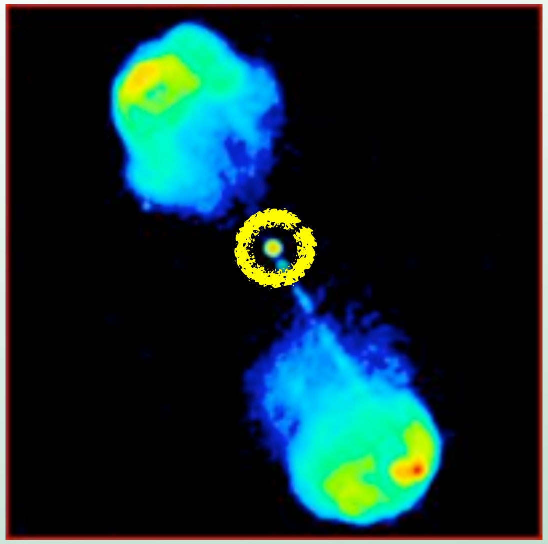

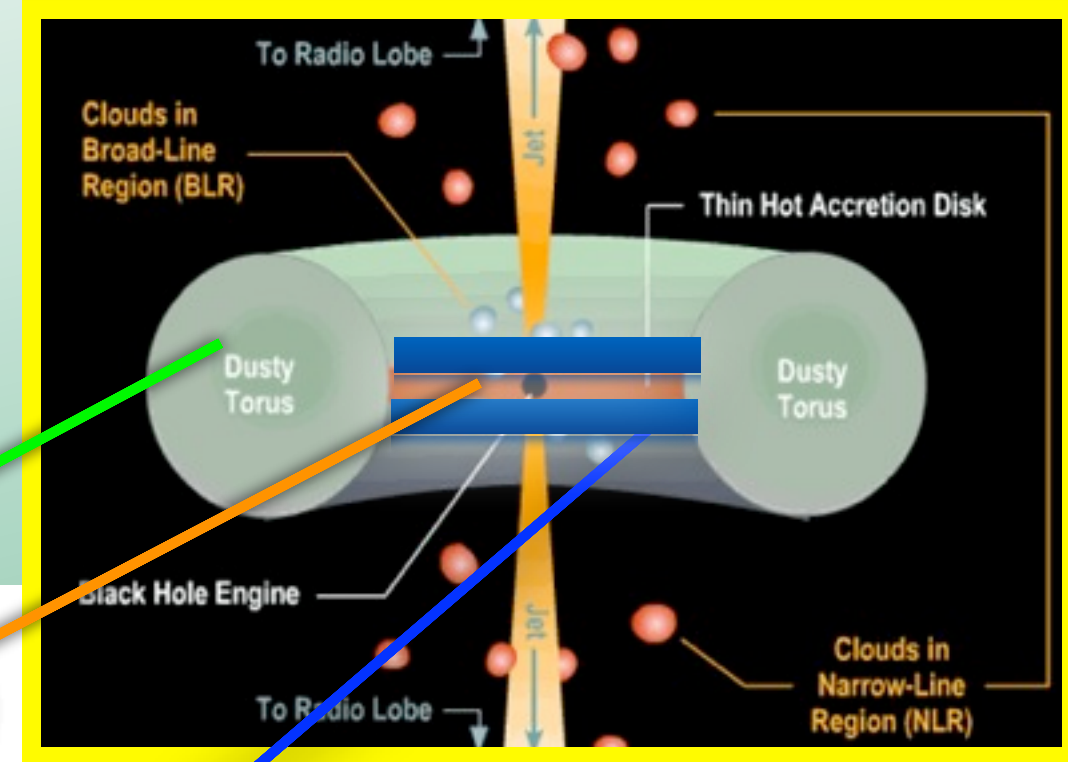

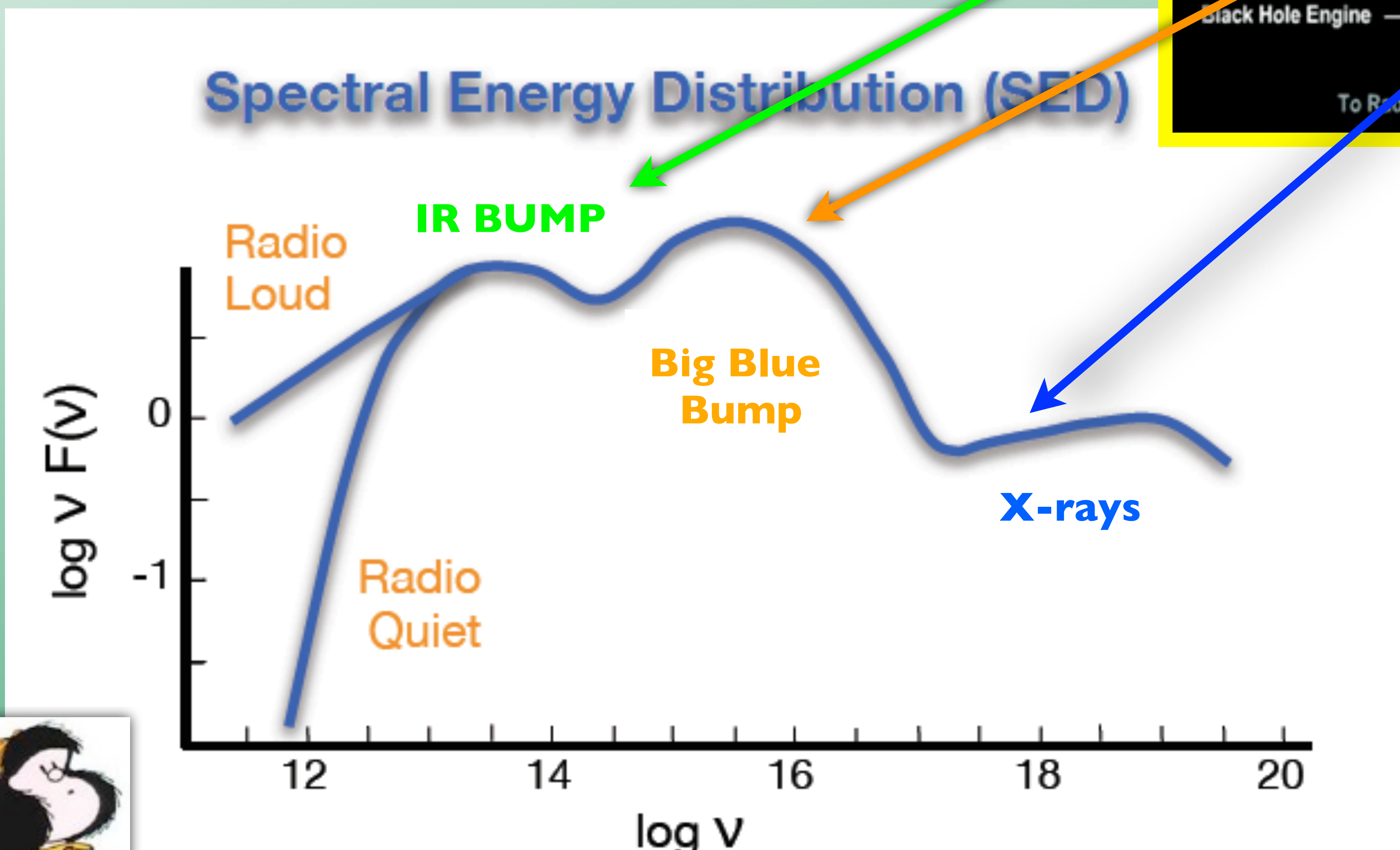

$F_X \sim 10^{-12}$ erg cm^{-2} s^{-1}
(X-ray source e.g. radio galaxy nucleus)

Radio Galaxies: kpc components

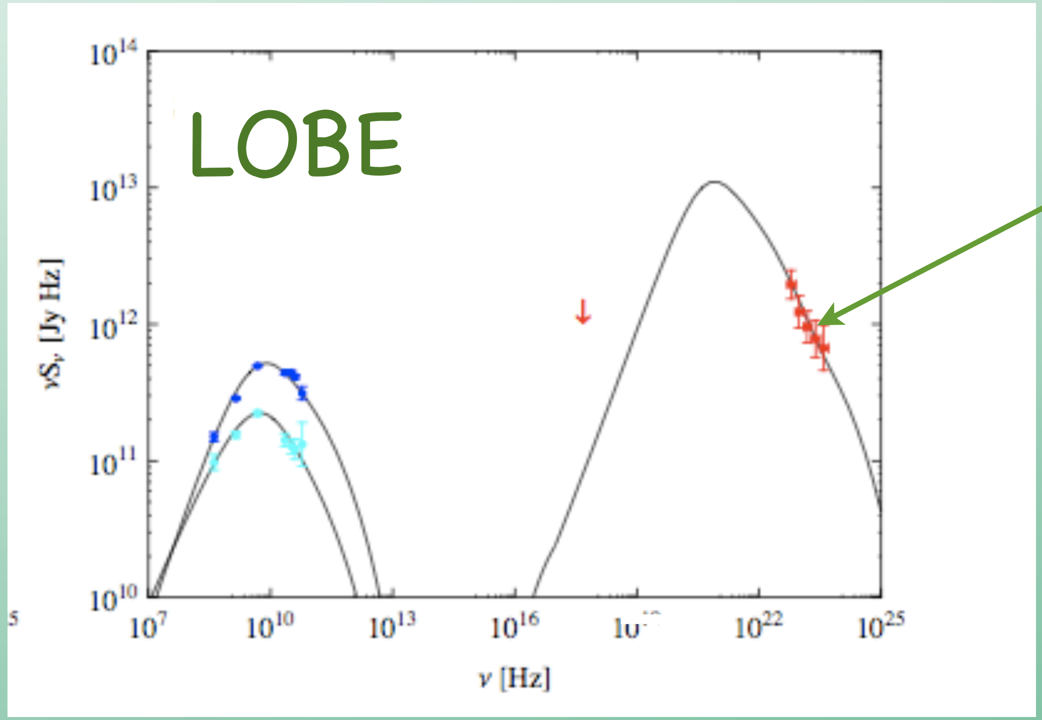

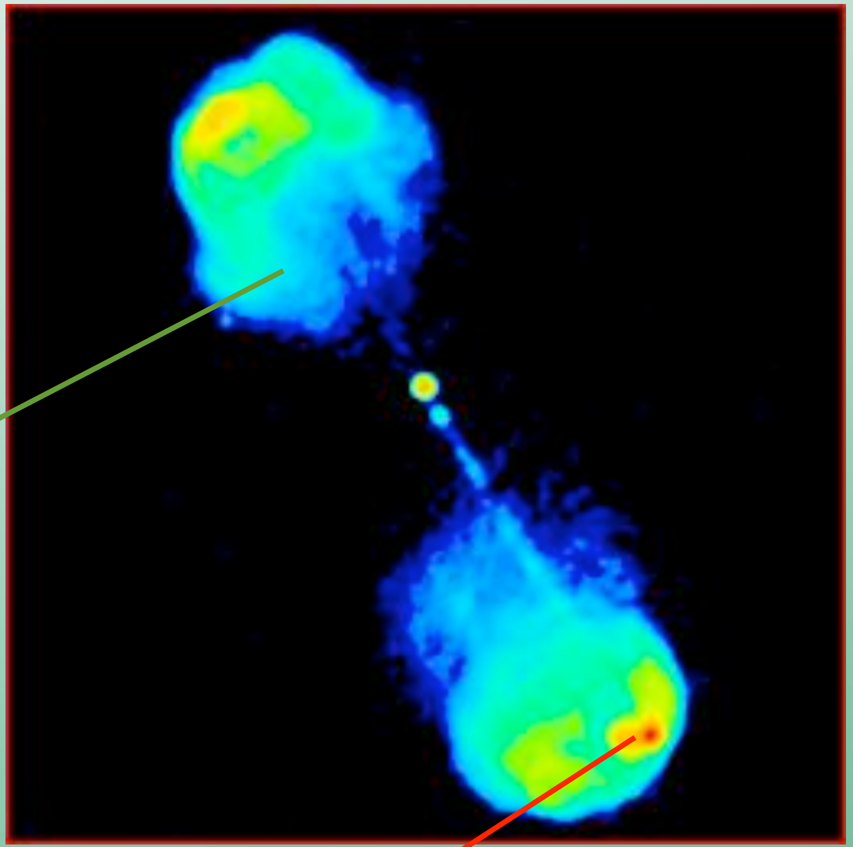

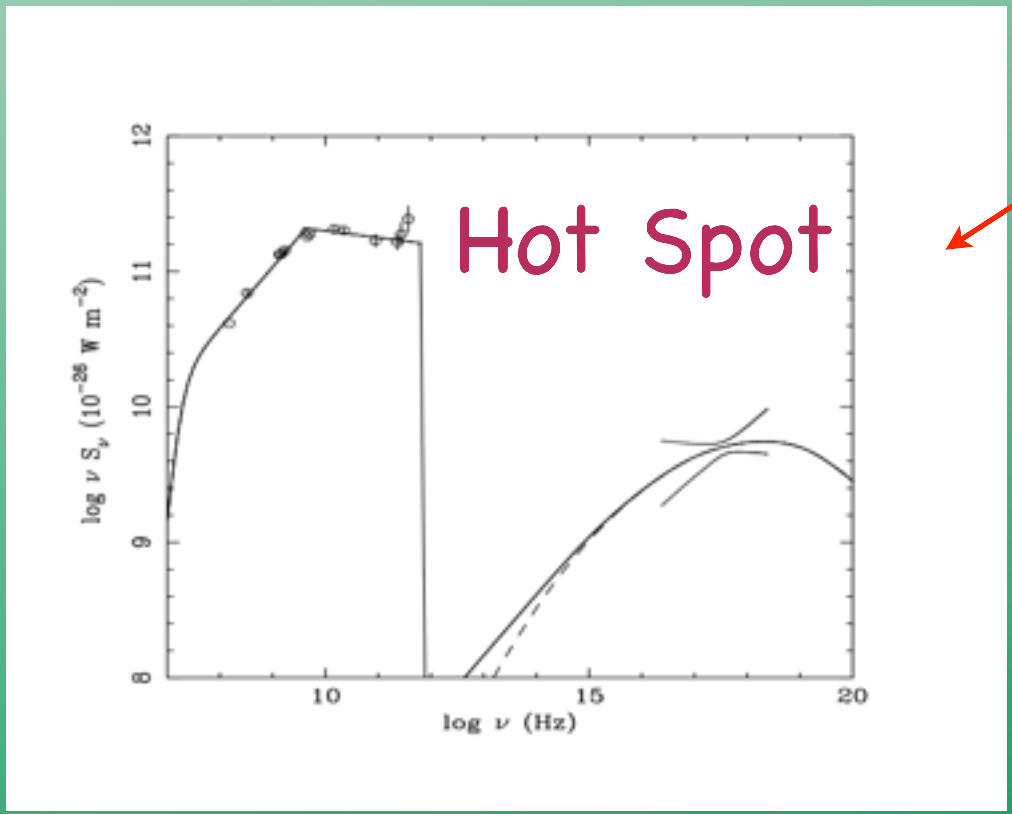

F_X~10^{-14} erg cm^{-2} s^{-1}
(X-ray source e.g. radio lobes or hot-spots)

BLAZARS

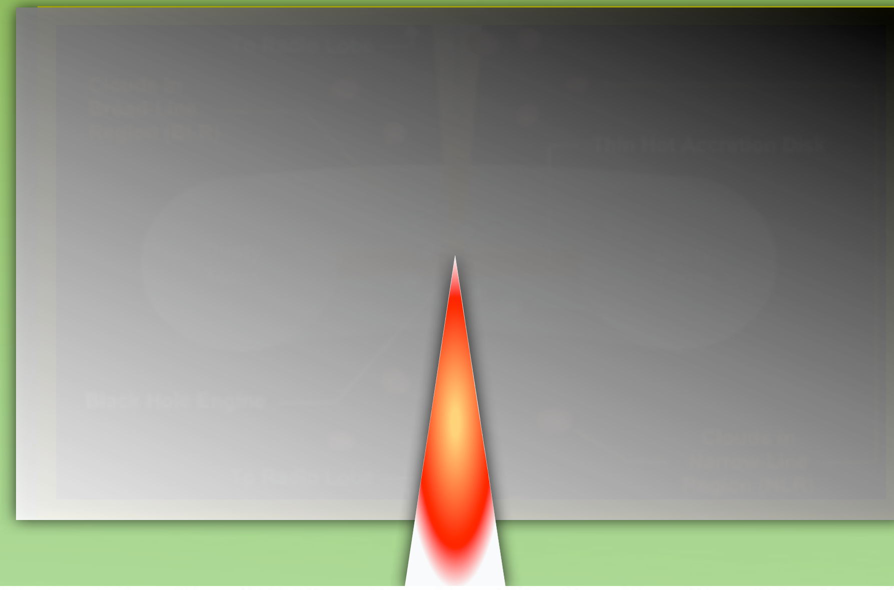

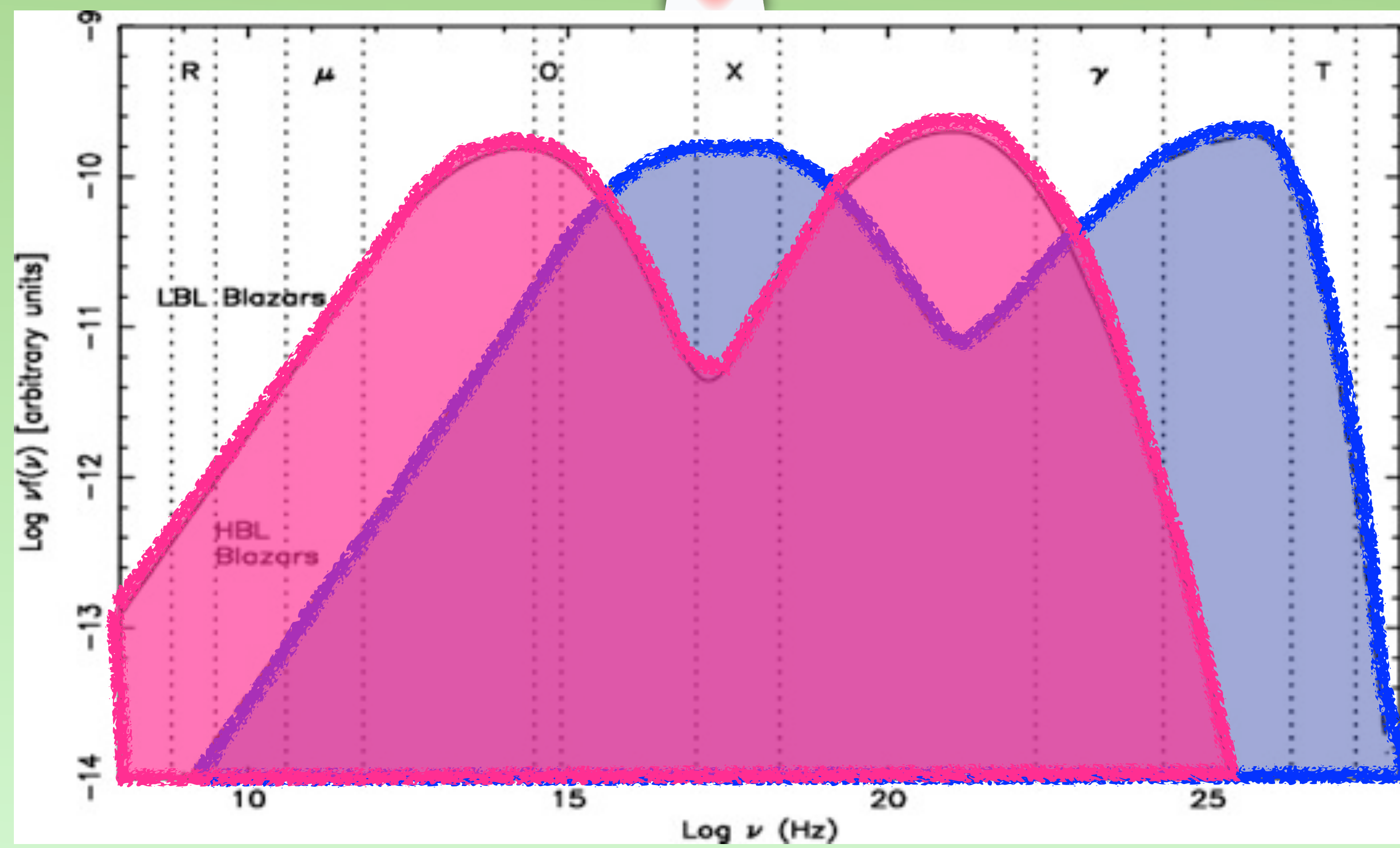
R
μ
O
X
γ
T
LBL Blazars
HBL Blazars
Log νf(ν) [arbitrary units]
−9
−10
−11
−12
−13
−14
10
15
20
25
Log ν (Hz)

The jet emission from blazars is strongly Doppler boosted with respect to radio galaxies

The jet emission from blazars is strongly Doppler boosted with respect to radio galaxies

The key parameter is the **Doppler Factor** $\delta(\beta, \theta)$

$$\delta = [\gamma(1-\beta cos\theta)]^{-1}$$

γ $=1/\sqrt{(1-\beta^2)}$ Lorentz factor

β =v/c bulk velocity

θ angle between the jet axis and the line of sight

The Doppler factor relates intrinsic and observed flux for a moving source at relativistic speed $v=\beta c$.

For an **intrinsic** power law spectrum: $F'(\nu') = K (\nu')^{-\alpha}$ the **observed** flux density is

$$F_\nu(\nu) = \delta^{3+\alpha} F'_{\nu'}(\nu)$$

$$\Delta t = \Delta t' / \delta$$

The jet emission from blazars is strongly Doppler boosted with respect to radio galaxies

The key parameter is the Doppler Factor $\delta(\beta, \theta)$

$$\delta = [\gamma(1-\beta cos\theta)]^{-1}$$

$=1/\sqrt{(1-\beta^2)}$

Lorentz factor

=v/c

bulk velo

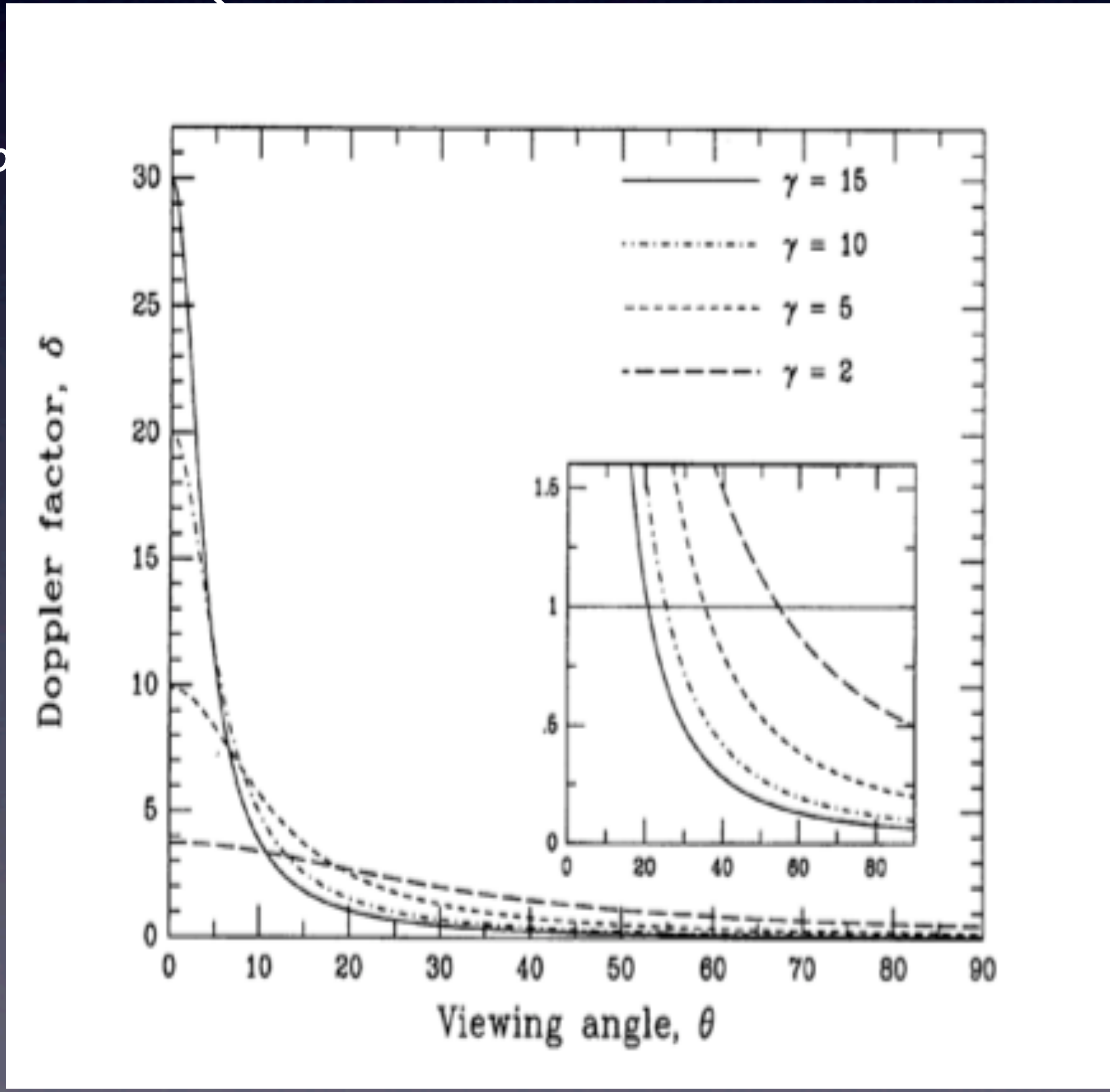

The Doppler factor relates intrinsic and observed flux for a moving source at relativistic speed v=β c.

For an **intrinsic** power law spectrum: $F'(\nu') = K (\nu')^{-a}$
the **observed** flux density is

$$F_\nu(\nu) = \delta^{3+\alpha} F'_{\nu'}(\nu)$$

$$\Delta t = \Delta t'/\delta$$

3. The FRI/FRII dichotomy

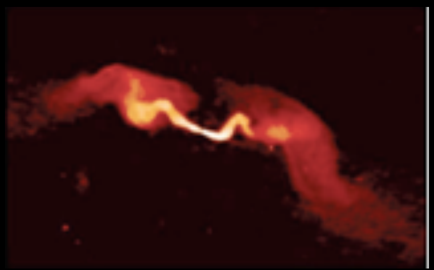

It is still unclear what causes the FRI/FRII dichotomy

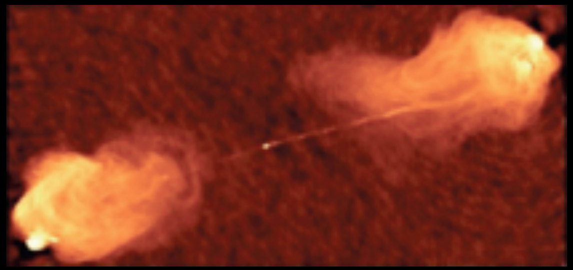

1) Ledlow & Owen (1994) found a correlation between the radio power at the FRI/FRII transition and the host galaxy magnitude

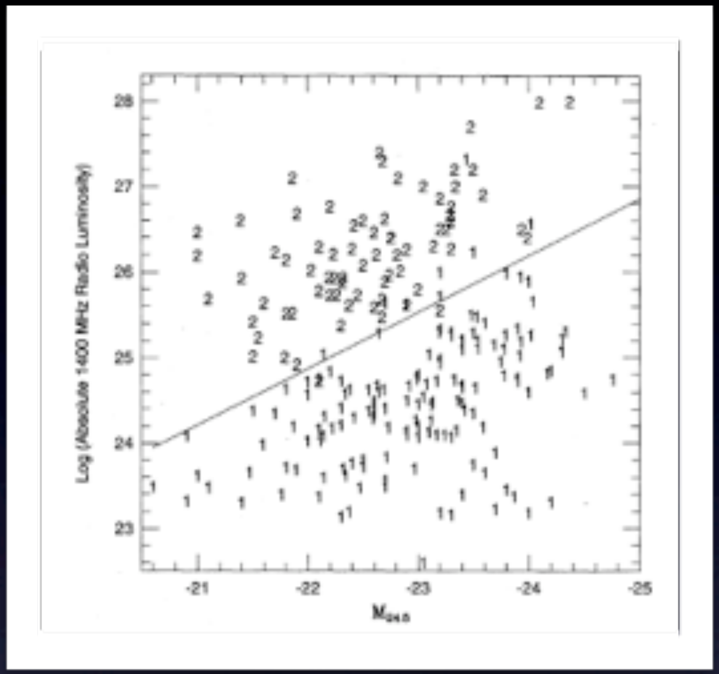

2) Bicknell 1995 points to different ways in which the jet interacts with the ambient medium: the FRI jets start highly relativistic and decelerate between the sub-pc and kpc scales

3) Baum et al. (1995) and Reynolds et al. (1996) suggest different nuclear intrinsic properties of the accretion and jet formation and the jet content

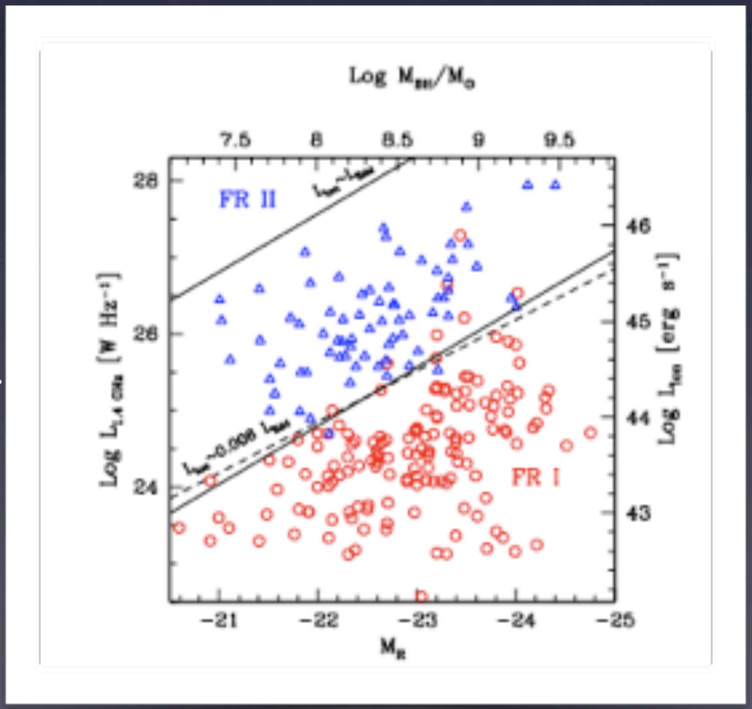

4) Ghisellini & Celotti (2001) indicate that the **accretion process** itself might play a key role in the deceleration and dichotomic behavior by affecting the pc-kpc scale environment

Optical observations seem to indicate that FRIs and FRIIs have different accretion regimes

The optical flux of FRIs shows a strong correlation with the radio core one over four decades, arguing for a non-thermal synchrotron origin of the nuclear emission
(Chiaberge et al. 2002)

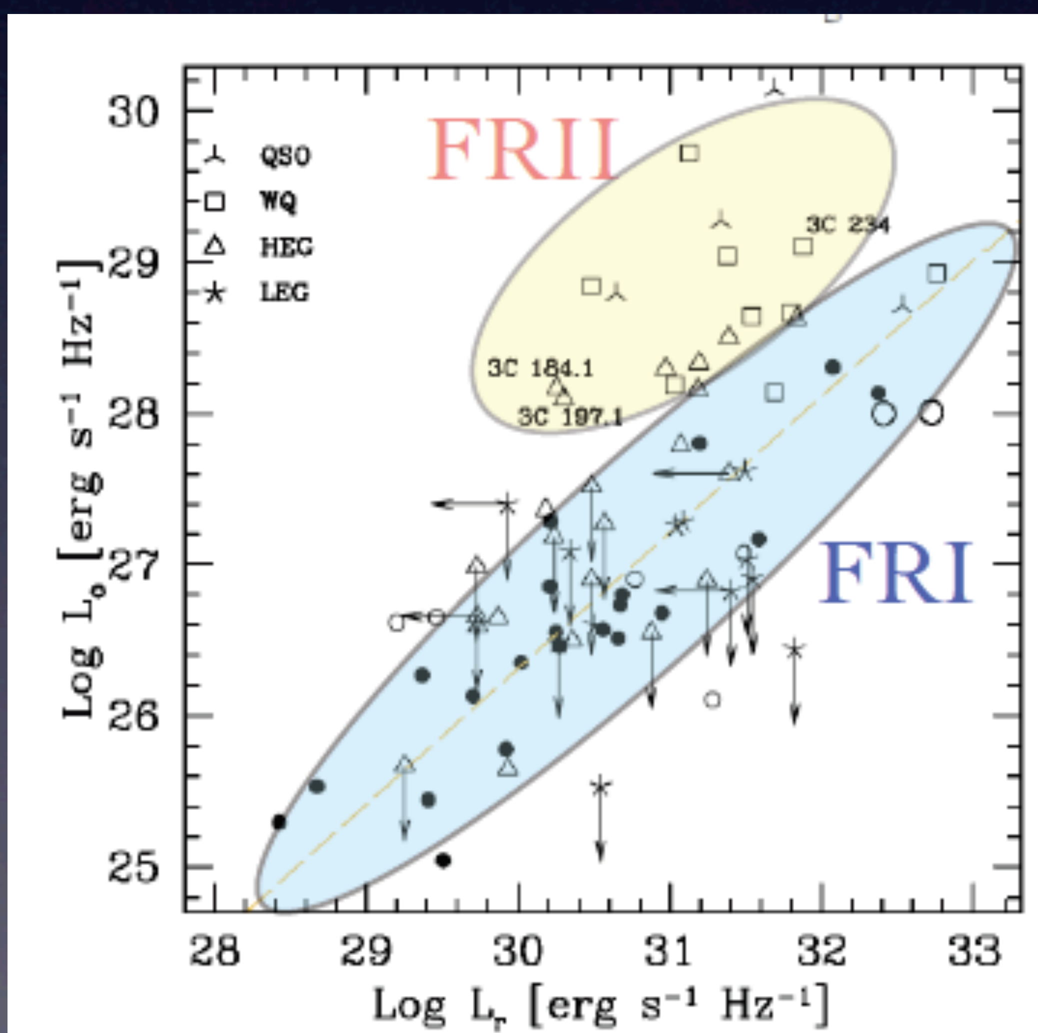

There is no nuclear absorption in FRI HST images. The weakness of the optical lines is not due to obscuration
(Chiaberge et al. 2002)

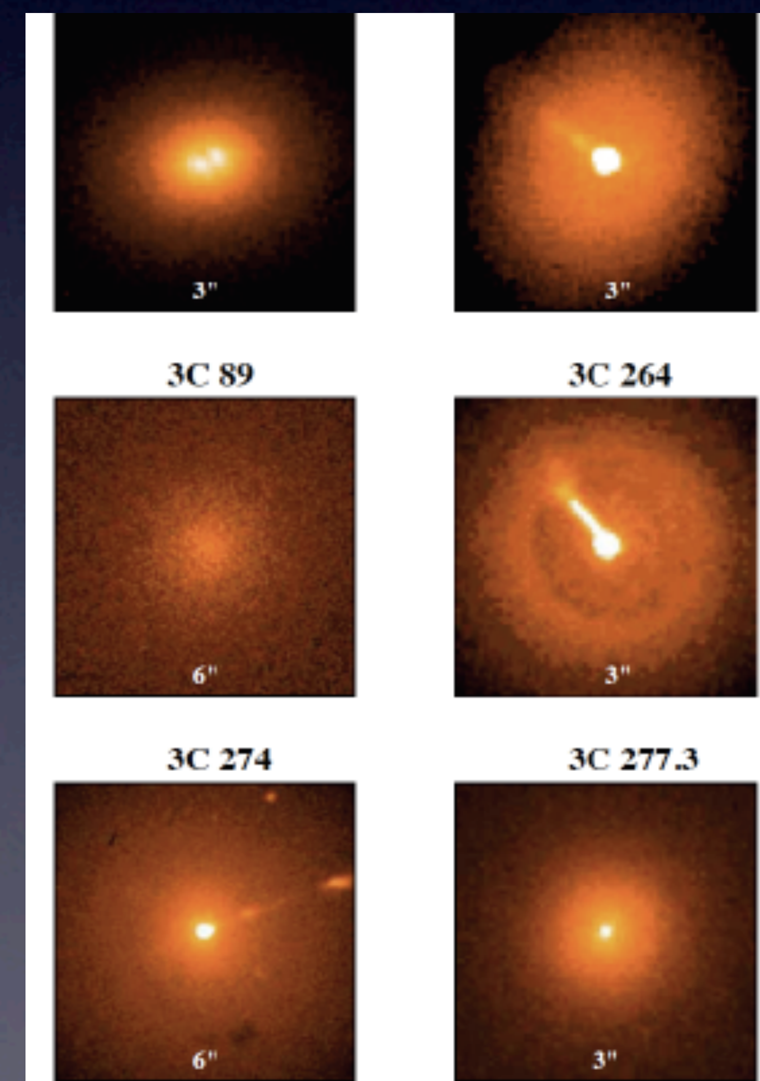

The accretion rate distribution is bimodal:
Low accretion rate => FRI
High accretion rate => FRII +Quasar

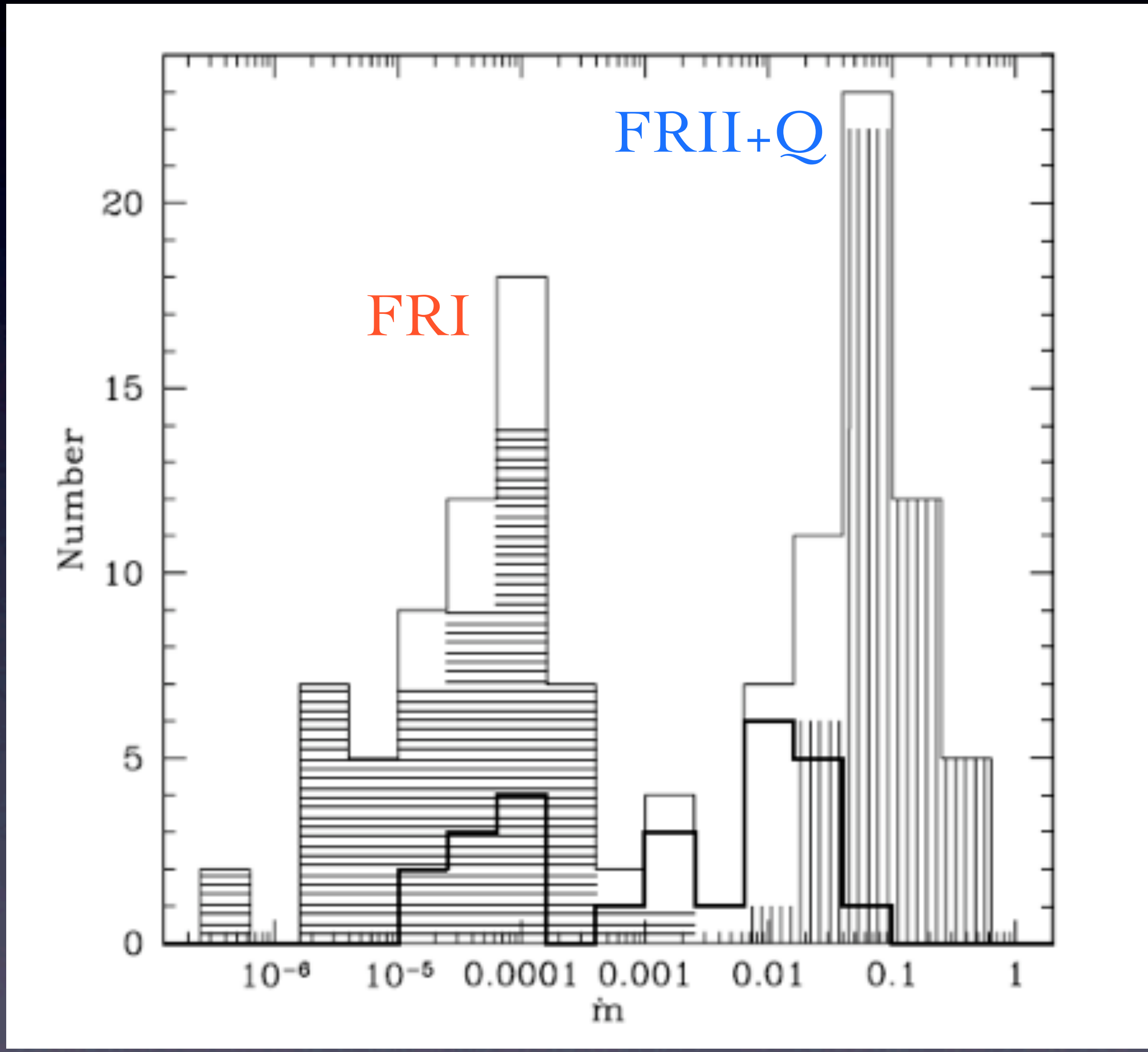

Marchesini et al. 2004

$\dot{m} = \dot{M} / \dot{M}_{Edd}$, mass accretion rate in Eddington units

4. The X-ray spectra of radio galaxies

X-rays

BLRGs →

different spectral behavior with respect Seyfert 1s (Grandi + 2006):

➡ weaker Compton reflection

➡ weaker FeKa line

➡ no clear evidence of ionized absorbing gas

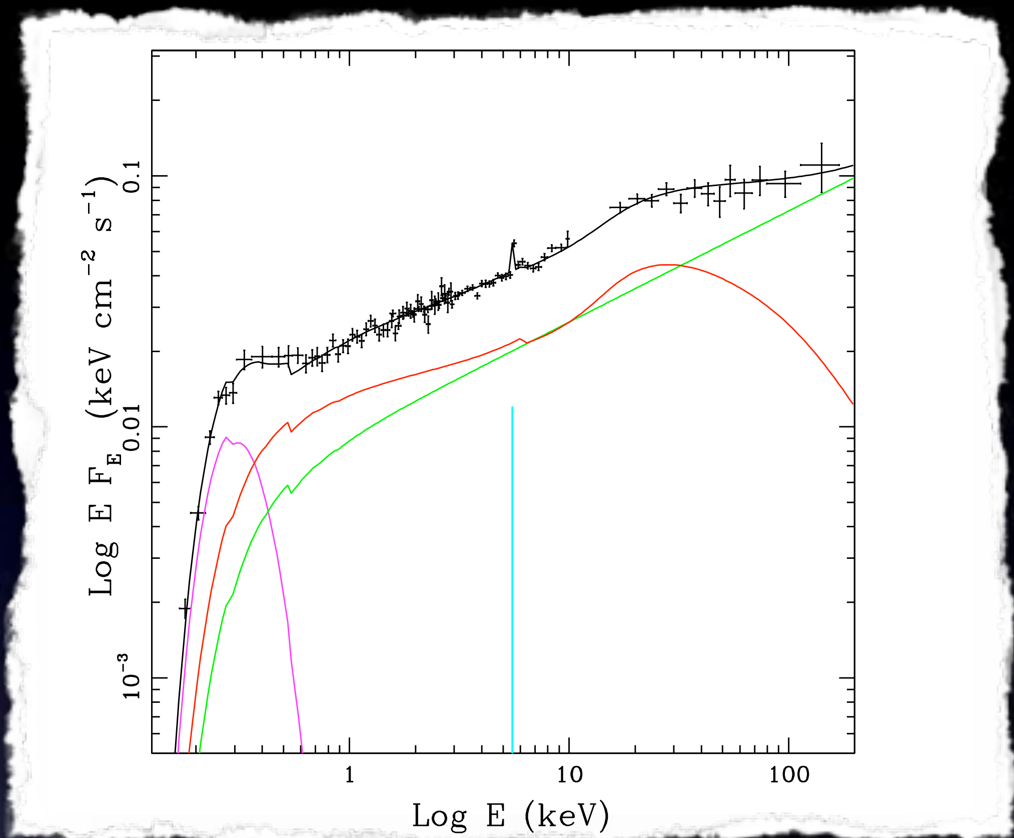

NLRGs →

➡ obscured but strong continuum related to an accretion flow

➡ dusty torus

➡ soft excess

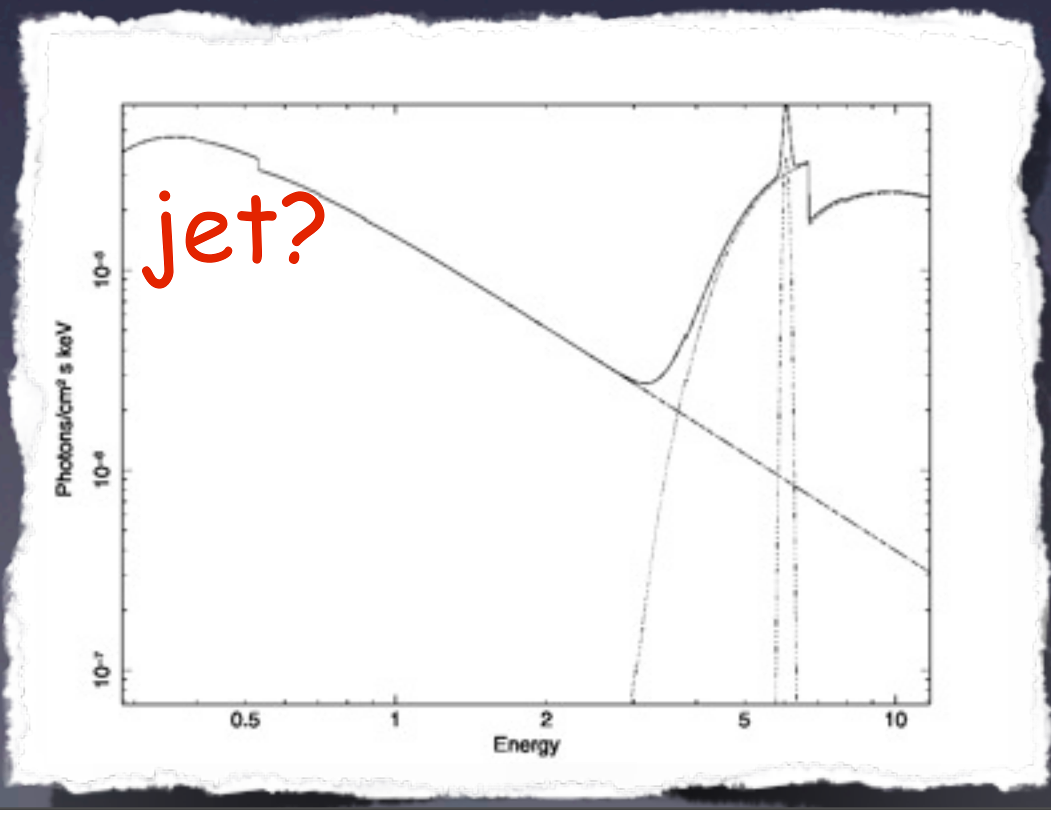

In FRII BLRGs and NLRG/HEGs, X-ray spectra show reprocessing features typical of cold matter surrounding an efficient accretion disk

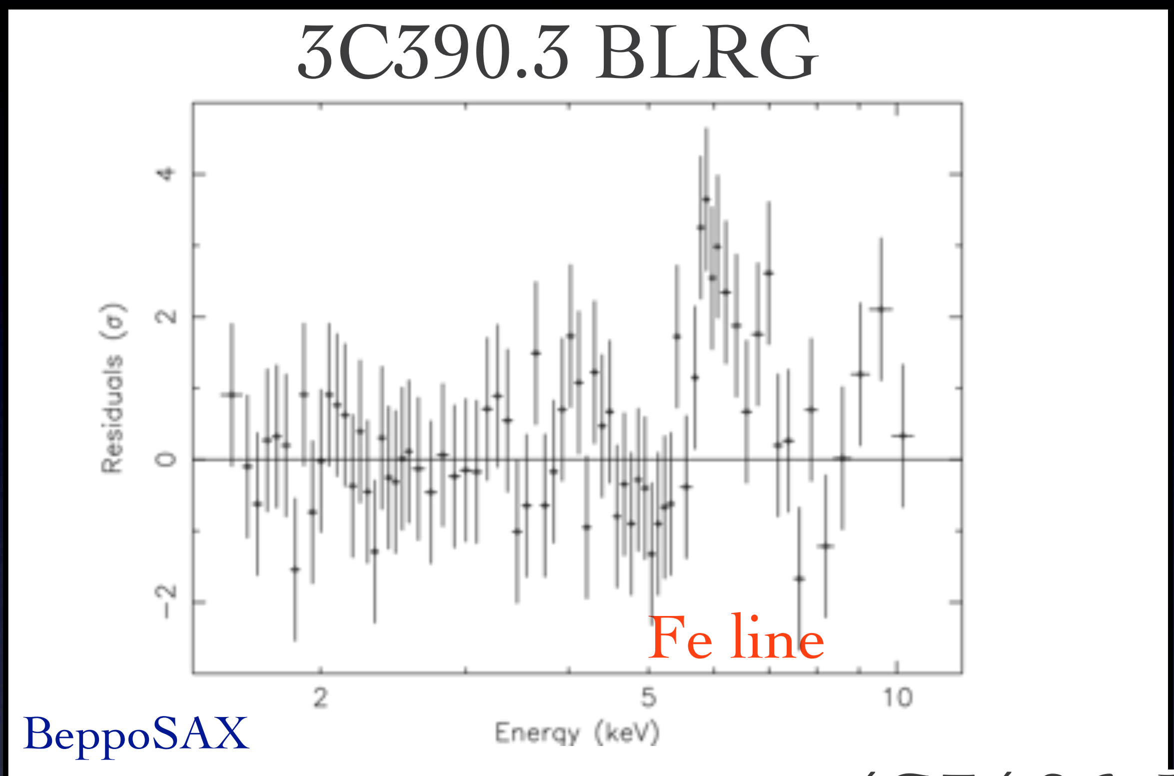

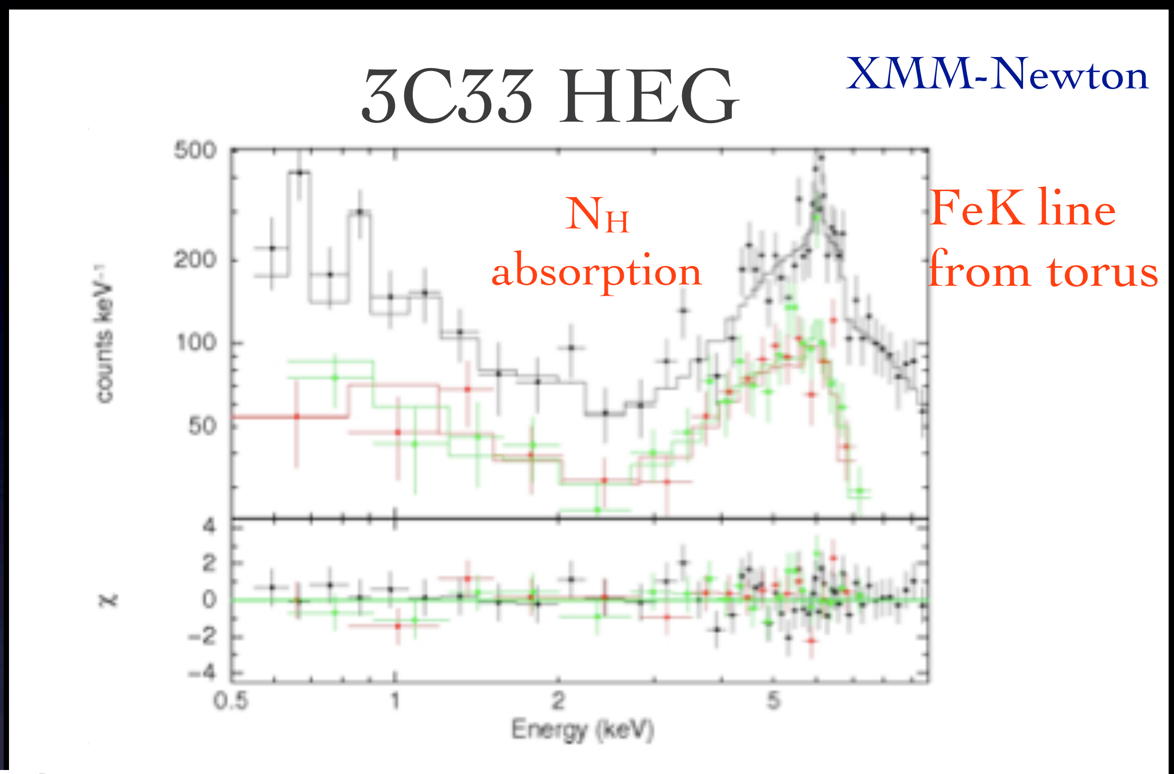

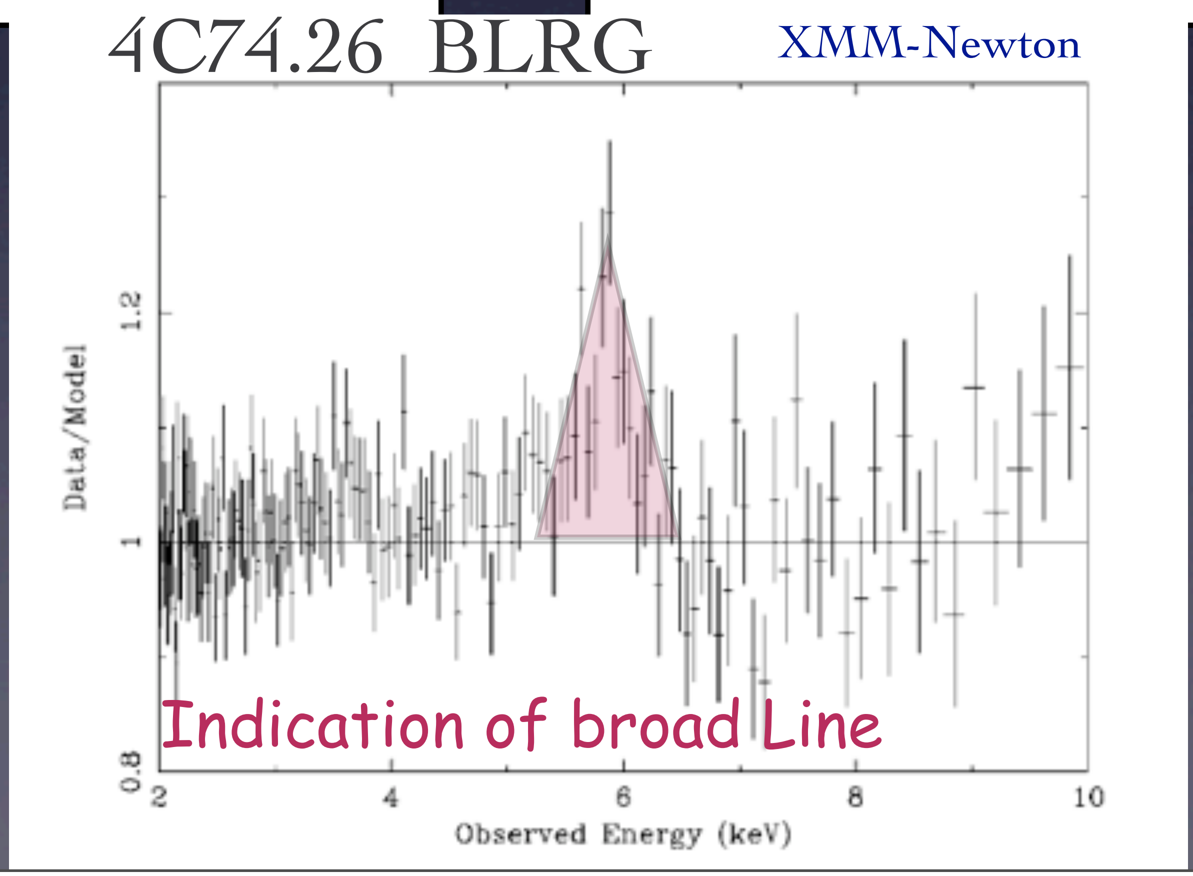

5. Radiative processes

Thermal emission

Accretion flow

Thermal Comptonization

Reprocessed features

Non-thermal emission

Synchrotron

Inverse Compton

Accretion

THERMAL PROCESS

Disks usually rotate such that each fluid element is moving almost in a circular orbit. As the angular velocity is a function of radius, there is a shearing flow. This means that coupling between adjacent radii exerts a force. Given that the outer parts rotate more slowly, inner try to speed up outer, giving it a higher velocity. This increases the angular momentum of the outer, decreases the angular momentum of the inner, so net result is that angular momentum is transferred outwards and mass flows inwards.

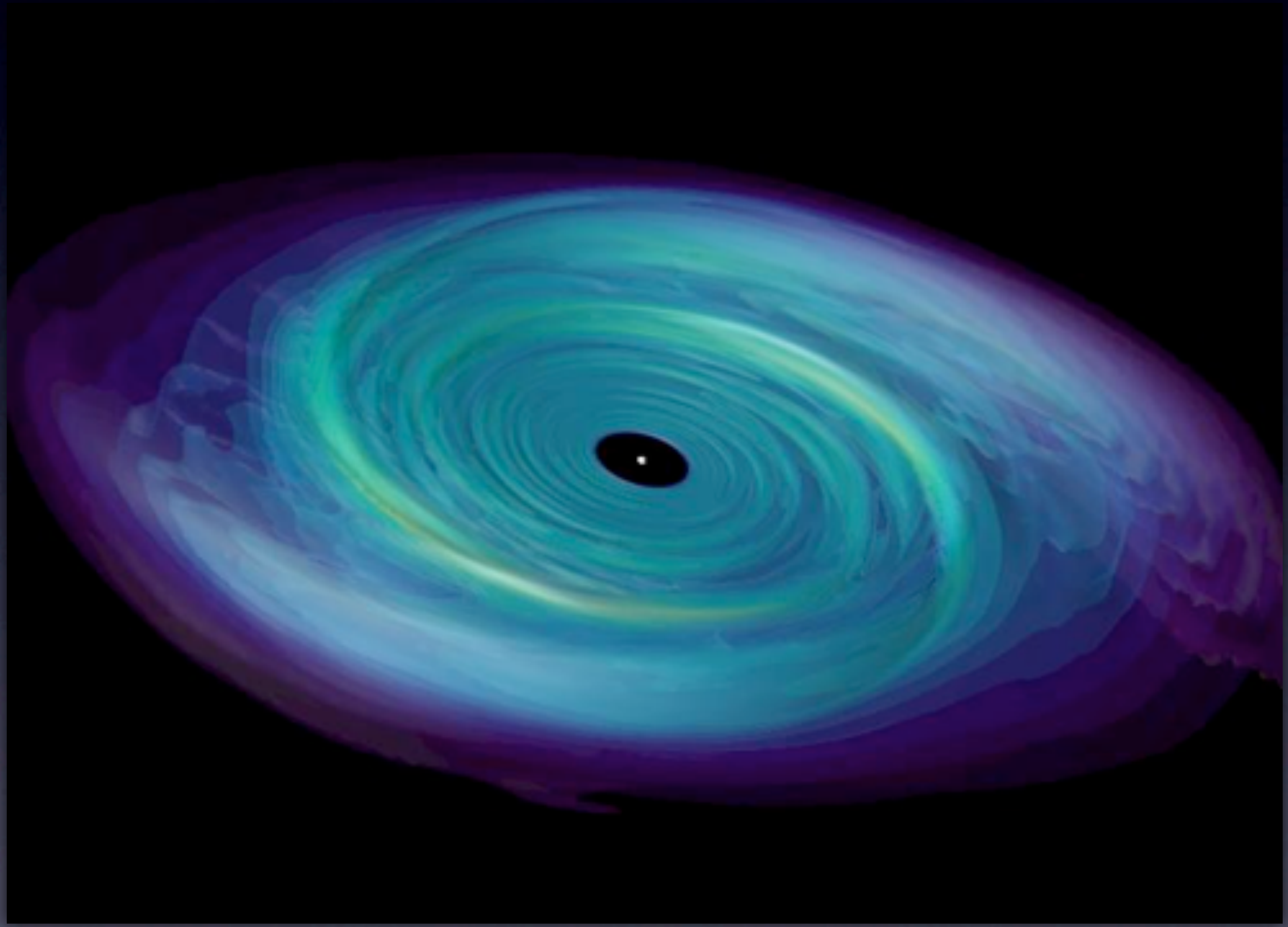

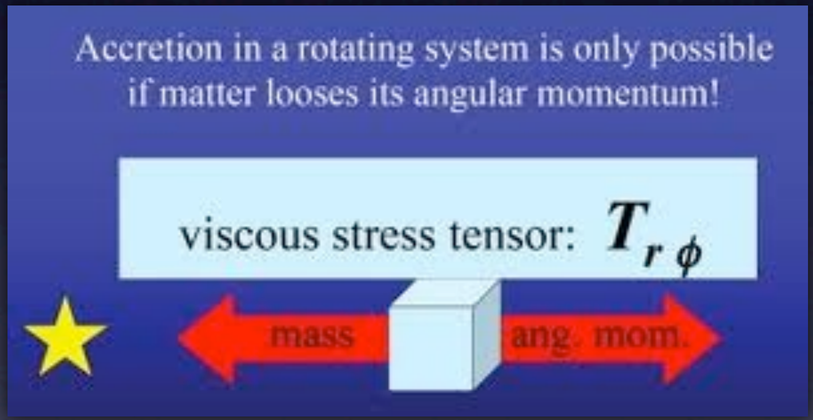

Viscosity transports angular momentum outward, allowing the accretion gas to spiral in toward the BH. Viscosity acts as a source of heat that is radiated away.

Accretion is the physical process by which black hole aggregates matter from their surroundings. The gravitational energies that such matter must release for accretion to occur is a powerful source of luminosity L.

$$L_{rad} = \eta \dot{M} c^2$$

The EFFICIENCY of the process is η

with $\eta \propto M/R$ (compactness of the system)

and $\dot{M}$ accretion rate in $M_{\odot} yr^{-1}$

In case of a black hole the size is defined in terms of the Schwarzschild radius

$$R_s = \frac{GM}{c^2} \sim 3 \times 10^{13}\ M_8\ \ cm$$

This efficency is maximized in the case of a black hole the size of which can be defined as

$$R_s = \frac{2GM}{c^2}$$

that can be derived by the escape velocity of the light

$$V_{escape} = c = (\frac{2GM}{R})^{1/2}$$

Eddington Luminosity L_E is the luminosity at which the outward force of the radiation pressure is balanced by the inward gravitational force

$$L_E = \frac{4\pi G m_p c}{\sigma_e} M \sim 1.3 \times 10^{38} \; (M/M_\odot) \; (erg \; s^{-1})$$

$$L_{\rm Edd} = \frac{4\pi G M c m_{\rm p}}{\sigma_{\rm T}}$$

from which

$$M = 7 \times 10^8 M_\odot .$$

And from our Eddington accretion rate, using $\epsilon = 0.1$ we have

$$\dot{M}_{\rm Edd} = \frac{4\pi G M m_{\rm p}}{\epsilon c \sigma_{\rm T}} \approx 3 M_\odot {\rm yr}^{-1}$$

$$L_{rad} = \eta \dot{M} c^2$$

Accretion processes around black holes involve rotating gas flow. Therefore the accretion flow structure is determined by solving simultaneously four conservation equations:

1. conservation of vertical momentum
2. conservation of mass
3. conservation of energy
4. conservation of angular momentum

Four solutions are currently known. In these solutions viscosity transports angular momentum outward, allowing the accretion gas to spiral in toward the BH. Viscosity acts a source of heat that is radiated away.

The most famous solutions are:

i) Shakura & Sunyaev thin optically thick disk model (standard model)
ii) Optically thick Advection-Dominated Accretion Flow (ADAF)

Shakura & Sunyaev thin optically thick disk model (standard model)

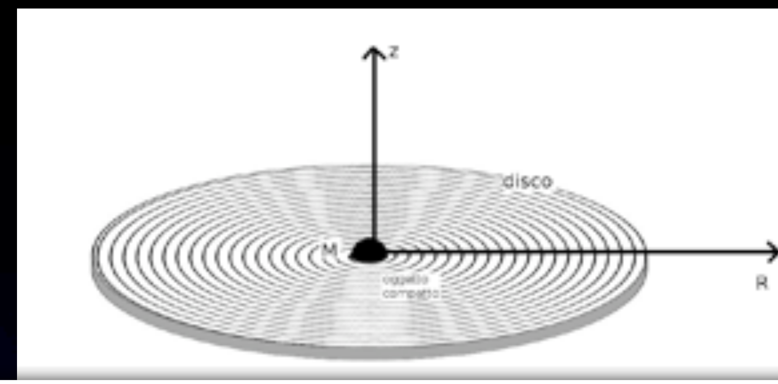

Thin $H/R \ll 1$

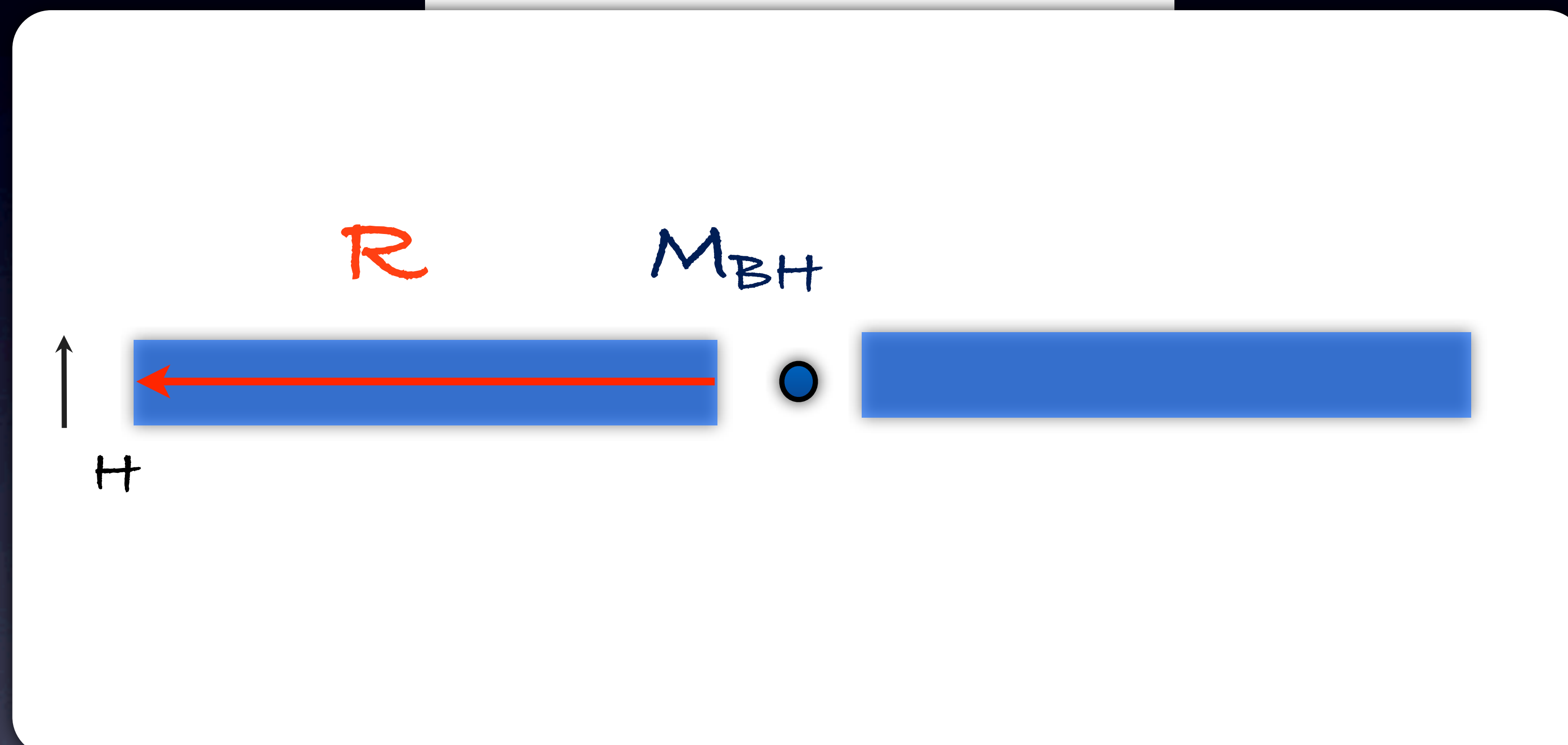

Thick, in the sense that each element of the disk radiates as a black body

If the the disk is optically thick, we can approximate the local emission as blackbody and the effective temperature of the photosphere

$$T(r) \sim 6.3 \times 10^5 (\frac{\dot{M}}{\dot{M}_E})^{1/4} M_8^{-1/4} (\frac{r}{R_s})^{-3/4} \quad K$$

For AGN with $M_{BH} = 10_8 = 10^8 M_\odot$ $\dot{M} \sim \dot{M}_E = \frac{L_E}{\eta c^2}$

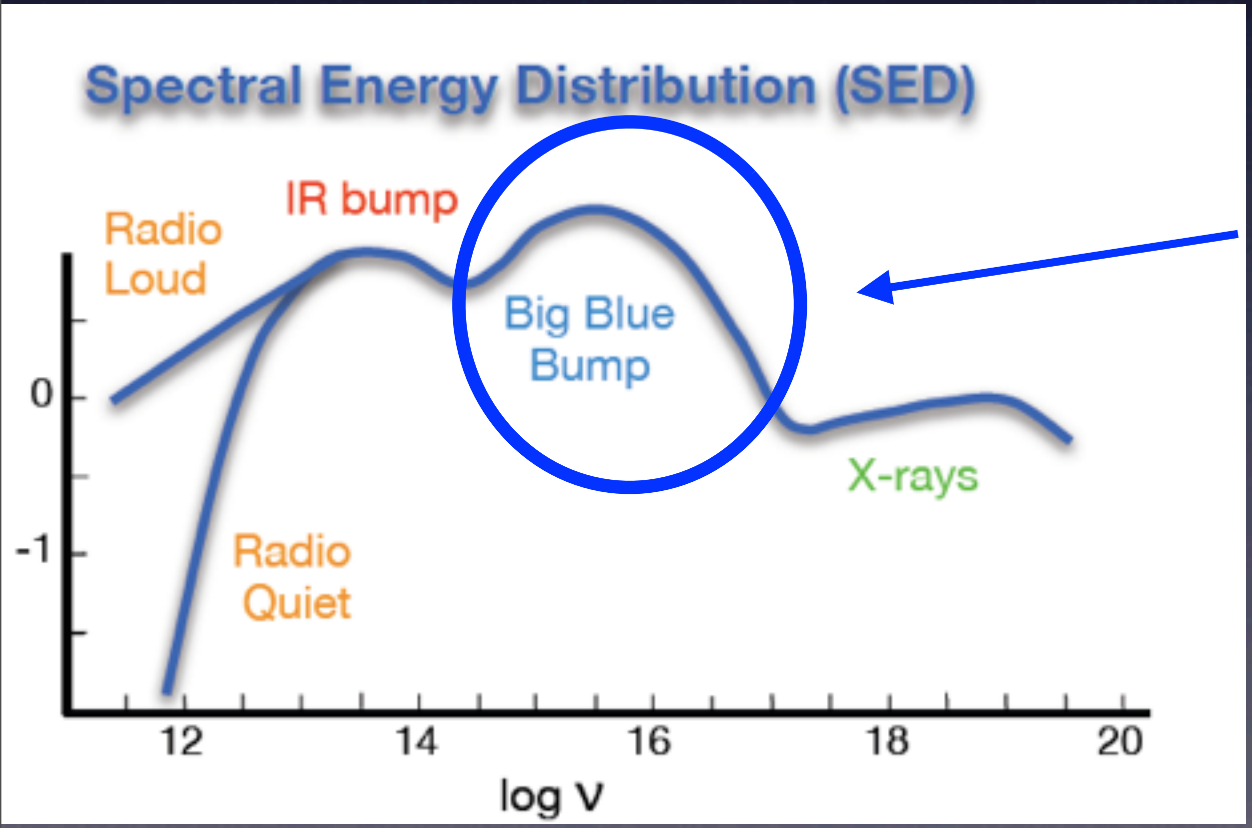

the peak occurs at UV-soft-X-ray region

$$\frac{\partial B}{\partial \nu} = 0 \qquad B(\nu) \propto \nu^3 [e^{\frac{h\nu}{kT}} - 1]^{-1}$$

$$\nu_{max} = 2.8kT/h \sim 10^{16} \quad Hz$$

Corona

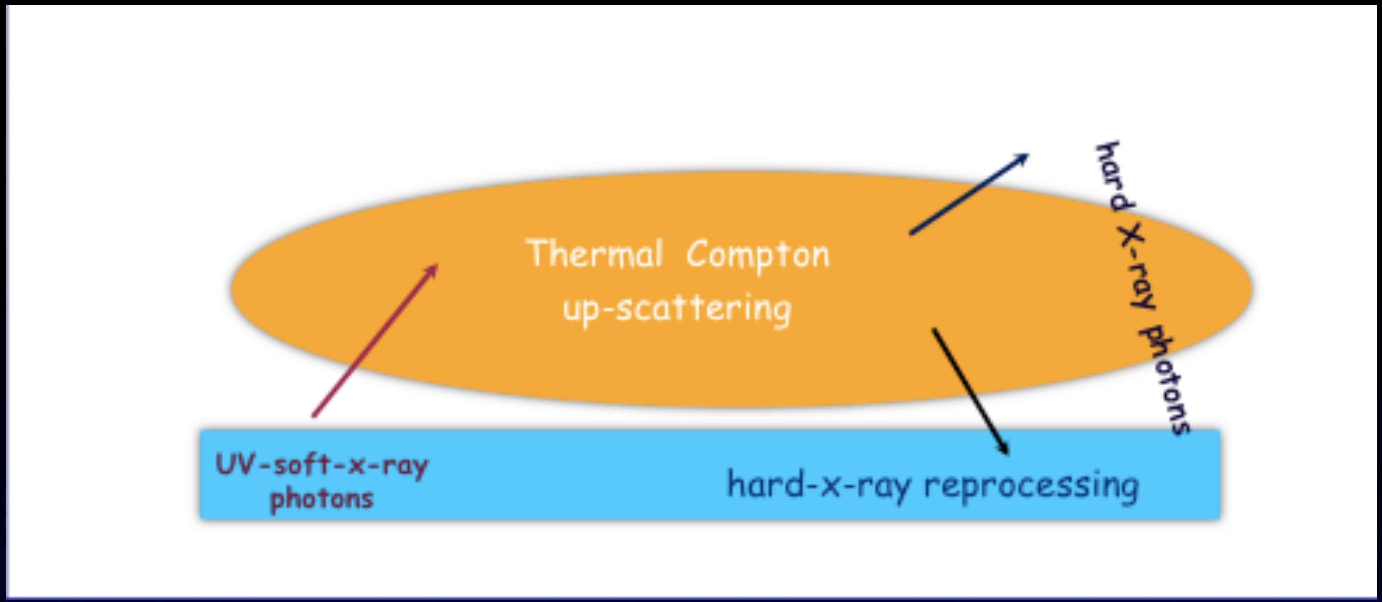

Disk

Thermal Comptonization

With this term we mean the process of multiple scattering of a photon due to a **thermal (Maxwellian)** distribution of electrons.

There is one fundamental parameter measuring the importance of the Inverse Compton process in general, and of multiple scatterings in particular: the Comptonization parameter, usually denoted with the letter **y**.

y = [average # of scatt.] x[average fractional energy gain for scatt.]

Thermal Comptonization

Comptonization on a thermal plasma of electrons characterized by a temp. T and optical depth τ

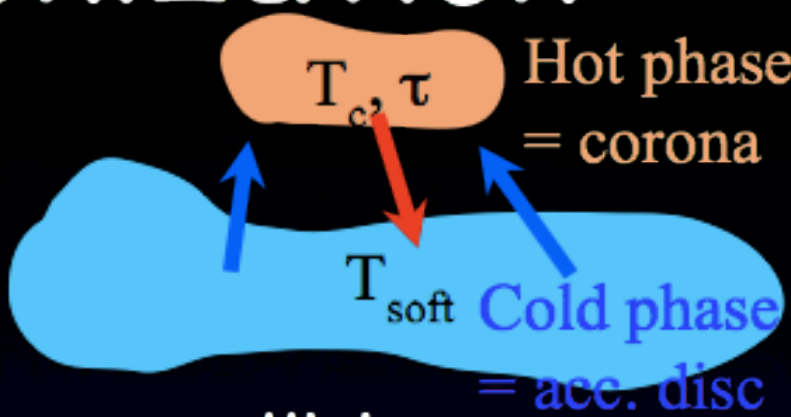

✓ mean relative energy gain per collision

$$\frac{\Delta E}{E} \simeq \left(\frac{4kT}{mc^2}\right) + 16\left(\frac{kT}{mc^2}\right)^2 \quad \text{for } E \ll kT$$

$$\leq \quad 0 \quad \text{for } E \gtrsim kT$$

✓ mean number of scatterings

$$N \simeq (\tau + \tau^2)$$

➡ Compton parameter $y = \frac{\Delta E}{E} N$

$E_f = E_i \, e^y$

Thermal Comptonization Spectrum: the continuum

$$F_E \propto E^{-\Gamma(kT,\tau)} \exp\left(-\frac{E}{E_c(kT,\tau)}\right)$$

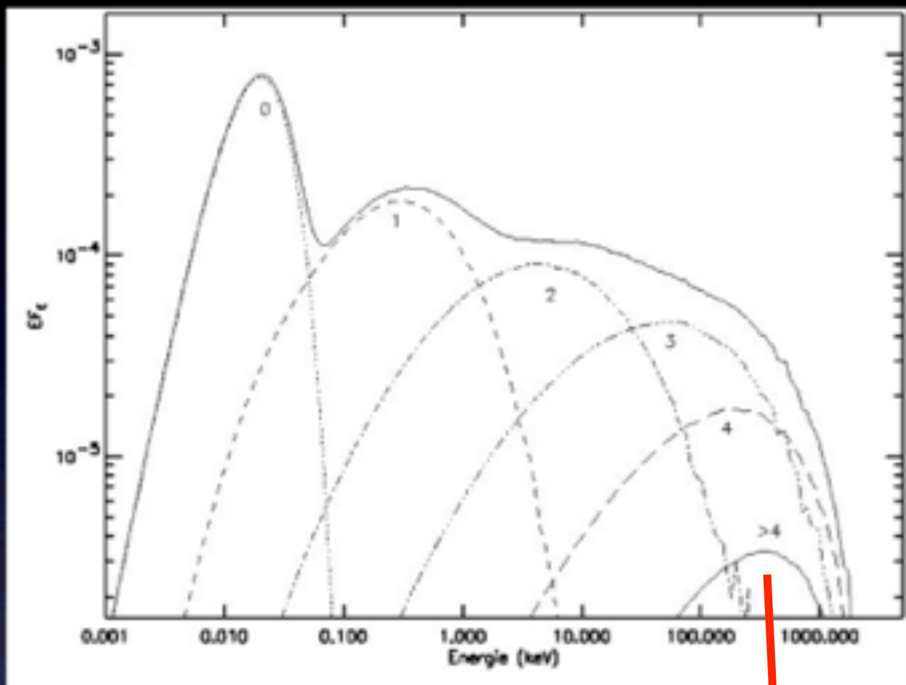

$$\Gamma(\tau, kT)$$

The exact relation between spectral index and optical depth depends on the geometry of the scattering region.

$$E_c \simeq kT$$

As photons approach the electron thermal energy, they no longer gain energy from scattering, and a sharp rollover is expected in the spectrum.
The observed high energy spectral cutoff yields information about the temperature of the underlying electron distribution.

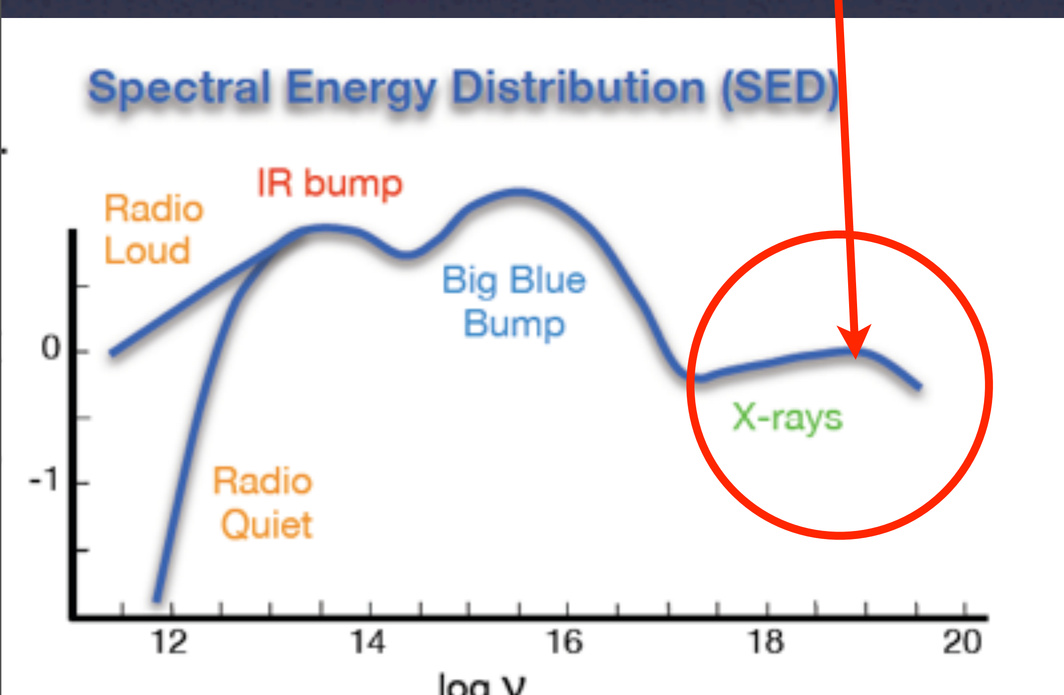

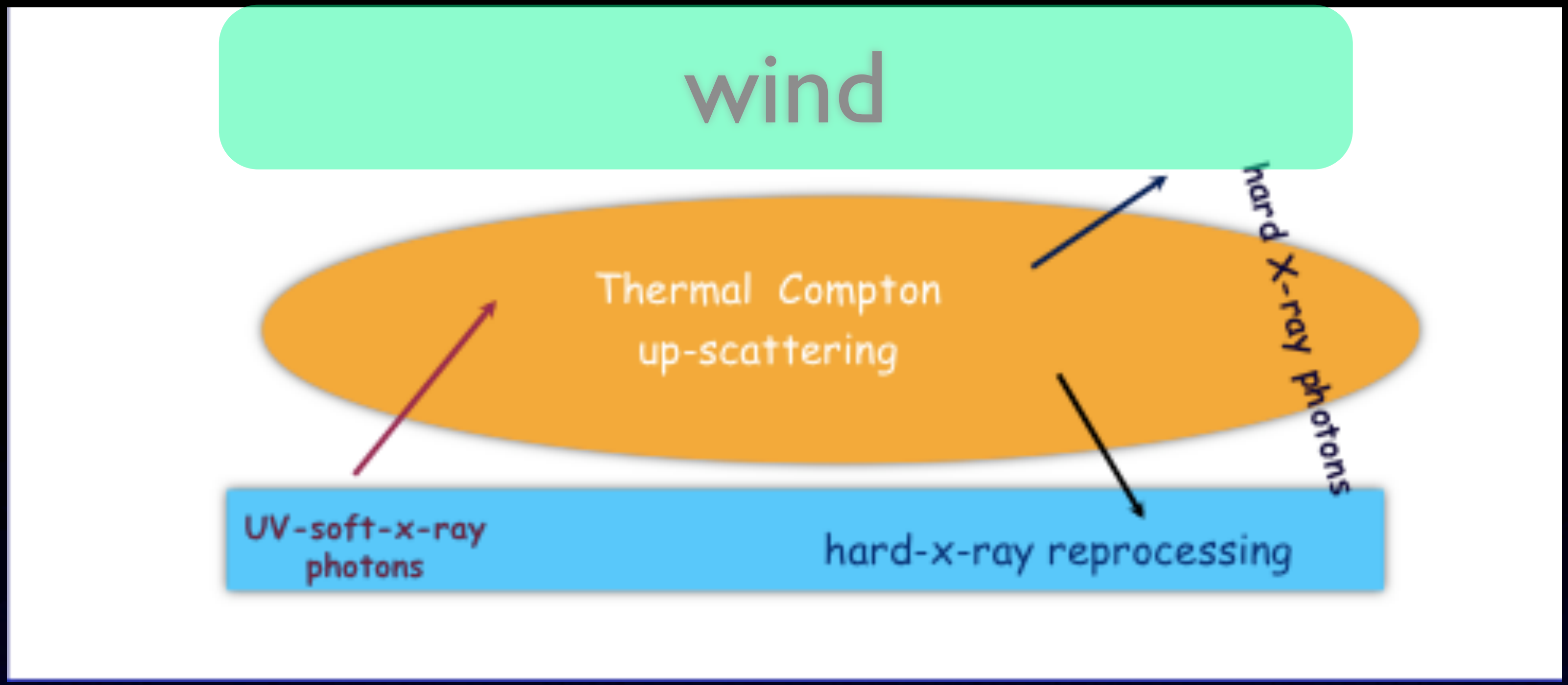

- Thermal Comptonization
- Hard X-ray reprocessing

Iron line

Compton hump

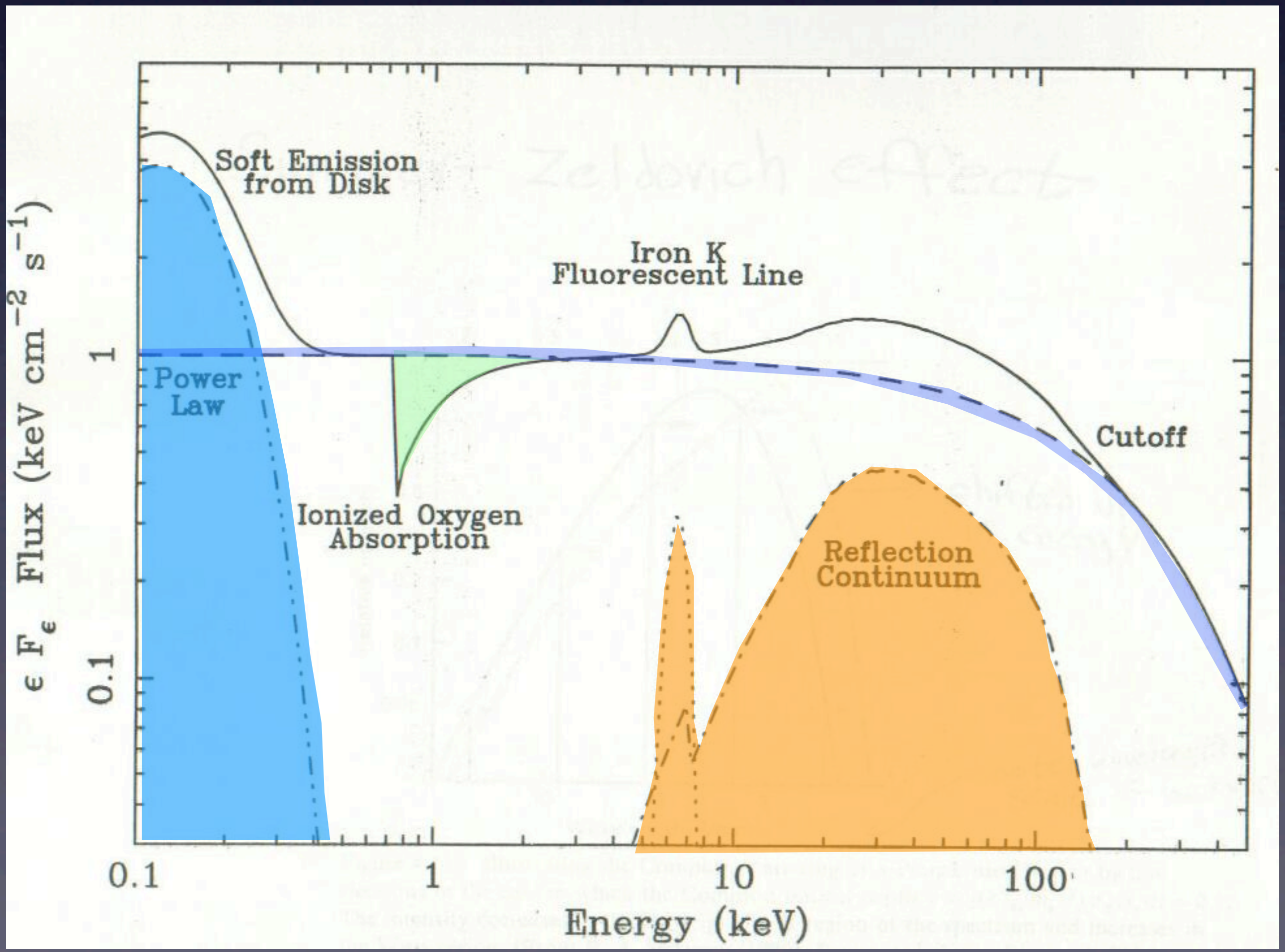

Reflection

At low energies <10 keV the high-Z ions absorb the X-rays. A major part of the opacity above 7 keV is due to Fe K-edge opacity.

At high energies the Compton shift of the incident photons becomes important.

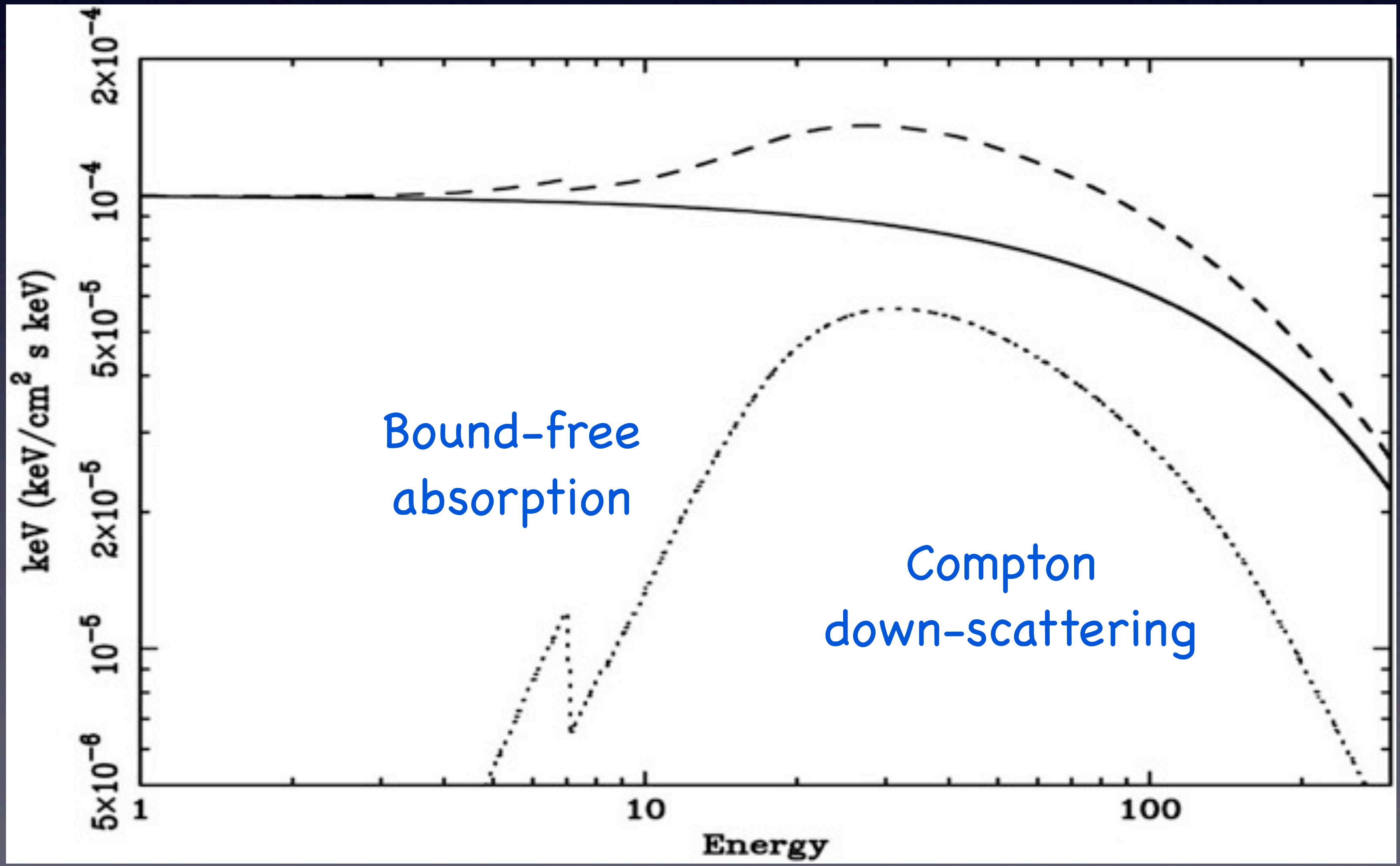

Photon-electron interaction

Direct Compton Scattering

In this process the photon is absorbed and immediately re-radiated by the electron into a different direction but it looses part of its initial energy. It can be thought as an heating mechanism.

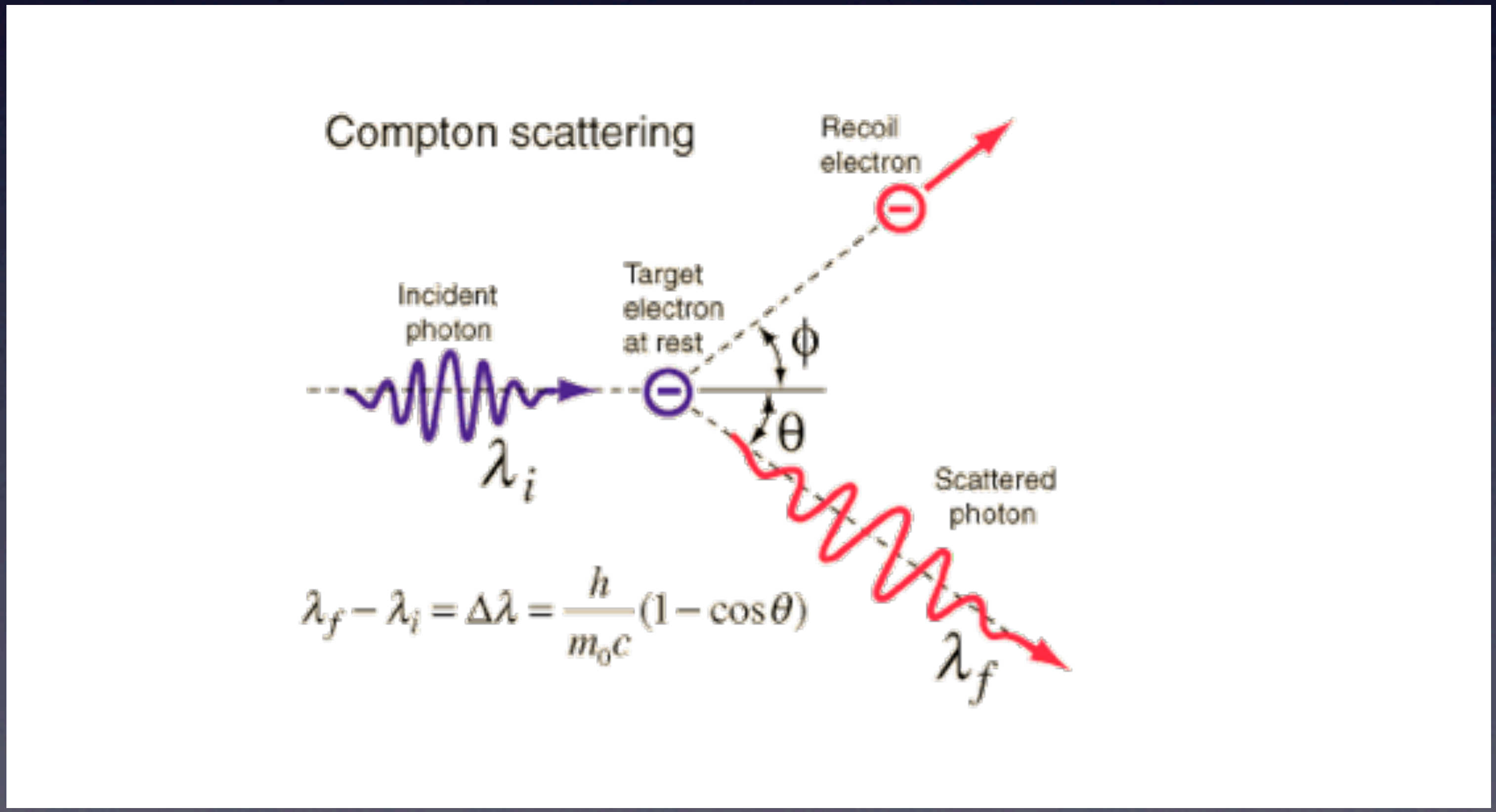

Iron Line

The fluorescent iron line is produced when one of the 2 K-shell (n=1) electrons of an iron atom (or ion) is ejected following photoelectric absorption of an X-ray. Following the photoelectric event, the resulting excited state can decay in one of two ways. An L-shell (n=2) electron can then drop into the K-shell releasing 6.4 keV of energy either as an emission line photon (34 % probability) or an Auger electron (66 % probability).

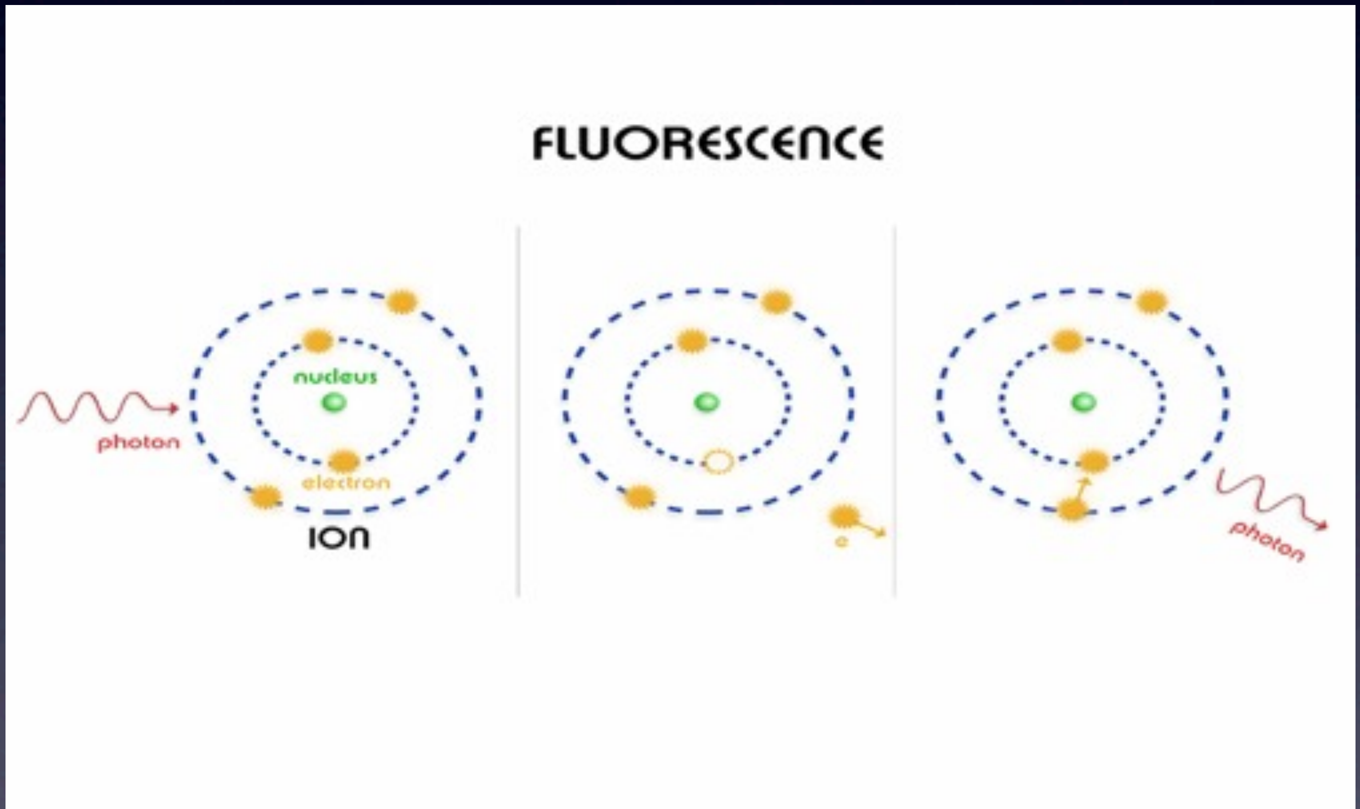

For ionized iron, the outer electrons are less effective at screening the inner K-shell from the nuclear charge and the energy of both the photoelectric threshold and the K line are increased.

BROAD LINE

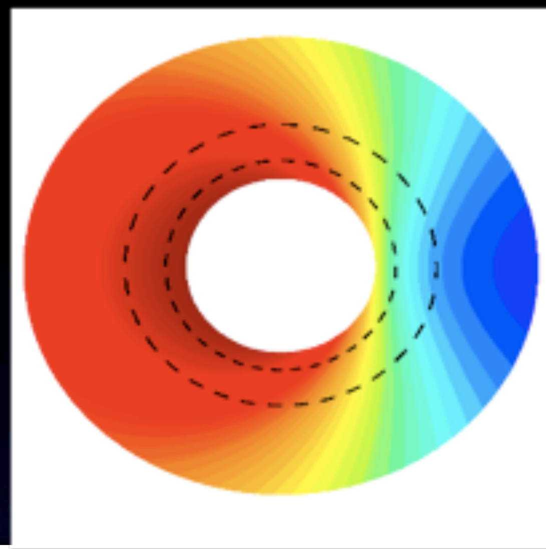

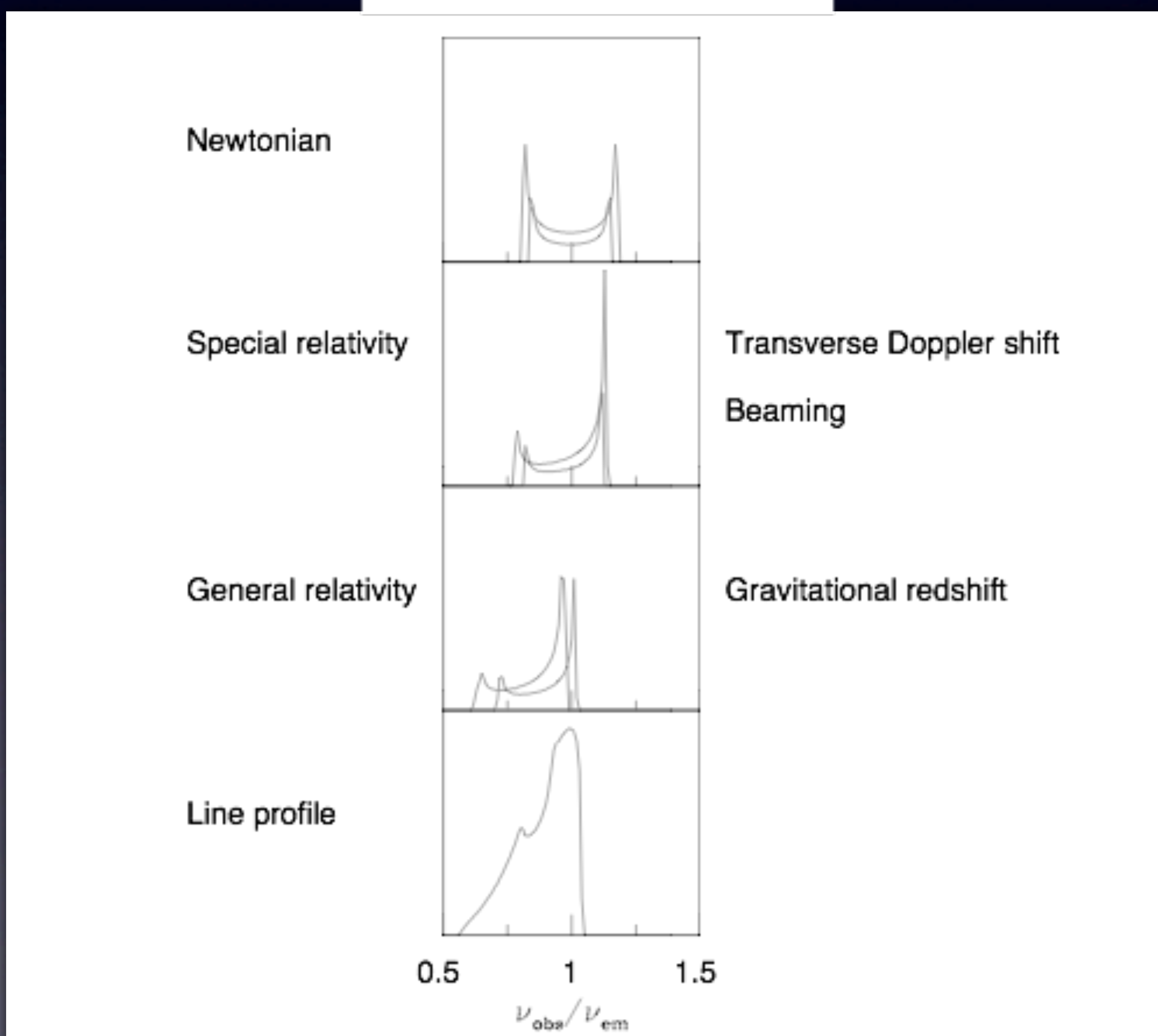

Newtonian
Special relativity
Transverse Doppler shift
Beaming
General relativity
Gravitational redshift
Line profile
0.5
1
1.5
ν_{obs}/ν_{em}

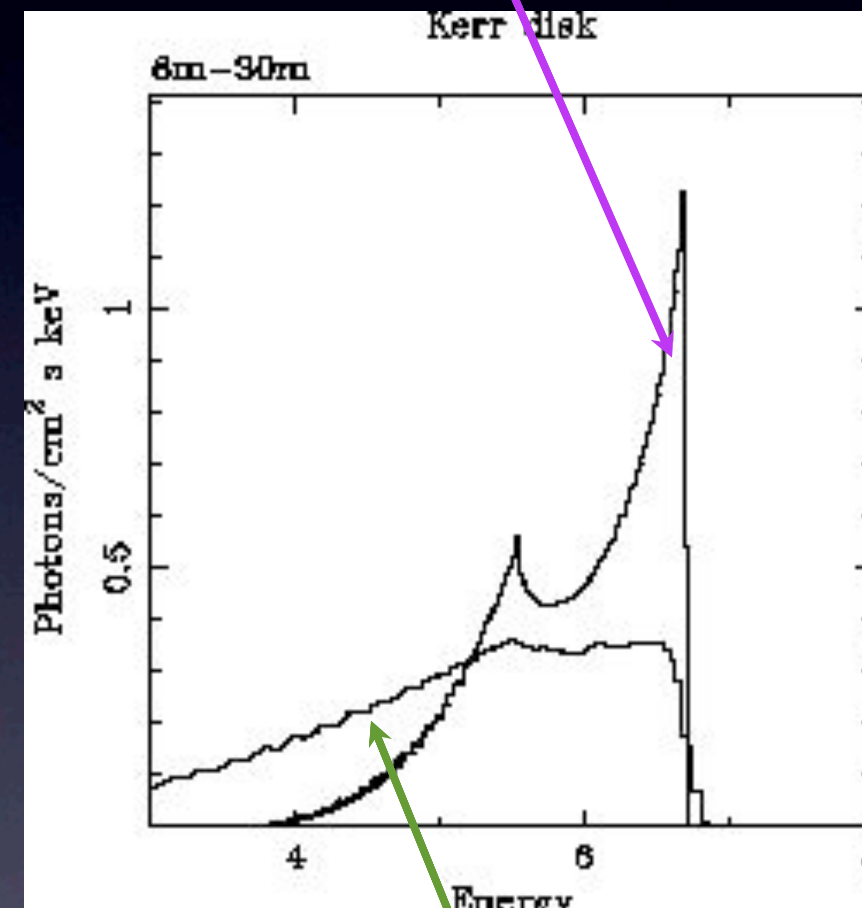

Schwarzschild
Kerr disk
6m–30m
Photons/cm^2 s keV
1
0.5
4
6
8
Energy
Kerr

Shape of the iron line and spin of the BH

The shape of the iron line allows to measure the spin of the black hole

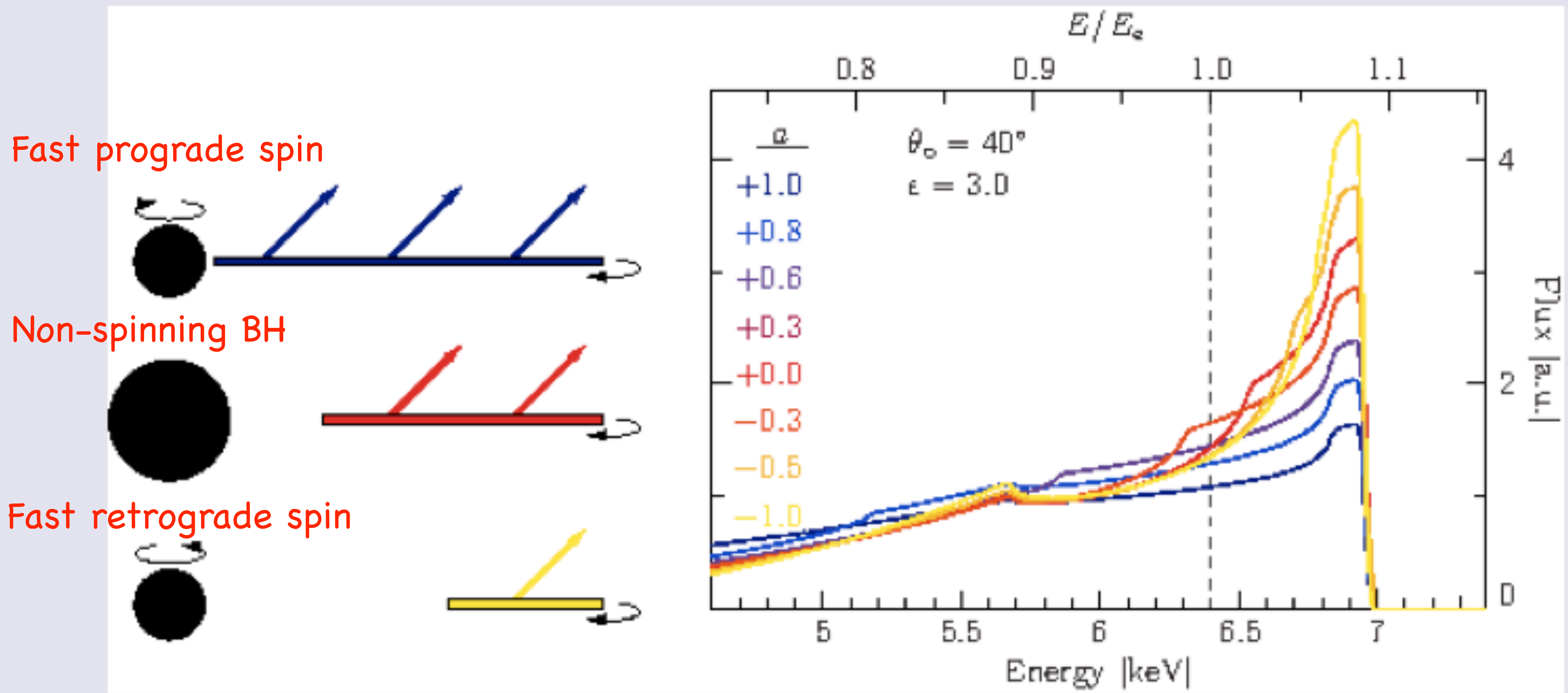

Line evolution for different spin of the black hole.

Image from
http://www.sternwarte.uni-erlangen.de/~dauser/research/broad_lines/index.html

Energy Equation

$$q^{+} = q^{-} + q^{adv}$$

Thin Accretion Disk

(Shakura & Sunyaev 1973; Novikov & Thorne 1973;...)

Most of the viscous heat energy is radiated

$$q^{-} \approx q^{+} \gg q^{adv}$$

$$L_{rad} : \ 0.1 \dot{M} c^2$$

Advection-Dominated Accretion Flow (ADAF)

(Ichimaru 1977; Narayan & Yi 1994, 1995; Abramowicz et al. 1995)

Most of the heat energy is retained in the gas

$$q^{-} \ll q^{+} \approx q^{adv}$$

$$L_{rad} \ll 0.1 \dot{M} c^2$$

$$L_{adv} : \ 0.1 \dot{M} c^2$$

q+ is the energy generated by viscosity per unit volume
q- is the radiative cooling per unit volume
q_{adv} represents the advective transport of energy

ADAF

In this solution the accreting gas has a very low density and is unable to cool efficiently. The viscous energy is stored in the gas as thermal energy instead of being radiated and is advected onto the BH. Ions and electrons are thermally decoupled.

- Very Hot: Ti~ 10^{12}K (R_S/R), Te~ 10^{9-11}K (since ADAF loses very little heat).
- Geometrically thick: H~R (most of the viscosity generated energy is stored in the gas as internal energy rather than being radiated, the gas puffes up
- Optically thin (because of low density)

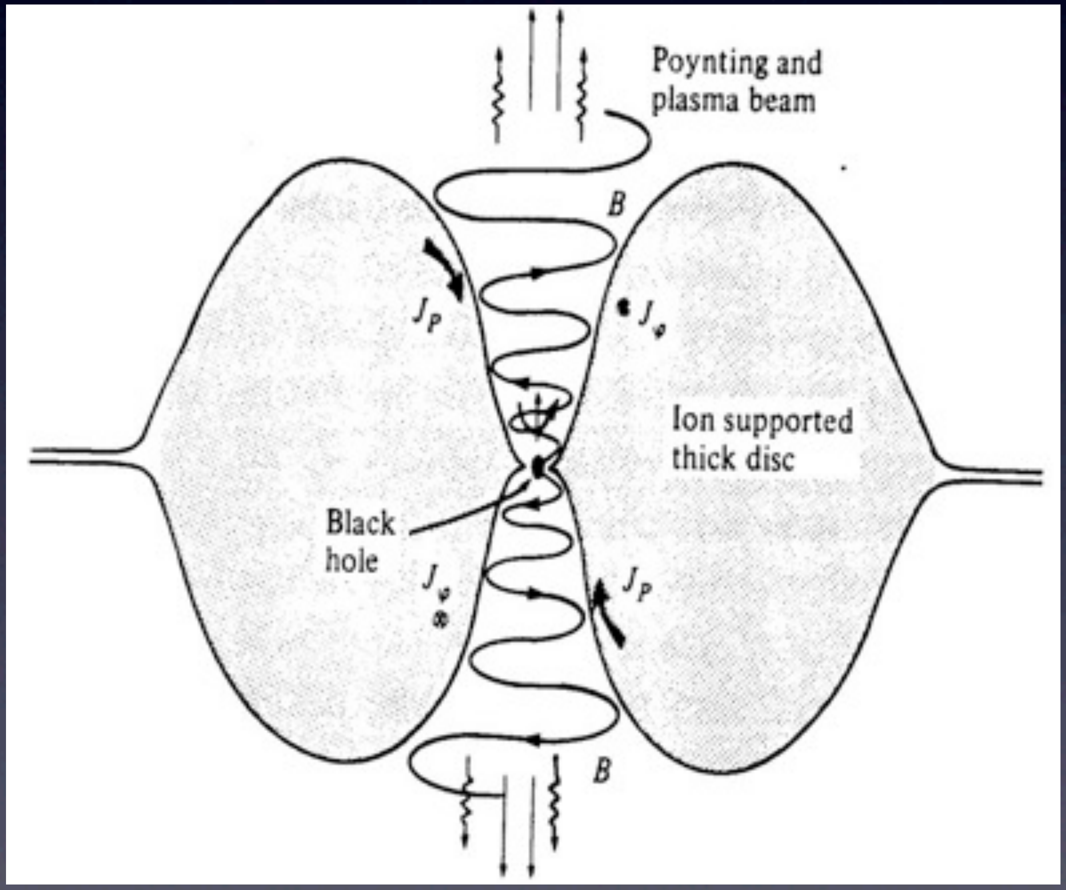

Jets, Lobes

NON-THERMAL PROCESSES

Synchrotron Radiation

Synchrotron radiation is due to the movement of an electron charge in a magnetic field. As a particle gyrates around a magnetic field, it will emit radiation at a frequency proportional to the strength of the magnetic field and its velocity.

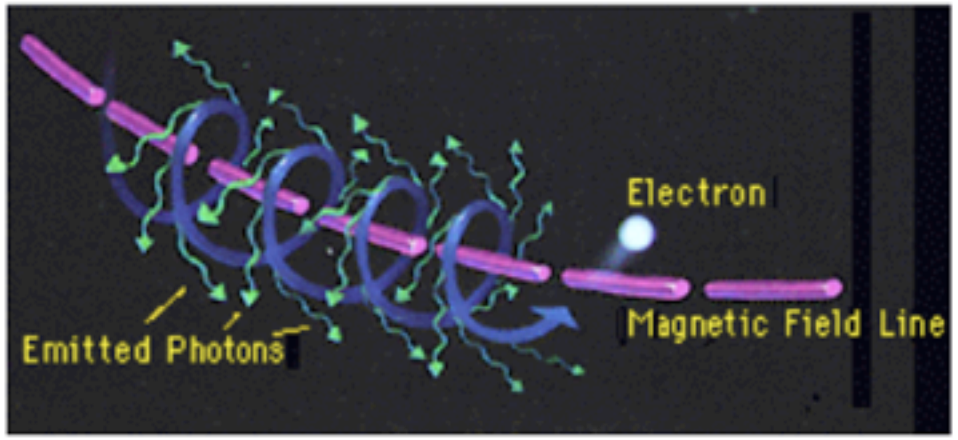

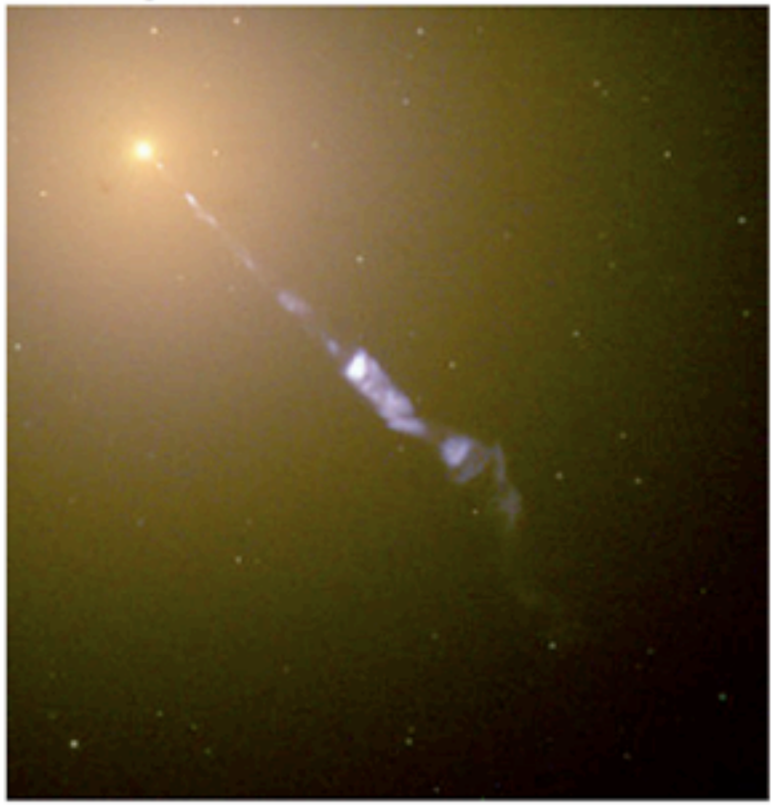

Synchrotron radiation is highly polarized and is seen at all wavelengths. At relativistic speeds, the radiation can also be beamed. It is very common in radio spectrum, but can be seen in x-rays. It is usually fit as a power law. For full details, see the review by Ginzburg & Syrovatskii (1969)

The synchrotron radiation of a power law distribution of electron energies

Synchrotron

$$N(\gamma_e) = K\gamma_e^{-p}\,, \quad \gamma_{min} < \gamma_e < \gamma_{max}\,, p = 1 + 2\alpha$$

$$\epsilon_{sin}(\nu) \propto K B^{\alpha+1} \nu^{-\alpha} \quad \text{erg cm}^{-3}\,\text{s}^{-1}\,\text{sr}^{-1}$$

Inverse Compton scattering

When the electron is not at rest, but has an energy greater that the typical photon energy, there can be a transfer of energy from the electron to the photon. This process is called Inverse Compton to distinguish it from the direct Compton scattering, in which the electron is at rest, and it is the photon to give part of its energy to the electron.

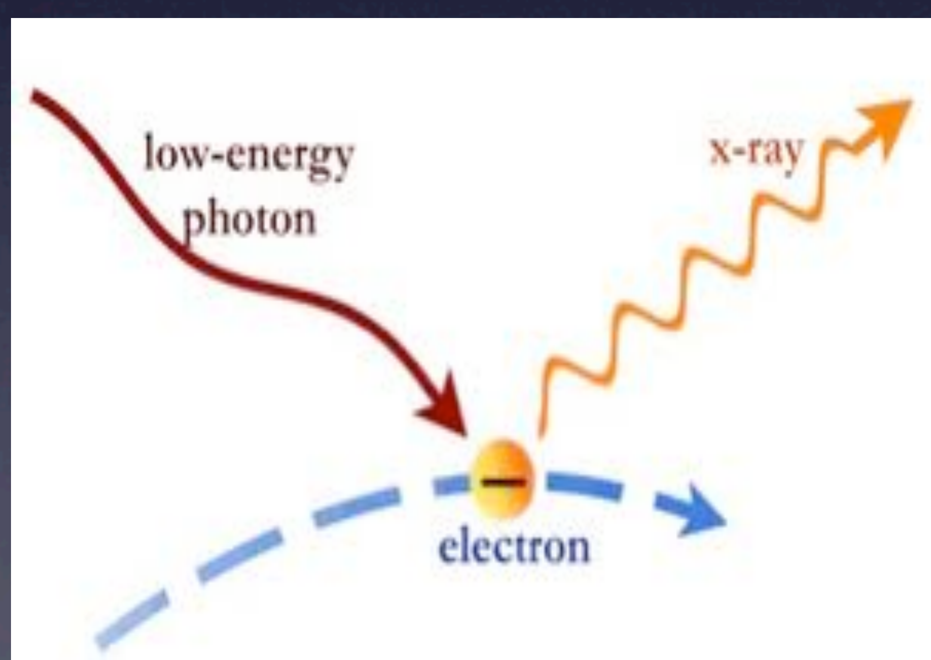

$$< \nu >= \frac{4}{3}\gamma^2\nu$$

Inverse Compton Radiation

The general result that the frequency of the scattered photons is $\nu \approx \gamma^2 \nu_0$ is of profound importance in high energy astrophysics. We know that there are electrons with Lorentz factors $\gamma \sim 100 - 1000$ in various types of astronomical source and consequently they scatter any low energy photons to very much higher energies. Consider the scattering of radio, infrared and optical photons scattered by electrons with $\gamma = 1000$.

Waveband	*Frequency (Hz)* ν_0	*Scattered Frequency (Hz) and Waveband*
Radio	10^9	10^{15} = UV
Far-infrared	3×10^{12}	3×10^{18} = X-rays
Optical	4×10^{14}	$4 \times 10^{21} \equiv 1.6$MeV = γ-rays

Thus, inverse Compton scattering is a means of creating very high energy photons indeed. It also becomes an inevitable drain of energy for high energy electrons whenever they pass through a region in which there is a large energy density of photons.

Inverse Compton

For a power law distribution of electrons:

$$N(\gamma_e) = K\gamma_e^{-p}, \quad \gamma_{min} < \gamma_e < \gamma_{max}, p = 1 + 2\alpha$$

Inverse Compton

$$\epsilon_c(\nu_c) \propto K\nu_c^{-\alpha} \int \frac{Ur(\nu)\nu^\alpha}{\nu} d\nu \qquad \text{erg cm}^{-3} \text{ s}^{-1} \text{ sr}^{-1}$$

U_r is the radiation energy density

$$U_r = \int n(\epsilon)\epsilon d\epsilon$$

- Synchrotron photons in the jet
- Environment photons from Accretion Flow, BLR, NLR, Torus
- Cosmic Microwave Background (CMB) photons

6. Journey along the jet

pc-scale jet

kpc-scale jet

lobes

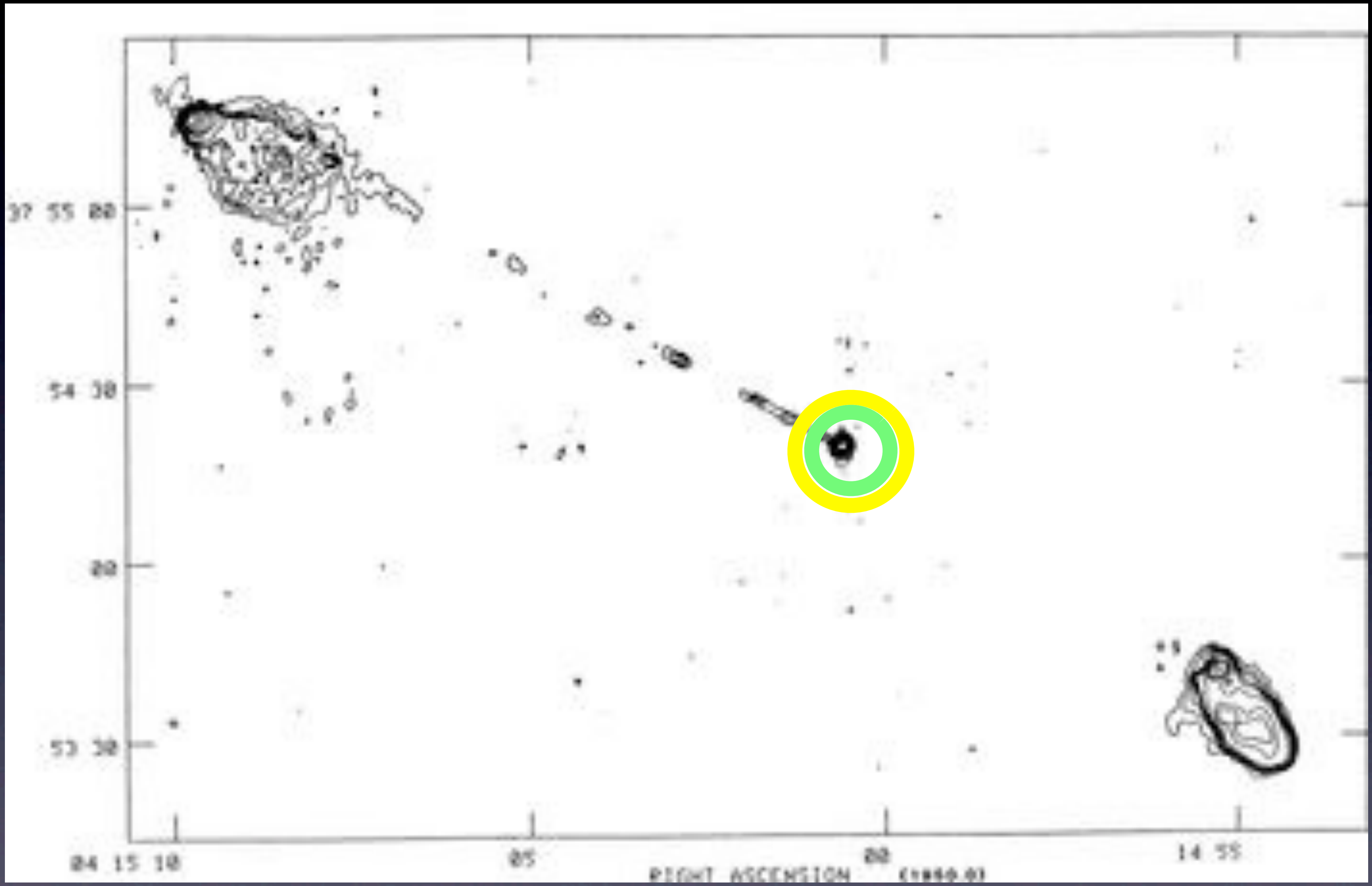
37 55 00
54 30
00
53 30
04 15 10
05
00
14 55
RIGHT ASCENSION

Radio Loud AGNs
JET at sub-pc scale (core)

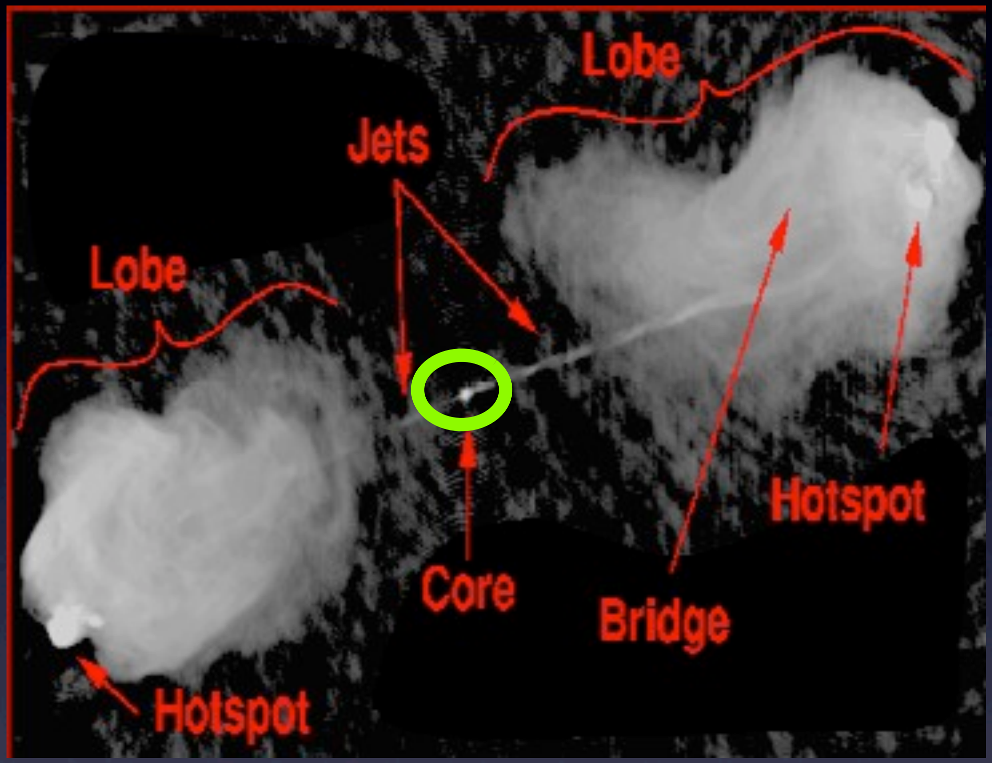

1mas=0.9 pc

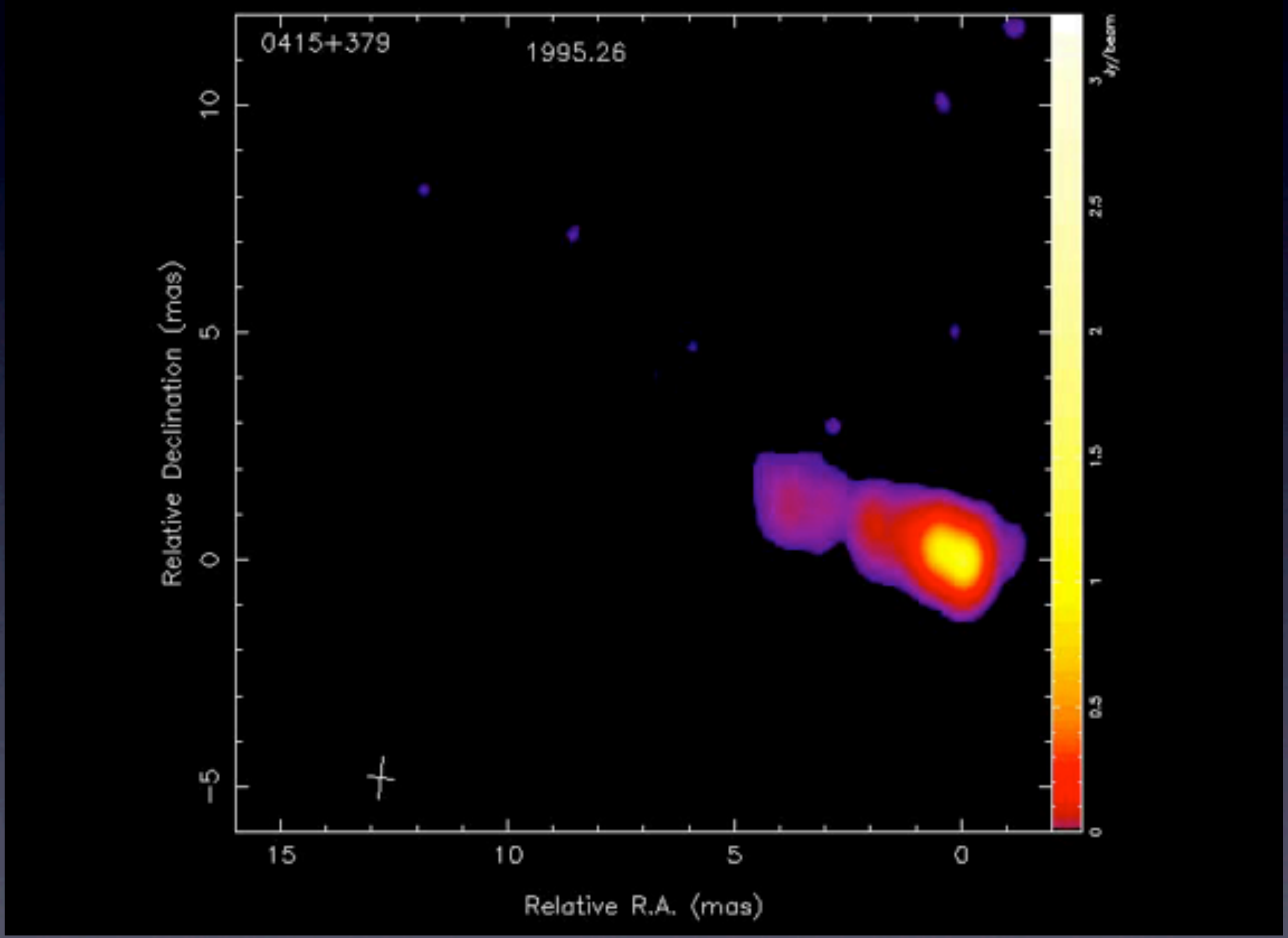

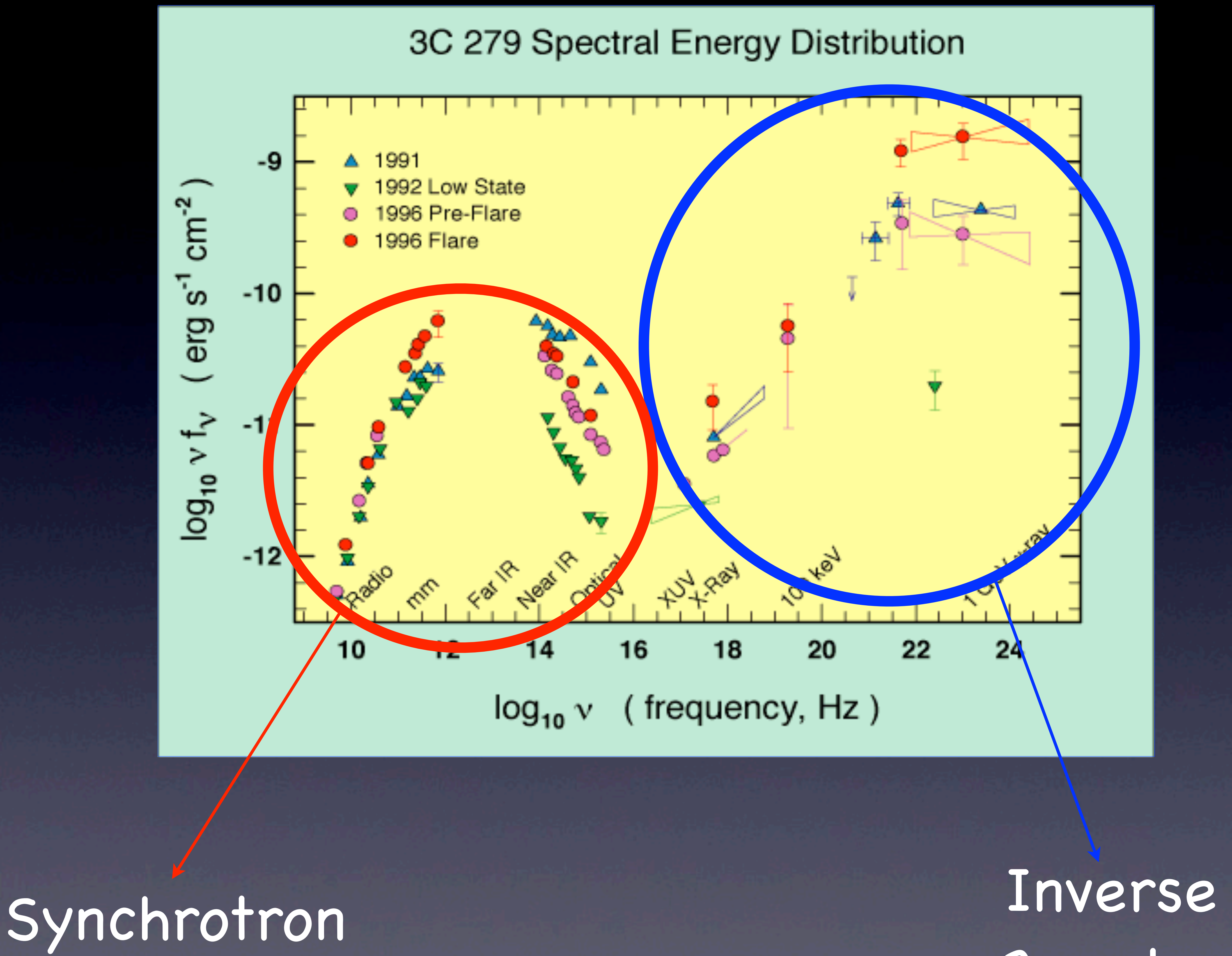
3C 279 Spectral Energy Distribution
1991
1992 Low State
1996 Pre-Flare
1996 Flare
Radio
mm
Far IR
Near IR
Optical
UV
XUV
X-Ray
log10 ν (frequency, Hz)
log10 ν fν (erg s-1 cm-2)
Synchrotron
Inverse Compton

Synchrotron Self–Compton

Consider a population of relativistic electrons in a magnetized region. They will produce synchrotron radiation, and therefore they will fill the region with photons. These synchrotron photons will have some probability to interact again with the electrons, by the Inverse Compton process. Since the electron "work twice" (first making synchrotron radiation, then scattering it at higher energies) this particular kind of process is called synchrotron self-Compton, or SSC for short.

External Compton

The population of relativistic electrons in a magnetized region can also interact with photons externa to the jet produced in the accretion disk, in the broad/narrow line regions in the torus. This particular kind of process is called External Compton, or EC for short.

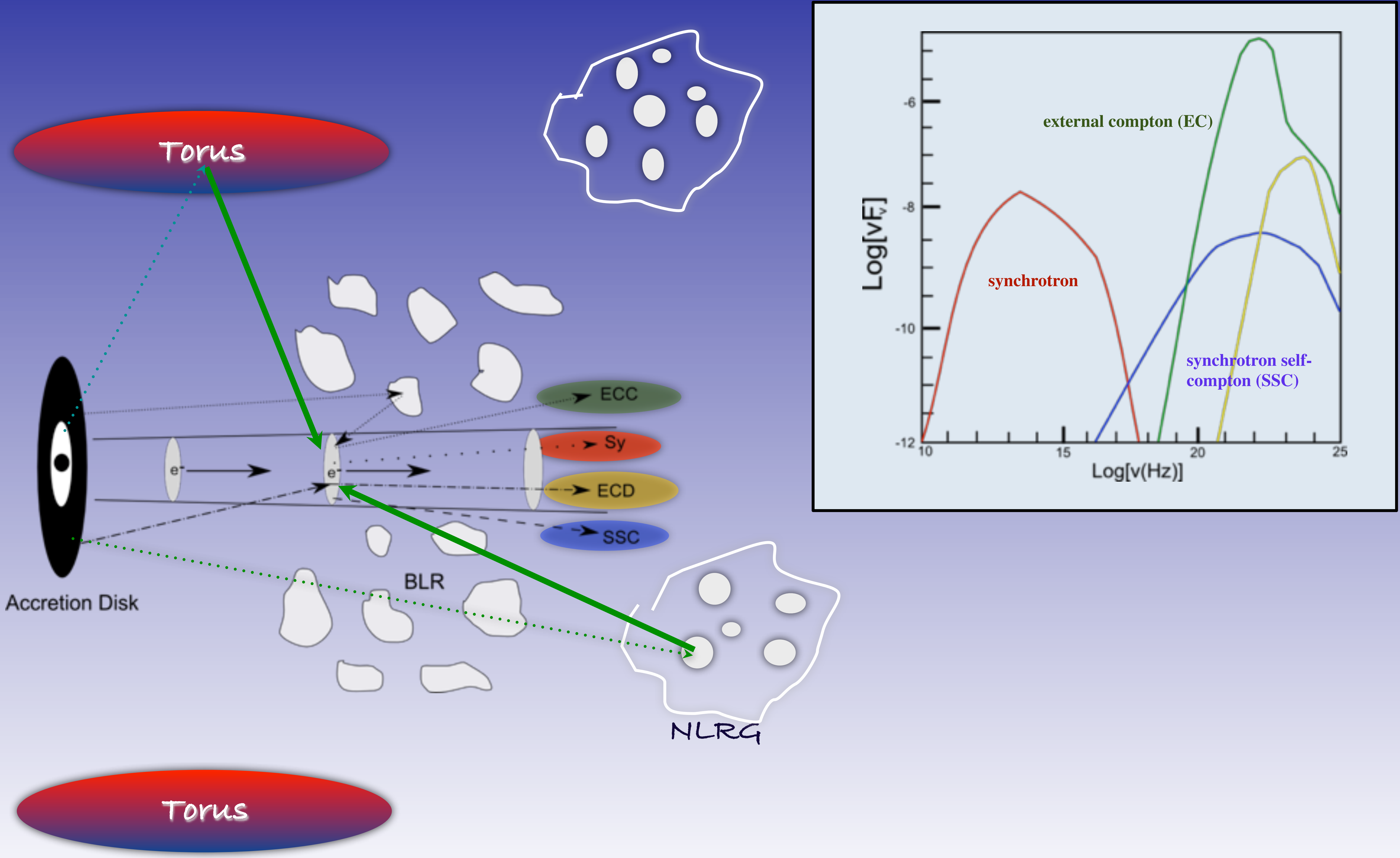
Torus
Accretion Disk
e-
e-
ECC
Sy
ECD
SSC
BLR
NLRG
Torus
Log[νF_ν]
-6
-8
-10
-12
external compton (EC)
synchrotron
synchrotron self-compton (SSC)
10
15
20
25
Log[ν(Hz)]

Competition between jet and disk

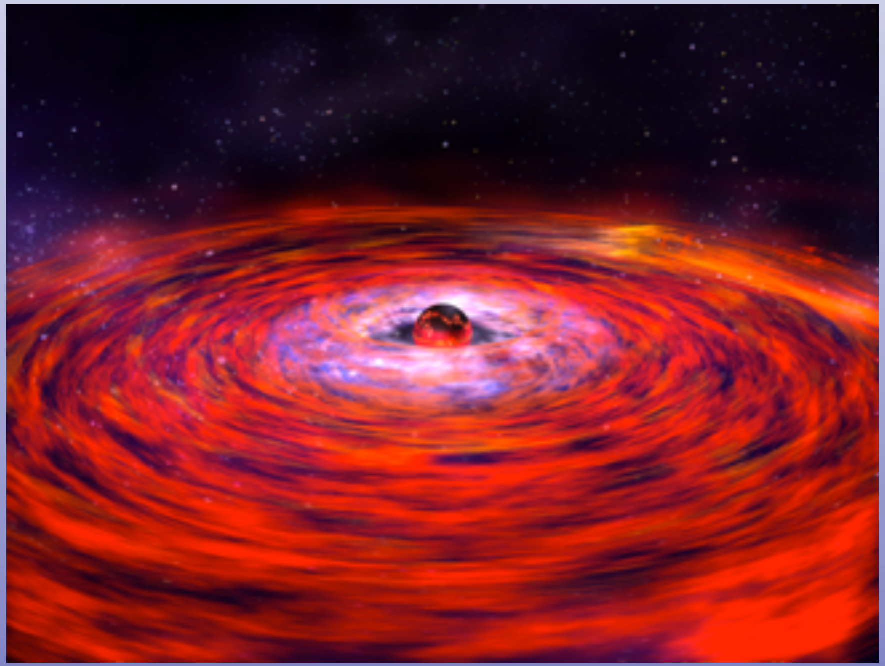

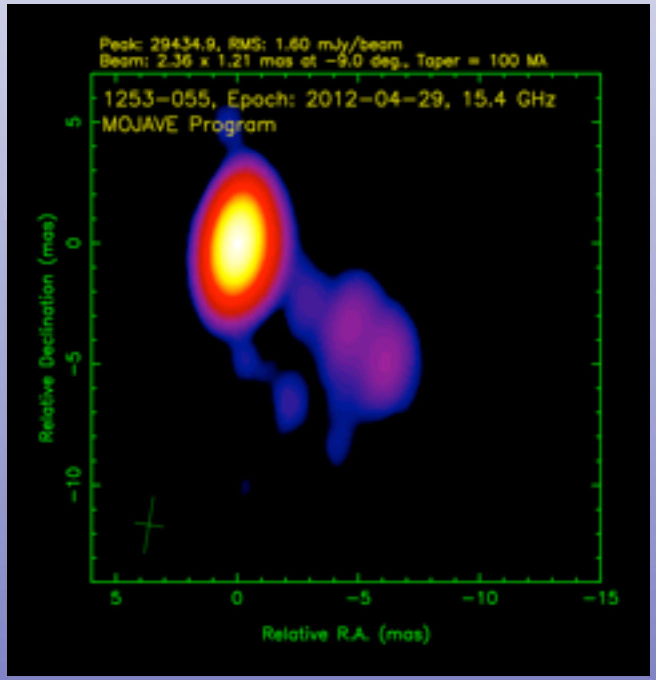

X-ray Spectra:Accretion Disk and pc-scale Jet emission are in competion:

Angle of sight = 0° ==> Jet radiation dominates

Angle of sight = 90° ==> Accretion disk dominates

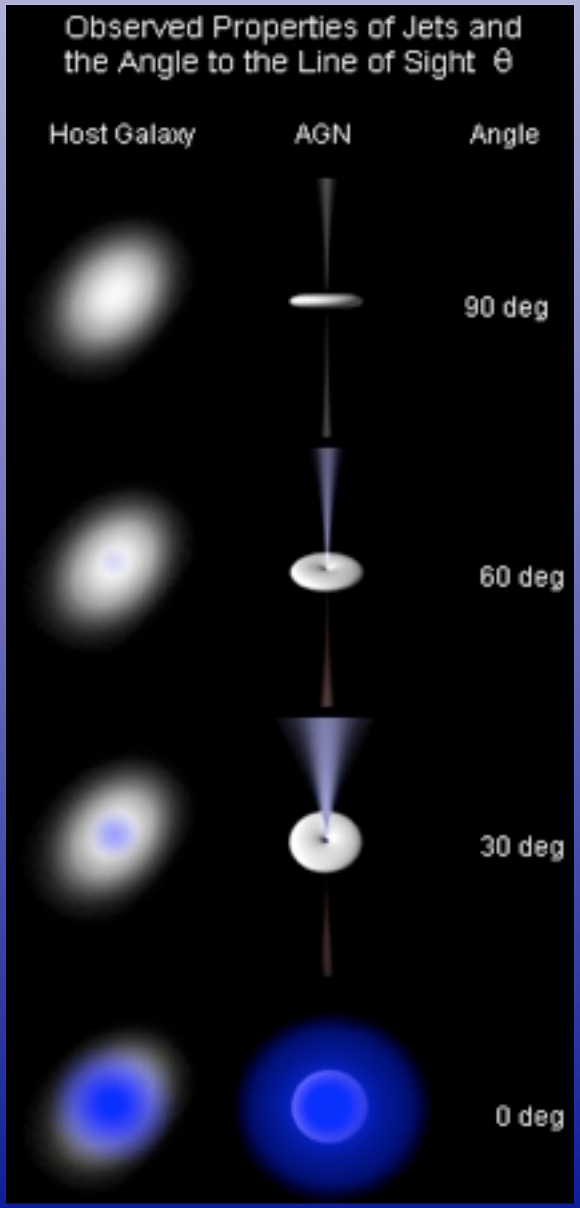

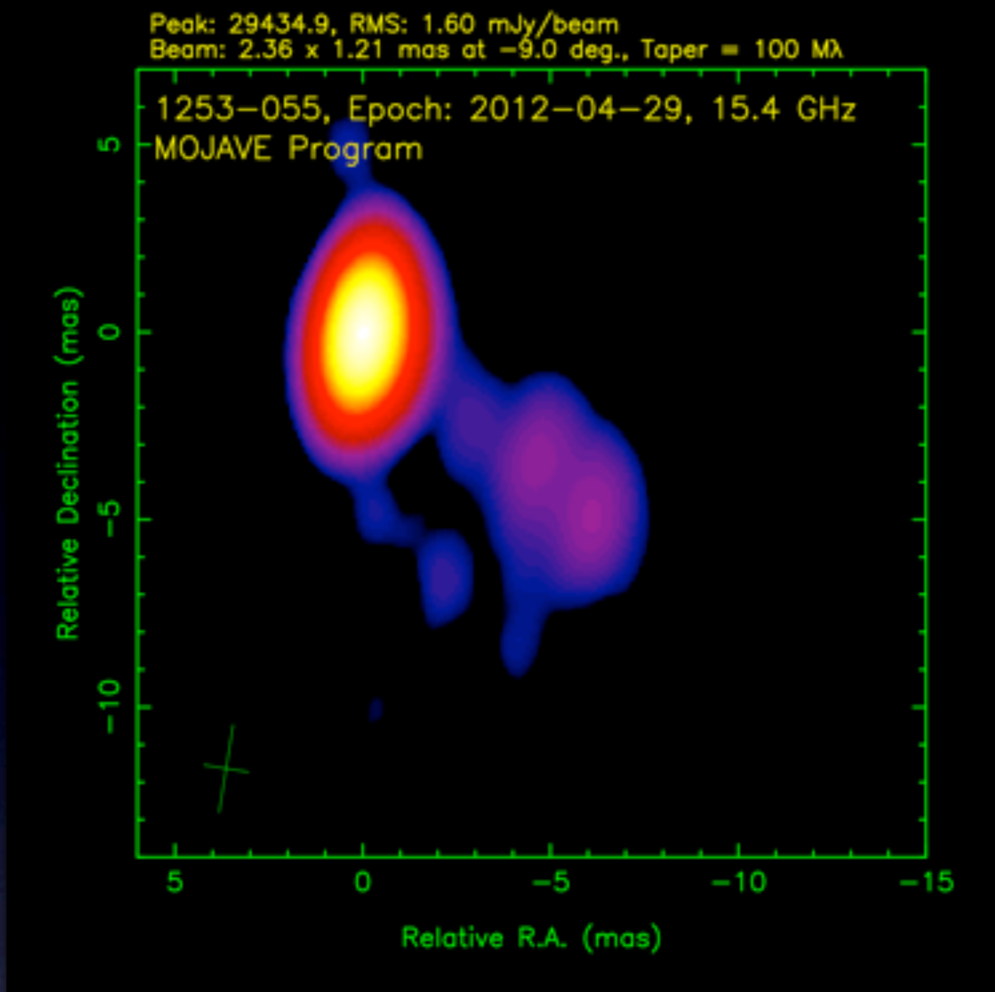
Peak: 29434.9, RMS: 1.60 mJy/beam
Beam: 2.36 x 1.21 mas at -9.0 deg., Taper = 100 MΛ
1253-055, Epoch: 2012-04-29, 15.4 GHz
MOJAVE Program
Relative Declination (mas)
Relative R.A. (mas)
5
0
-5
-10
-15

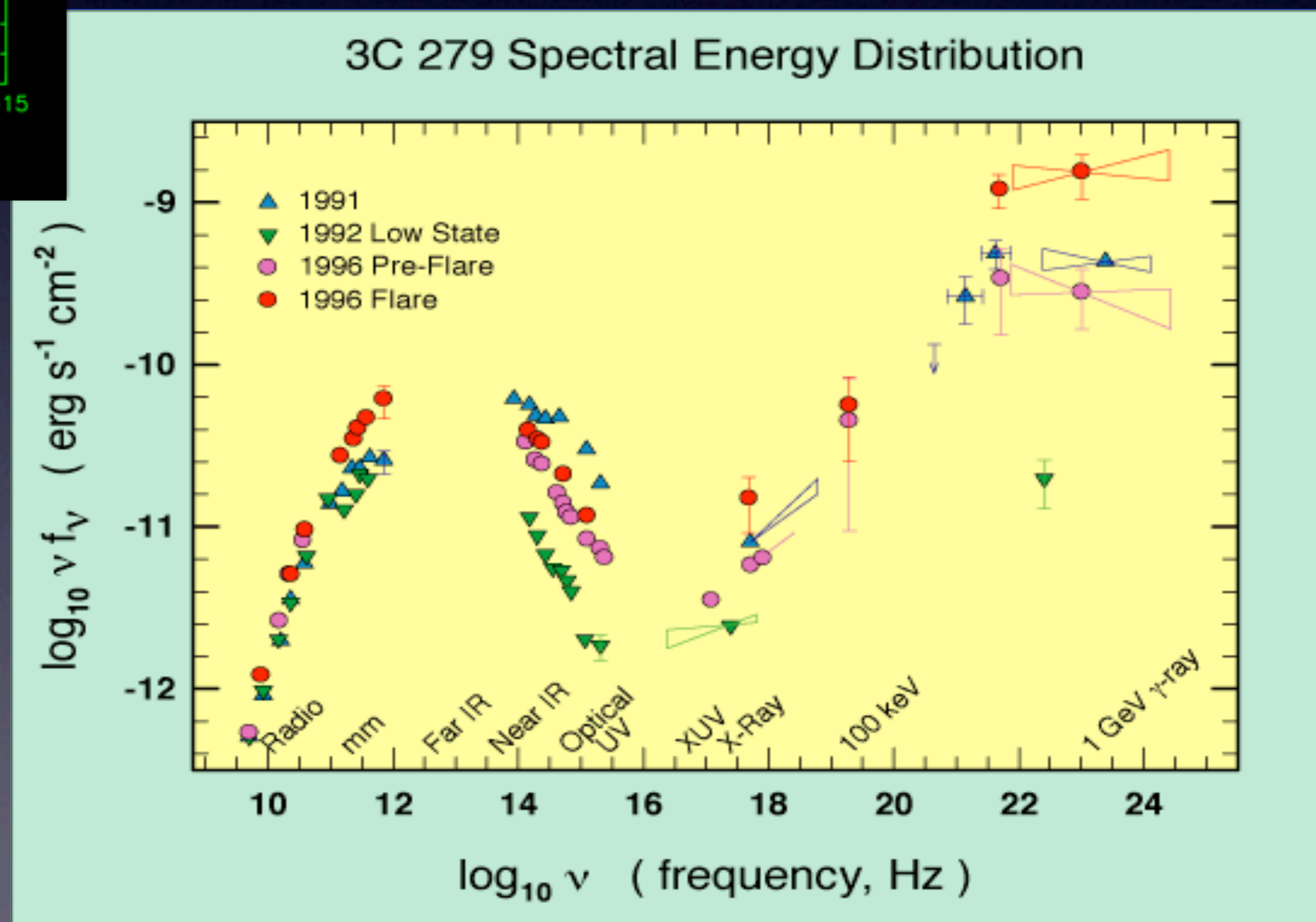
3C 279 Spectral Energy Distribution
1991
1992 Low State
1996 Pre-Flare
1996 Flare
log10 ν fν (erg s-1 cm-2)
log10 ν (frequency, Hz)
-9
-10
-11
-12
10
12
14
16
18
20
22
24
Radio
mm
Far IR
Near IR
Optical
UV
XUV
X-Ray
100 keV
1 GeV γ-ray

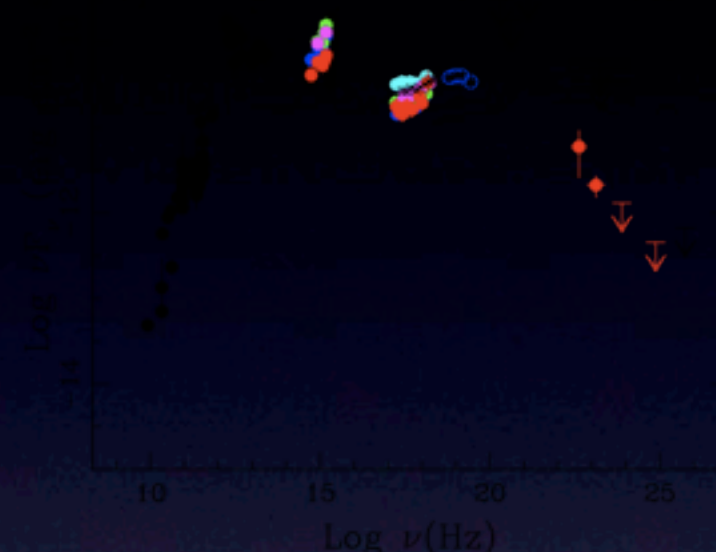
10
15
20
25
Log ν(Hz)

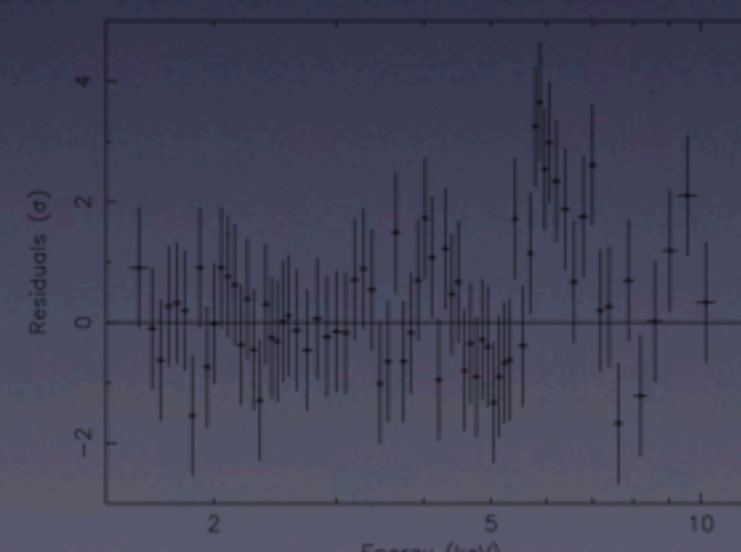
Residuals (σ)
4
2
0
-2
2
5
10
Energy (keV)

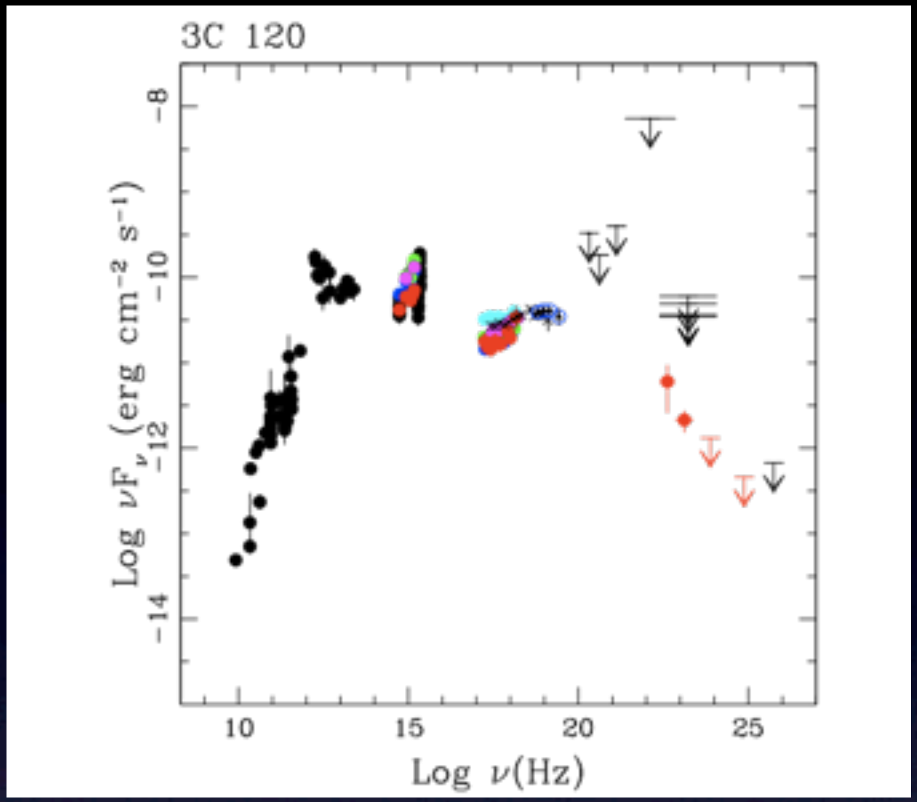
3C 120
Log νF_ν (erg cm^{-2} s^{-1})
Log ν(Hz)
−8
−10
−12
−14
10
15
20
25

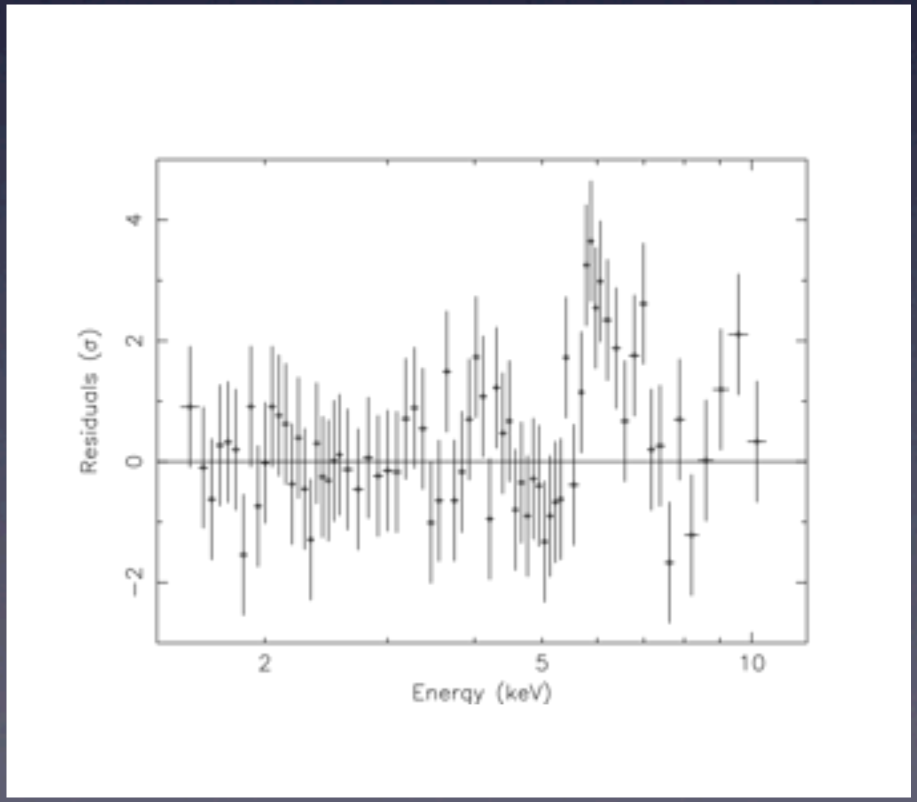
Residuals (σ)
Energy (keV)
4
2
0
−2
2
5
10

kpc-scale Jet

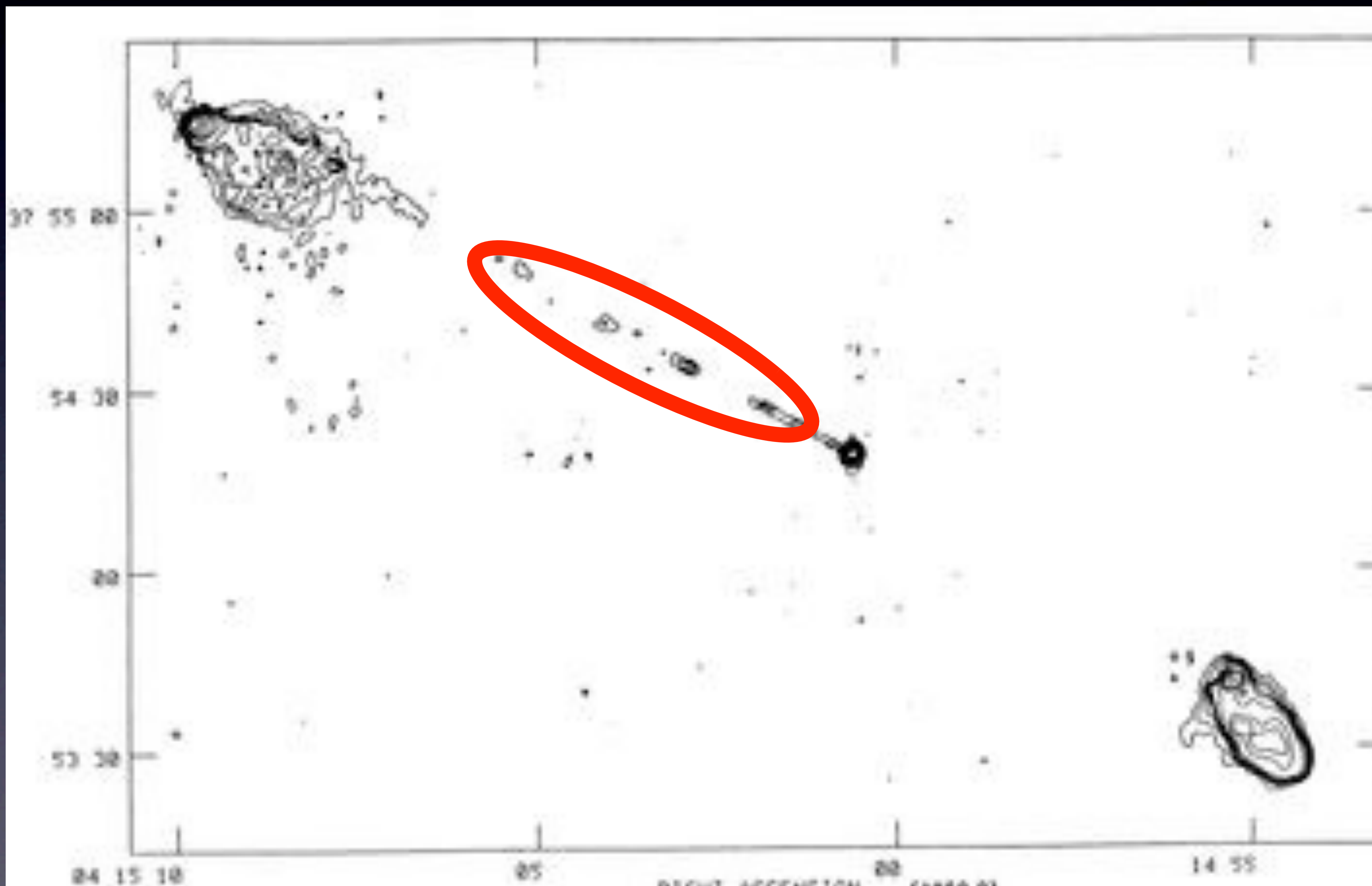

kpc-scale Jet

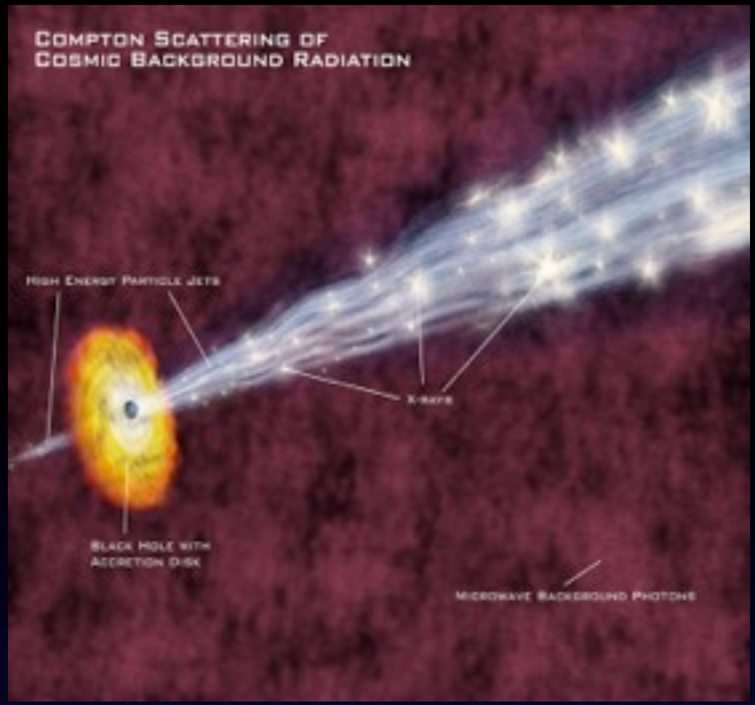

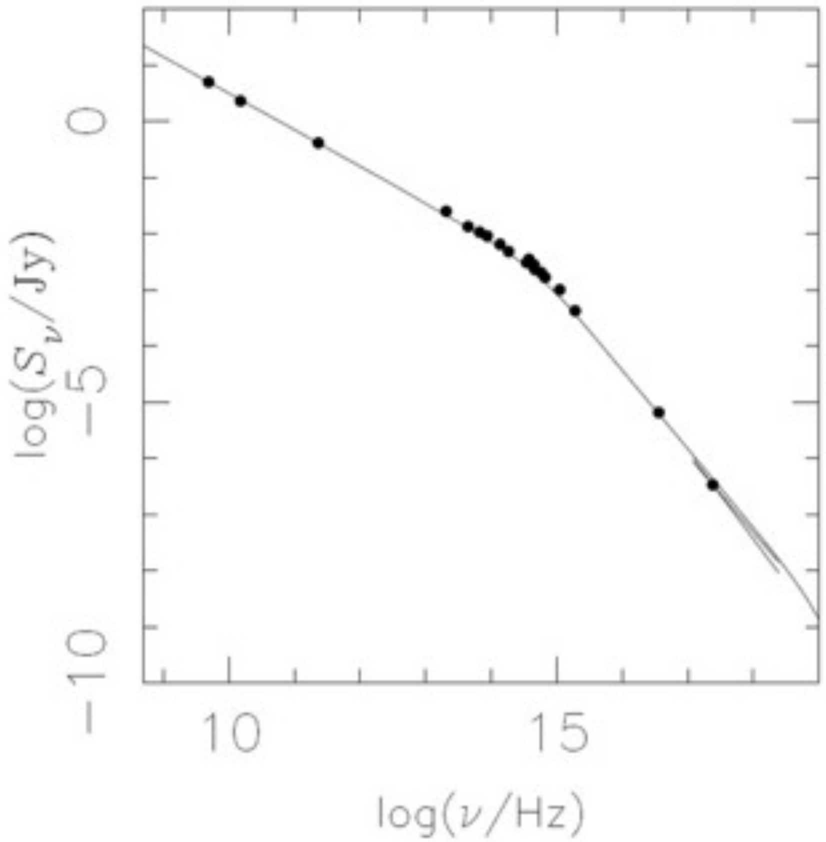

FRI-M87

For low-luminosity (FRI) radio sources, there is strong support for the synchrotron process as the dominant emission mechanism for the X-rays, optical, and radio emissions

Synchrotron process

FRII sources require multi-zone synchrotron models, or synchrotron and IC models (seed photons: CMB).
The most popular model postulates very fast jets with high bulk Lorentz factors Γ.

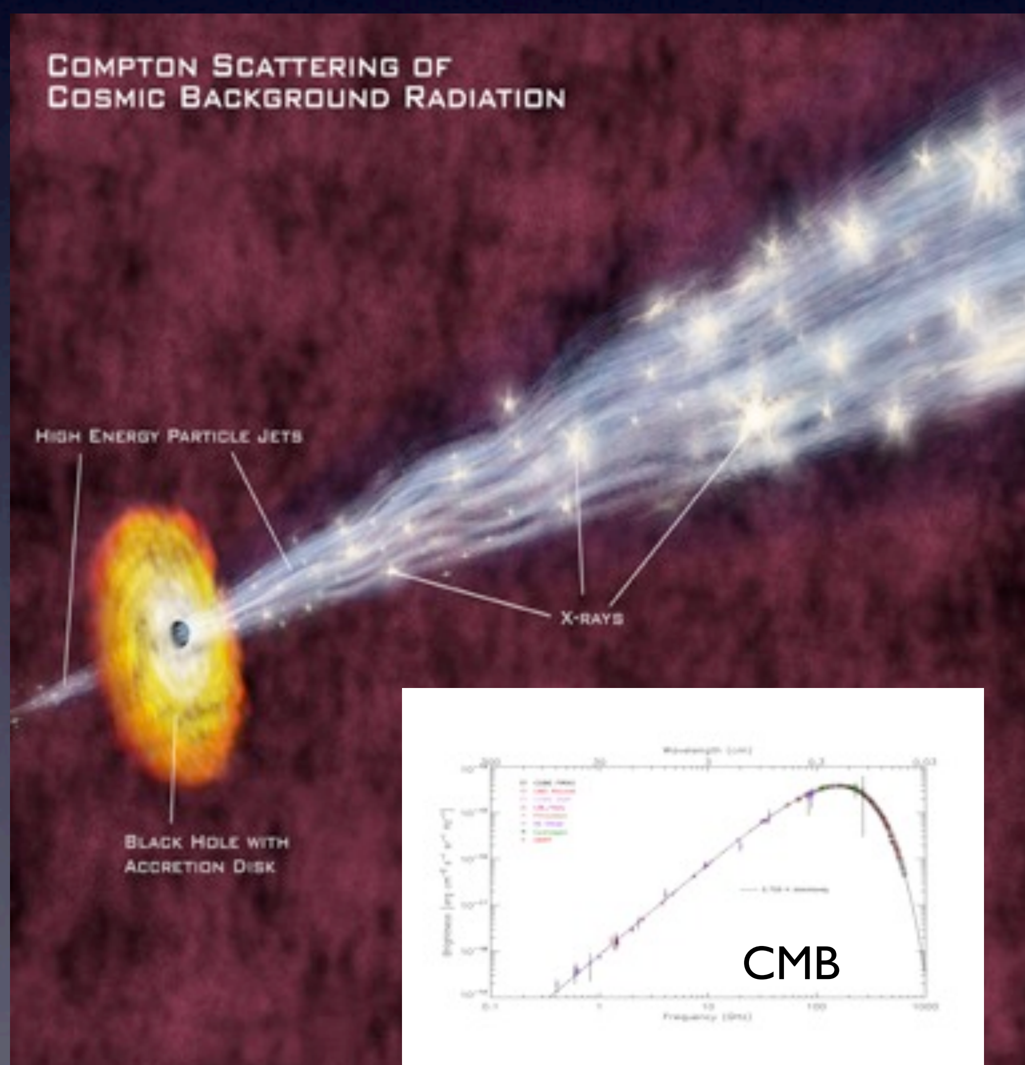

FRII-PKS0637-75

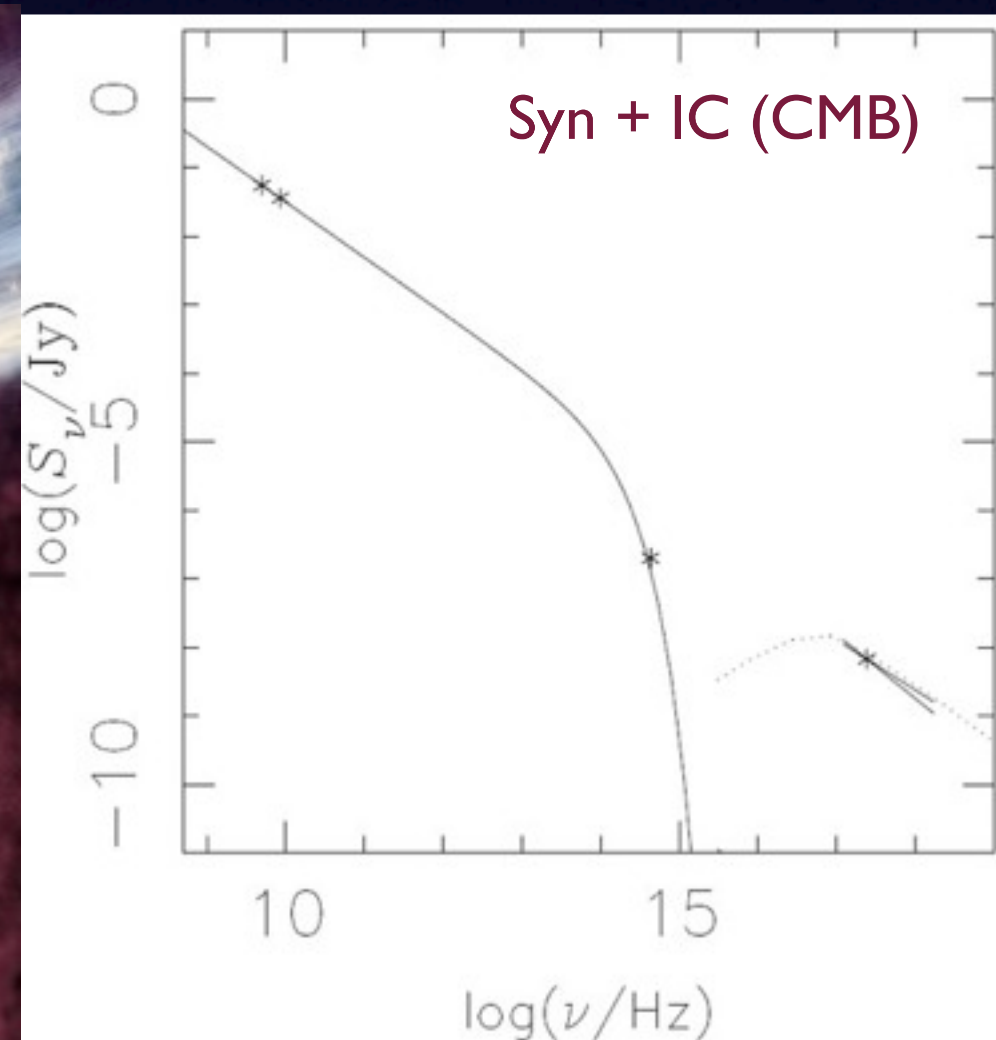

Lobes

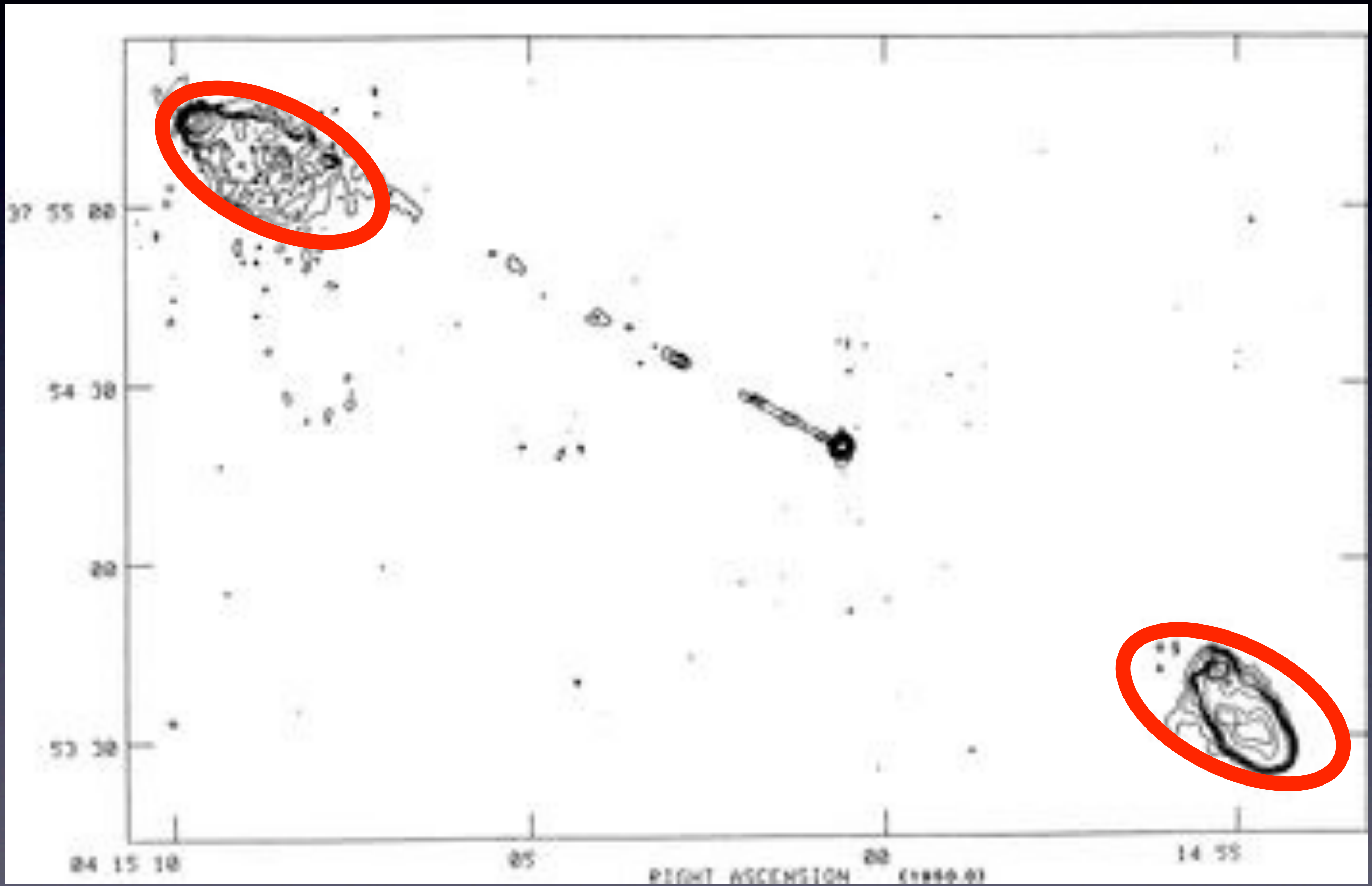

Lobes

relativistic electrons

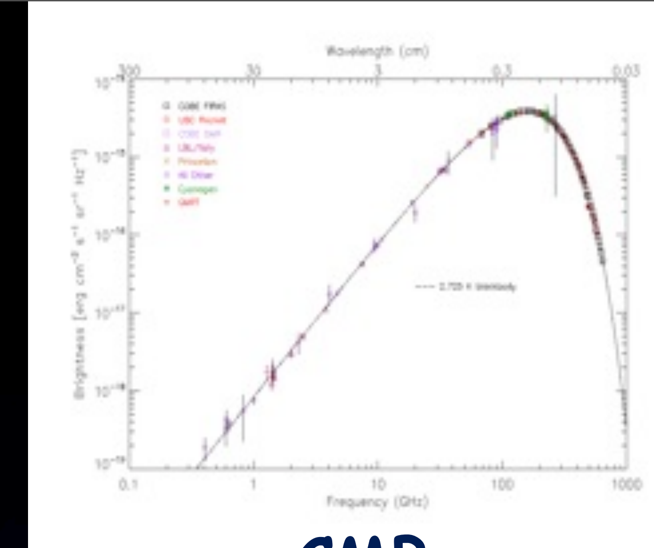

CMB

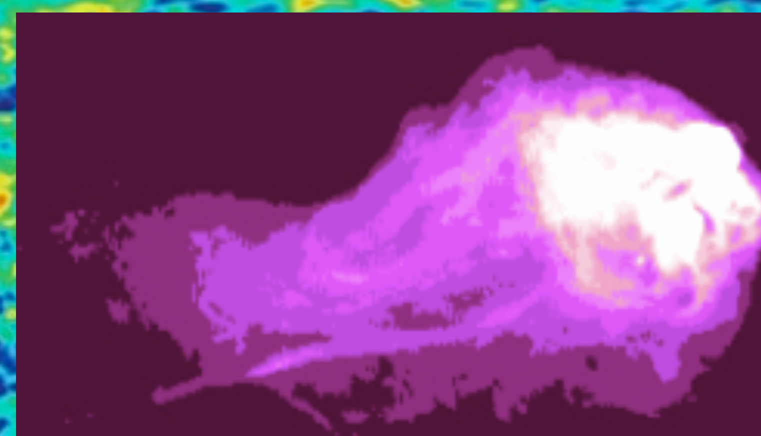

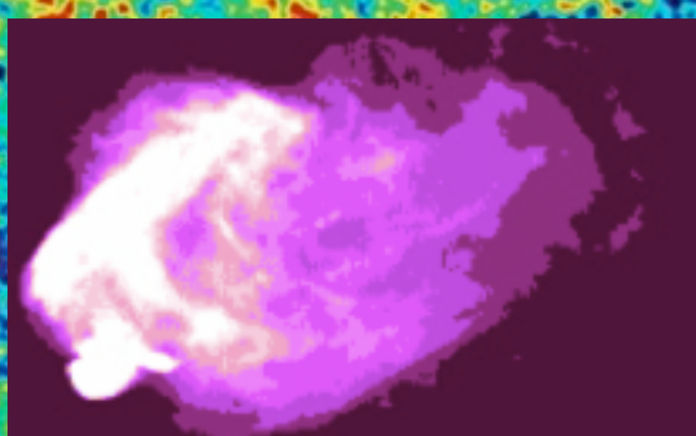

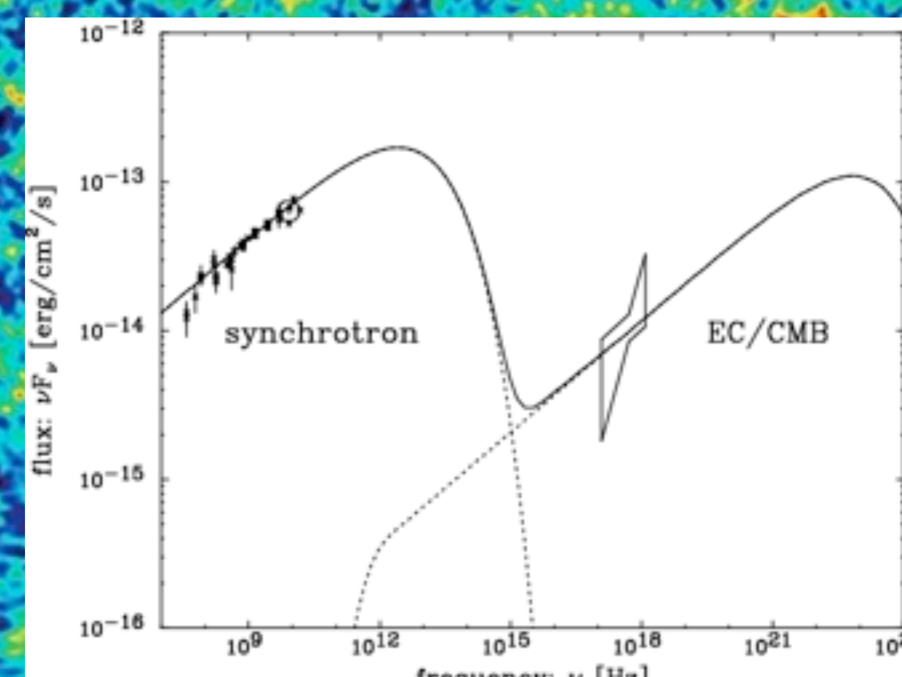

Hot Spots

Terminal hotspots, like knots, are thought to be localized volumes of high emissivity which are produced by strong shocks or a system of shocks. Hot spot spectra are generally consistent with SSC predictions but a significant number appeared to have a larger X-ray intensity than predicted. This excess could be attributed to a field strength well below equipartition, IC emission from the decelerating jet 'seeing' Doppler boosted hotspot emission or an additional synchrotron component, ecc

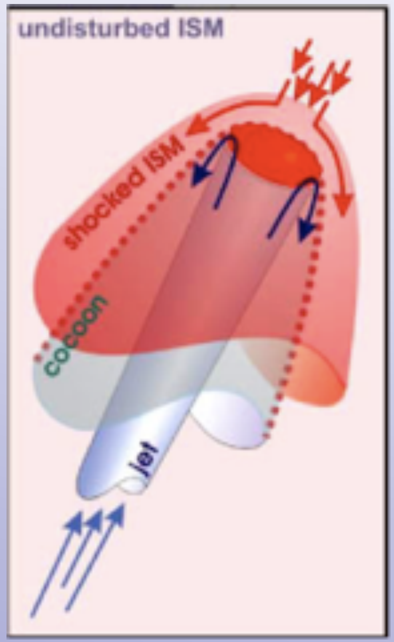

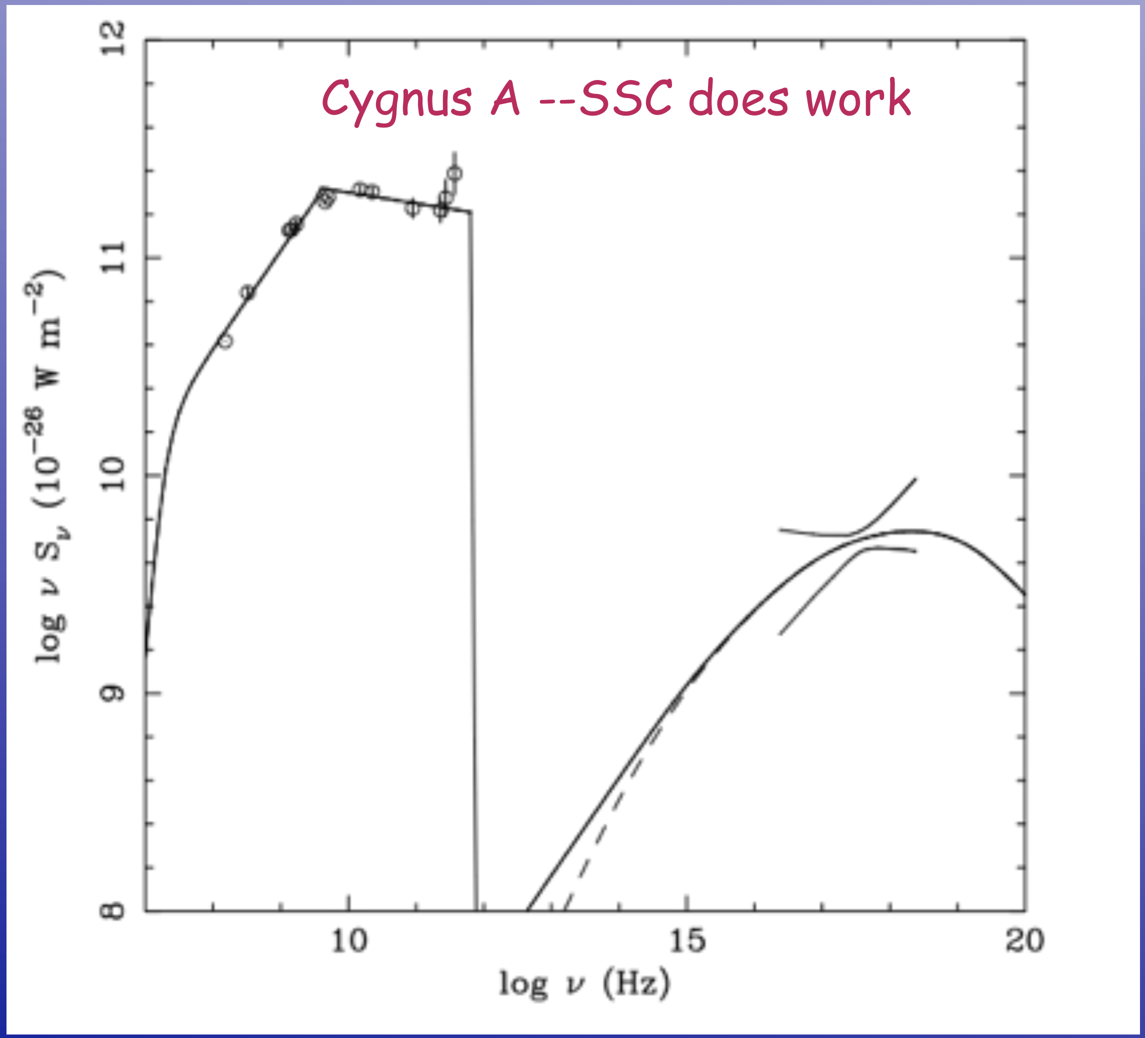

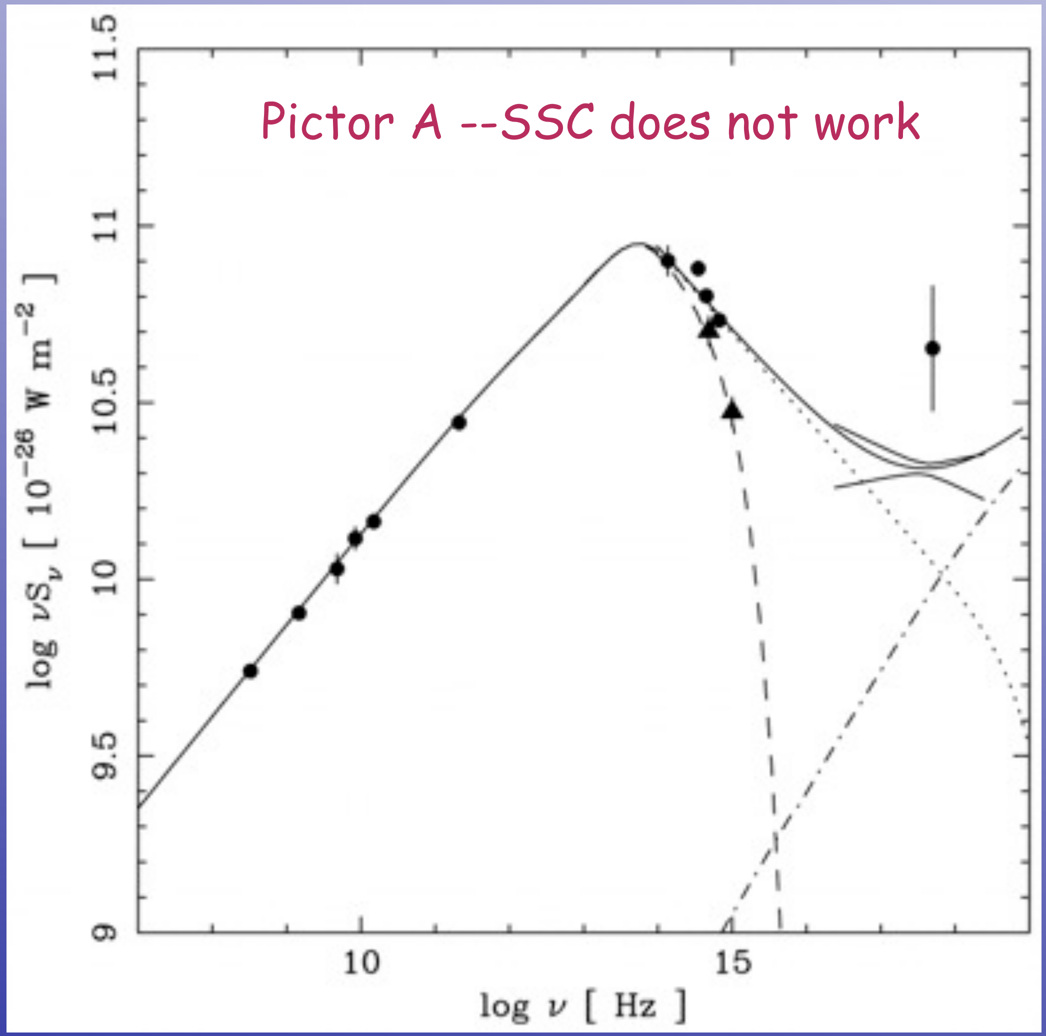


Questions?